Response to Reviewer 1

Original text is in black. Our responses are in blue text. References to the revised text take the following format: RP78,L54-55 (Revised Page 78, Lines 54-55). The references are to the manuscript with changes tracked.

This paper compares the atmospheric distributions of CO2 resulting from two sets of optimized fluxes derived from GEOS-Chem using different observing systems based on in situ data and GOSAT data respectively. The results show the differences in the optimized fluxes and how their correction is transported in the atmosphere. An evaluation of the seasonal cycle and inter-hemispheric gradient is also provided. Finally, the zonal variability of the flux correction signal at different vertical levels (boundary layer, free troposphere and stratosphere) is also explored. The differences between the two sets of posterior fluxes and their atmospheric distributions highlight problems associated with spatial and temporal coverage of observing systems and their ability to constrain the surface CO2 fluxes at different temporal and spatial scales. Overall, the results point to the conclusion that the in situ observations do a better job at constraining the fluxes at global and annual time scales, leading to smaller biases in their fit with independent observations. While GOSAT data is able to better capture the seasonal cycle at northern extratropical sites. The paper is well written and well structured. However, I have some concerns on the use of atmospheric differences associated with flux correction patterns to draw conclusions on the potential representation of zonally asymmetric patterns by different observing systems. It is not possible to say that GOSAT is (potentially) better at constraining the zonal patterns without substantiating this with an assessement of the errors in zonal variability based on independent observations (e.g. zonal gradients using TCCON or in situ data). The analysis of the seasonal cycle could also be improved by looking at the seasonal amplitude and phase, instead of just providing seasonal biases which is too qualitative in my opinion. The results and conclusions would also be more robust if more than just one year and a half of data was used.

Response: The question raised by the Reviewer here and in the second and third bullets under General comments is an important one. The question ultimately concerns our approach of drawing conclusions from comparing posterior atmosphere adjustments due to flux increments with posterior atmospheric adjustments due to uncertain meteorology. Because it is such a different approach from any other in the literature, it should have been better explained. Therefore, we are grateful for the opportunity to clarify this. In the revised manuscript, we add a new section which mathematically describes the posterior atmospheric adjustment (referred to as the "flux signal" in the original manuscript) and shows that it comprises components due to flux adjustments, initial state adjustments and meteorological uncertainty. Clearly, if the posterior atmospheric adjustment due to flux increments is not the dominant term (for certain spatial or temporal scales), then caution must be exercised when utilising the retrieved fluxes on those scales. Thus we introduce a new diagnostic for retrieved fluxes and we use this to show that assimilating GOSAT observations gives zonal standard deviations that exceed those associated with meteorological uncertainties. We also agree (and we noted this in several places in the original manuscript) that the conclusion of whether GOSAT is better at constraining final spatial scales must rely on the availability of dense network of independent observations. Such a network does not currently exist. The TCCON and in situ surface networks are not sufficiently dense. But, but we can still point to the *potential* ability of GOSAT to see finer spatial scales, using our diagnostic since spatial scales produced by in situ-constrained fluxes do not exceed those produced by uncertain meteorology. In general, larger values of zonal standard deviations means more spatial structure is seen, but *more* does not mean *better*. However, if the threshold (of posterior atmospheric adjustments due to uncertain meteorology) is not exceeded, the spatial structure seen should not be trusted since a perturbed but equally valid wind field would give different spatial structures. Finally, it is always better to have longer runs but we all balance this desire with what is computationally feasible. Because of the systematic and consistent differences between the posterior atmospheric adjustments obtained with the two different posterior fluxes over the course of our experiments, we believe that our conclusions concerning the global/annual time scale and seasonal cycle are robust. We also note that our diagnostic is model dependent so there is inherent difficulty in generalizing results but our use of two very different models yielded the same patterns for atmospheric flux adjustments. To be sure, the data assimilation problem refers to a "best" estimate projected onto a given model's basis and is thus diagnostics of data assimilation systems are inherently model dependent. We had emphasized this in our original conclusions section along with the need for independent confirmation with other models. We further clarify this point in the revised manuscript.

In summary, we appreciate the thoughtful and thought-provoking comments of the Reviewer and we feel that in the course of addressing the questions raised by the Reviewer, the manuscript has been significantly improved.

GENERAL COMMENTS

- The use of CO_2 flux signal to denote the cumulative impact of the flux corrections/adjustments in the atmosphere is a bit misleading. A flux signal gives the impression that it is associated to a process or phenomenon, while here it just reflects a correction (or analysis increment) which depends on the specific model, prior flux and observation used. I would think that using the term 'posterior atmospheric adjustment' would be a better term to describe the difference between posterior and prior atmospheric distributions of CO_2 or alternatively 'flux correction signal'.

  Response: We struggled with to find a good name for "flux signal" and had considered "analysis increment". However, since it was the flux that was incremented not the concentrations, we thought that term would not work. We also agree that the term "flux signal" is not entirely appropriate as it suggests a physical phenomenon. We like the reviewer's suggestion of "Posterior Atmospheric Adjustment (PAA)" and have replaced the term "flux signal" with PAA in the revised manuscript.

- Spatial variability of flux correction signal in the atmosphere does not necessarily translate in better provision of information by observations nor an improvement in spatial/regional patterns. If the observations are very noisy (e.g. GOSAT has larger errors than the in situ observations assimilated in flux inversion systems) or observations are not homogeneously distributed (e.g. many more data over land than sea as it is the case in northern extratropical regions) then the flux corrections can create artifacts in the zonal variability which increase the zonal variability but are nevertheless not realistic.

  Response: We agree with this point: zonal structures in the flux signal do not necessarily imply that the inversion is capturing the true zonal structures. As the reviewer points out, biases in the observations or artifacts due to the uneven spatiotemporal distribution of the observations could plausibly result in zonal structures in the posterior fluxes. Therefore, since we do not validate the zonal structures introduced by the inversion, we cannot conclude that their presence implies that the GOSAT inversion is better capturing the true zonal structures. Although we do point this out in the previous manuscript (Page 21 lines 12-18, Page 22, line 23-28), there were also some places where we erroneously made this connection and have removed these statements. In addition, we have expanded the text discussing the possibility of spurious results. Here are some details. Newly added text is in red, deleted text is struck-out:

  Page 1, line 9 (Key point 1 was revised to): ~~The potential for GOSAT data to better resolve zonally asymmetric structures in the tropics year round and in the northern extratropics except during boreal winter is demonstrated.~~ Inversions constrained with GOSAT data introduce zonally asymmetric structures in posterior atmospheric adjustments that exceed those due to uncertain meteorology in the lower troposphere year round in the tropics and outside the boreal winter in the northern extratropics. (RP1,L10-13)

  Page 19, line 23: ~~This suggests GOSAT is capable of picking up finer spatial scales due to the high density of observations in this region when the satellite shifts its view to the northern hemisphere (Figure 2).~~ (RP25,L20-21)

  Page 20, line 18-25: "In the lower troposphere, zonal asymmetry in GOSAT flux signals exceeds that arising from wind field uncertainty except in November, December and January (Figure 1~~7~~6a). However, for in situ data, the zonal structure can only be trusted in boreal summer (June, July and August). Thus the satellite data are potentially able to retrieve fluxes on finer spatial scales than are in situ data through most of the year, but it is important to note that more spatial structure does not mean better spatial structure. Validation of spatial structures in posterior distributions needs to be made against a dense network of independent observations in order to determine if the increased spatial variation is correct. Given the difference in observation densities (Figures 1 and 2), this result is not surprising. The lack of ability of in situ data to produce zonal asymmetry in flux signals that are larger than those arising from uncertainty in wind fields outside of boreal summer may indicate why it has been difficult for flux inversions to regionally attribute sources with this observation network (e.g. Gurney et al., 2002, Peters et al., 2010, Bruhwiler et al., 2011, Peylin et al., 2013)." (RP26,L19-22)

Page 22, lines 2-6: "Zonal standard deviations of the ~~flux signal~~ PAAF (which reveal spatial structures in the zonal direction) are much larger when GOSAT-informed posteriors are used (in the northern extratropics outside of boreal winter and in the tropics throughout the year) (Figure 16, 17). ~~This indicates a potential for GOSAT data to retrieve finer scale fluxes since the accuracy of such finer scale features requires a dense network of independent measurements to validate.~~ (RP28,L22-23)

Page 22, line 18-30: "In situ observations were found to generate zonal standard deviations larger than this minimum level only in boreal summer whereas GOSAT data exceeded this threshold through most of the year (Figure 16, 17). This potential for retrieving finer spatial scales with GOSAT sampling relative to the in situ network makes sense given the density of GOSAT observations (Figure 2) and is consistent with the prediction of Takagi et al. (2014) or Deng et al. (2016). Moreover, the ability to retrieve zonal structure is evident throughout the year in the tropics and in all seasons except boreal winter in the northern extratropics is rather encouraging. However, verifying such finer scales will be challenging given the limited spatial coverage of validating measurements from TCCON or aircraft platforms and temporal and spatial scales resolved may depend on the characteristics of the flux inversion system. Indeed, the current dispute over the enhanced European sinks obtained with GOSAT data (Feng et al., 2016; Reuter et al., 2014; Houweling et al., 2015) indicates that the finer spatial scales retrieved are not necessarily correct and are difficult to validate. It is plausible that spurious zonal structures in the PAAF could be introduced by spatially varying biases in the observations or uneven spatial coverage. However, there is also evidence supporting the ability of space-based observations to recover zonal asymmetries in the CO_2 fields. Liu et al. (2017) use observations from GOSAT and OCO-2 to isolate tropical flux anomalies between continents during the 2015-2016 El Niño event, while Chatterjee et al. (2017) found that zonal asymmetries in XCO_2 anomalies could be isolated during the same El Niño event. Furthermore, the fact that the spatial structure seen in ~~flux signals~~ PAAFs obtained with in situ data surpassed the minimum uncertainty level only in boreal summer implies that regional attribution of fluxes may be challenging with the in situ observation network alone when the inversion integrates signals over many seasons." (RP29,L15-19)

Page 23, line-14-15: As noted in response below.

Newly added citations:

Liu et al. (2017): J. Liu et al., Contrasting carbon cycle responses of the tropical continents to the 2015–2016 El Niño. Science 358, eaam5690 (2017).

Chatterjee et al. (2017): A. Chatterjee, Influence of El Niño on atmospheric CO2 over the tropical Pacific Ocean: Findings from NASA's OCO-2 mission. Science 358, eaam5776 (2017)

- The paper would benefit from a better quantification of error reduction at different scales based on TCCON and in situ observations which could be presented in tabular format.
  Response: Given that there are only 14 TCCON stations available worldwide in our period of study, it is not possible to assess spatial scales with this network. The surface network is more plentiful, but with only around 40 stations reporting hourly, this too will not be enough to compute zonal asymmetry since most of the sites are clustered in Europe and North America. This is why we had stressed (abstract, last line; p.21, lines 14-15; p.22, line 5) that a dense network of independent observations is needed to verify an improvement in spatial scales achieved by any system, but that such a network does not yet exist.

- The fact that the minimal level of uncertainty in the zonal variability associated with imperfect knowledge of winds is around 0.5 ppm and the global zonal variability of flux corrections is of similar magnitude does not make the posterior zonal flux correction pattern is unreliable. The objective of the flux inversion systems is to reduce the uncertainty of the posterior fluxes and the flux corrections on their own do not necessarily reflect the uncertainty reduction. The posterior zonal patterns should be assessed with independent observations and their standard error compared to the minimal level of uncertainty associated with transport.

Response: The reviewer suggests that comparing posterior atmospheric adjustments due to fluxes with adjustments due to imperfect knowledge of winds is not the appropriate comparison. We disagree. The posterior atmospheric adjustment due to flux increments can and should be compared to the atmospheric adjustment due to uncertain meteorology and this can lead to new insights on the information provided by different observing systems. This becomes clear when we look at the mathematical definitions. Let us first define an atmospheric transport model (*T*) that integrates an initial state for CO_2 (c_0), a set of surface fluxes ($s_{0,n-1}$) and a set of meteorological fields ($x_{0,n-1}$) to yield a CO_2 distribution at time step *n*:

$$c_n = T\left(x_{0,n-1}, c_0, s_{0,n-1}\right). \qquad (1)$$

Subscripts refer to time steps and the model integration starts at time step 0 and yields a final CO_2 state at time step *n*. The posterior atmospheric adjustment (using the Reviewers' suggested name above) is simply the difference between the constituent distribution obtained with posterior fluxes and that obtained with prior fluxes:

$$\Delta c_n = T\left(x^a_{0,n-1}, c^a_0, s^a_{0,n-1}\right) - T\left(x^b_{0,n-1}, c^b_0, s^b_{0,n-1}\right) \qquad (2)$$

The superscripts *a* in (2) can be viewed as the "after adjustment" values and the superscript *b* refers to the before adjustment value. Note that (2) is a general form which allows for the adjustment of the initial concentrations (c_0), and imperfect meteorological states ($x_{0,n-1}$) at the same time that the fluxes are adjusted. Because initial concentrations are not adjusted in our GEOS-Chem flux inversions, we ignore the impact of potential variations of c_0 on Δc_n. However, we allow for the possibility that the meteorological states are not perfect. Thus $x^a_{0,n-1}$ is a set of meteorological states which are perturbed by realizations of meteorological analysis error (computed as explained in our supplemental section, using our operational Ensemble Kalman filter). Then (2) can be written as:

$$\Delta c_n = T\left(x^a_{0,n-1}, c^a_0, s^a_{0,n-1}\right) - T\left(x^a_{0,n-1} - \varepsilon_{0,n-1}, c^a_0, s^a_{0,n-1} - \Delta s_{0,n-1}\right) \quad (3)$$

Now, expanding (3) in Taylor series reveals that to first order, the posterior atmospheric adjustment has two components

$$\Delta c_n \cong \Delta c^s_n + \Delta c^x_n \qquad (4)$$

where

$$\Delta c^s_n = T\left(x^a_{0,n-1}, c_0, s^a_{0,n-1}\right) - T\left(x^a_{0,n-1}, c_0, s^b_{0,n-1}\right) = PAAF \qquad (5)$$

$$\Delta c^x_n = T\left(x^a_{0,n-1}, c_0, s^a_{0,n-1}\right) - T\left(x^b_{0,n-1}, c_0, s^a_{0,n-1}\right) = PAAM \qquad (6)$$

PAAF is the component of PAA due to flux adjustments while PAAM is the component of PAA due to uncertain meteorology. PAAF is computed by integrating the transport model with a set of posterior fluxes and again with the prior fluxes but both integrations use the same set of meteorological analyses ($x^a_{0,n-1}$) and initial concentrations. However, this is only one component of the posterior flux adjustment because the meteorological analyses are not perfectly known, and we can simulate that uncertainty by perturbing the meteorological analyses with realizations of meteorological analysis error (see supplemental material). In other words, for a given set of fluxes, the meteorological fields could have been slightly different but equally valid in the context of the meteorological analysis errors. This is what PAAM defines and it is computed by integrating the model twice (with perturbed and unperturbed meteorology) for a given set of posterior fluxes and where we again use the same initial concentrations in both integrations. A novel aspect of our work is the ability to compare the component of posterior atmospheric adjustment due to flux increments (PAAF) with that due to meteorological uncertainty (PAAM). If the PAA component due to flux increments alone (PAAF) does not exceed the component due to meteorological errors (PAAM), then it is not the dominant contribution in (5) and should not be accorded great significance.

In summary, a novel aspect of our work is the ability to compute two components of PAA with our coupled meteorological and tracer transport model. This comparison provides new insights into the atmospheric adjustments arising from flux increments associated with different types of observing systems. This information is complementary to direct comparisons of posterior CO_2 distributions to measurements made with a single set of meteorological analyses.

In the revised manuscript, the PAA is now defined mathematically in a new section (2.3). This greatly clarifies the arguments and results presented in our manuscript.

SPECIFIC COMMENTS

- Page 7, Line 14: Isn't the uncertainty of 22% associated with NEE very low?

Response: The uncertainty of 22% is applied to both GPP and Respiration because these are the quantities that are optimized in the GEOS-Chem inversion. These quantities are significantly larger than NEE. So too are their uncertainties.

- Page 7, Line 19: I would not call GOSAT coverage "dense".

Response: We changed "dense" to "more dense" since it is fair to say GOSAT coverage is more dense than the surface network. (RP9,L12)

- Page 8, Lines 2-3: "Note that ... " sentence is not clear.

Response: We clarified this statement from "Note that posterior fluxes contain total fluxes from unoptimized as well as optimized fluxes." To "Note that posterior fluxes contain the total of all optimized (GPP, Respiration, ocean, biomass burning and anthropogenic) fluxes and the small amount of un-optimized fossil fuel emissions from shipping (~0.19PgC/yr) and aviation (~0.16PgC/yr)." (RP9,L31-32 to RP10,L1-2)

- Page 9: Please provide a quantitative estimate of standard error and bias per month/season for the surface in situ evaluation in order to assess the seasonal cycle quantitatively. When the bias is shown to be smaller, it would help to know by how much

Response: This is a good suggestion. Table 2 was added to the manuscript. It contains the seasonally aggregated statistics (means and standard deviations) for 6 seasons used in the TCCON figures and table, for the four experiments (two models forced by posterior fluxes from GEOS-Chem inversions with GOSAT or in situ data). This new table is indeed helpful to the discussion of Figure 4 (revised Figure 5) on page 9 (RP13-14).

- Page 10, Line 2, Page 11, Line 23: Is the flux correction signal in the atmosphere "propagated" or "transported"?

Response: In the first instance, we changed "…before considering the vertical propagation of the flux signal in section 3.2." to "…before considering the vertical structure of the PAAF in section 3.2." (RP15,L6-7). In the second instance, we changed "…flux signal then propagates vertically…" to "flux perturbation is then vertically transported…" (RP17,L4-5)

- Page 12, Line 16: Why is GOSAT reducing meridional gradient? From Figs 8 and 10 it looks that the meridional gradient from the GOSAT posterior fluxes is worse than that from the in situ data.

Response: From our study, we cannot say why the meridional gradient is worse than that from the in situ data, but we noted here (page 3, line 19 and page 10, line 22) that other studies have seen the same thing. We also noted in Polavarapu et al. (2016, ACP on Page 3, Line 18): "It has been suggested that the GOSAT-based inversions shift some uptake from North Africa to Europe which reduces the north-south gradient in CO_2 and reduces agreement with observations (Houweling et al., 2015)"

- Page 14, Lines 22-25: How do you reconcile this with the larger bias of GOSAT versus TCCON in SH?

Response: It is difficult to reconcile the larger bias of GOSAT-based CO_2 distributions with TCCON in the southern hemisphere sites in all seasons (relative to CO_2 distributions informed by in situ data) (Figure 9) with the lower bias when compared to HIPPO3 data (Figure 10). However, we can speculate that it is due to difference in specific locations sampled by the two measurement networks. In addition, transport error does play a role because HIPPO comparisons using GEM-MACH-GHG are consistent with the TCCON results (Figure S12). Note that comparisons to independent surface (continuous) sites in the southern hemisphere also show a larger bias for GOSAT-based posteriors even with GEOS-Chem (e.g. at South Pole in new Table 2). For example, in Figure R1, we show monthly statistics from Cape Matatula for GEOS-Chem integrations (top panel) and GEM-MACH-GHG integrations (lower panel). This is also consistent with the TCCON results of Figures 8 and S11. Because there are some results that we cannot reconcile, we made conclusions based only on the results that are consistent. What is consistent is that lower CO_2 values are produced with in situ-constrained fluxes in both comparisons and both models and for long (12 or 18 month) time averages, CO_2 fields forced by in situ-based posteriors agree better with independent measurements.

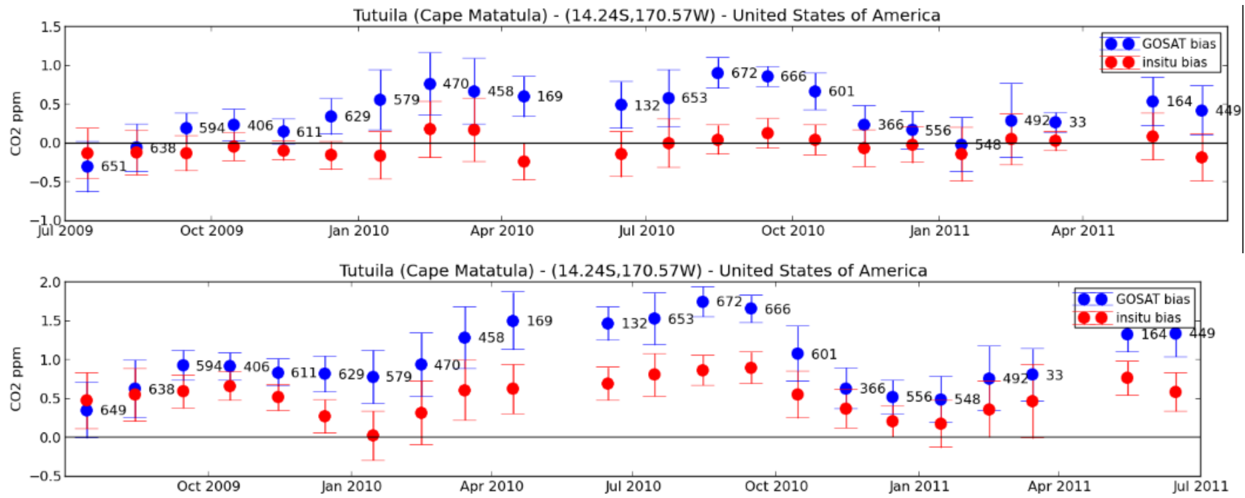

Figure R1: Comparison of model and in situ hourly observations at NOAA's Cape Matatula site with GEOS-Chem (top panel) and GEM-MACH-GHG (bottom panel). All observations (including night time) are used in statistics. The whiskers correspond to one standard deviation and the number to the right of each dot is the number of observations used in each calculation. Both GEM-MACH-GHG simulations produce more CO2 than the corresponding GEOS-Chem simulations due to transport error mismatches. For both models, in situ informed posterior distributions better match measurements.

- Page 16, Line 2: How do you explain that GOSAT produces better fit with observations in middle to upper troposphere in boreal winter?

Response: We can only speculate on this. We saw that in situ posteriors better match TCCON total columns at all times except boreal summer (Figs. 9, S11) and, on long time scales, they better match both TCCON (Figs. 8, S10) and NOAA aircraft profiles (Fig. S13). However, seasonal anomalies are better captured with GOSAT posteriors (Table S1) and there is seasonal variation to the agreement with the aircraft profiles (Figs. 11, S14). So, it is possible that the better fit of GOSAT posteriors to aircraft profiles is specific to the winter season, for North America. We cannot speculate on a reason for this. However, Figure 18 shows that zonal asymmetries (standard deviations) in CO_2 adjustments are well below those due to meteorological uncertainty (Fig. 18b,c) for the northern extratropics in boreal winter. So for the whole zonal band, zonal asymmetries (e.g. results for North America only) are not robust because they are likely sensitive to transport error.

- Page 21, Lines 11-18: The message that GOSAT observations have the potential benefit of improving the zonal structure seems to be contradicted by the results from flux inversions using GOSAT data published in Houwelling et al (2015). Therefore, the conclusion of the potential benefit of GOSAT highlighted in the abstract can be misleading.

Response: We did note that the "potential benefit" aspect is contradicted by the Howelling result a few lines later in the same paragraph. However, we revised the abstract to better correspond to the revised manuscript which focuses on our new diagnostic and its potential utility for understanding flux inversion results.

- Page 23, Line 15: "GOSAT better captures zonally asymmetric structure ..." should be rephrased as this has not been proven in the paper.

Response: The reviewer is correct. We only showed that there was more zonally asymmetric structure, not that it was better. We changed the statement to "GOSAT better captures the seasonal cycle at northern extratropical TCCON sites." (RP30,L6)

- Page 23, Lines 24-27: Note that this type of comparison has already been done by Locatelli et al. (2013, ACP) for CH4.

Response: What Locatelli et al. (2013, ACP) did was to use 10 different transport models with identical initial conditions and prior fluxes to simulate observations which were then used in an inversion system with a single model. Their experiment includes transport errors in the synthetic observations which are then assimilated with the reference inversion system. While this is an interesting and useful method of exploring transport error impact on flux estimation, what we suggested in the text was rather different. Instead of forcing different models to use specific initial conditions or fluxes, we simply suggest taking the results (posterior fluxes) from different inversion models and integrating them all with a reference transport model. This will create a convolution of transport model errors from the inversion model and the reference model (as seen in our work). If transport characteristics of the reference transport model are known, relative transport errors of the flux inversion models can be inferred, to some extent. Obviously, there are limitations with this method since it is *relative* transport errors that are obtained, but since it is very easy to do (does not require a common protocol), we suggest that it is worth considering.

- Page 24, Line 10: .. seasonal correlation of "error" covariances.
Response: Corrected. (RP31,L2)

- Figure 4 and Page 9: It would be good to include GEOS-Chem in Fig. 4.
Response: We agree that because of the content of the discussion in the text, it would be good to have curves corresponding to both models on the same plot. However, there would be too many curves if all the existing ones were retained. Therefore, we have modified Figure 4 (revised Figure 5) to show the GEM-MACH-GHG and GEOS-Chem posterior CO_2 distributions obtained with in situ data compared to observed time series. The analogous figure for posterior CO_2 distributions obtained with GOSAT posterior fluxes is not shown but the newly added Table 2 (as suggested by the Reviewer in specific comment on page 9) supports the discussion concerning both types of posterior fluxes. We also now use the quality flags on the observed data and show only those not flagged as suspicious. The text on page 9 was modified accordingly. (RP13-14)

Response to Reviewer 2

Original text is in black. Our responses are in blue text. References to the revised text take the following format: RP78,L54-55 (Revised Page 78, Lines 54-55). The reference are for the manuscript with changes tracked.

According to my understanding, this manuscript addresses two major topics. The first is how adjustments to surface fluxes (posterior minus prior) manifest themselves in the atmosphere. This is done by performing inversions for the first two years of GOSAT data using a variational GEOS-Chem system, and propagating the posterior and prior fluxes through a transport model. Along the way, the authors perform some evaluation of their inverse results, such as comparison to TCCON and HIPPO. The second is how that manifestation varies if a different higher resolution online atmospheric transport model is used. In my opinion, the authors spend too much time on the first topic and not enough on the second, which makes the work not significant enough for a journal like Atmospheric Chemistry and Physics. If this focus were reversed, or the first topic were explored further (explained below), it would make for a much more interesting and scientifically significant paper. The authors perform inversions of GOSAT and in situ data for two years, and look at the fluxes and resultant atmospheric CO_2 fields in the first two years of GOSAT, primarily focusing on 2010. They use a variational inversion technique using the GEOS-Chem transport model. Their conclusions are very similar to previously published literature, such as Houweling et al (2015), Basu et al (2013), Chevallier et al (2014), which they cite. In fact, a very similar (if not identical) set of inversions was already submitted by some of the co-authors to an intercomparison of GOSAT inversions published by Houweling et al (2015). As far as I can tell, there is nothing new or unique about their inversion or analysis compared to the multitude of GOSAT inversions already published for 2010, and this part of the work does not add to the body of existing knowledge about GOSAT retrievals and derived fluxes in and around 2010. GOSAT has been up for eight years now, and retrievals of column CO_2 from GOSAT exist for the majority of that period. I do not understand why the authors have limited their study to the first couple of years of GOSAT data. If the authors want to publish a GOSAT inversion study that would be of value to the scientific community, I would recommend performing a longer term study, such as (say) the inter-annual variability of fluxes as seen by GOSAT, or the longer term trends in atmospheric CO2 and CO2 fluxes as seen by GOSAT. The current inversion study, focused on 2010 (with some padding on either side), is of limited interest. The second thread in their work, however, is more interesting. They perform forward runs with two different models of atmospheric transport driven by the same fluxes and look at the difference in the "flux signal" in the atmosphere. The non-GEOS-Chem model is the higher resolution GEM-MACH-GHG, a fairly new addition to this community (Polavarapu et al, 2016). Not only did they transport CO_2 with GEM-MACH-GHG, they also perturbed the transport with analysis errors from the meteorological assimilation system, thereby simulating the impact of uncertainties in the met fields on CO_2 variations. They derive a "baseline" CO_2 variation from this error propagation, contending that variations smaller than this detected by an observing system cannot be reliably ascribed to fluxes. This, to my knowledge, is fairly unique in the tracer transport community, and provides a recipe for deriving transport errors in CO_2 space. Such errors can be used, e.g., if GEM-MACH-GHG or a derived offline model is used for trace gas inversions. This technique may also be valid for deriving "baseline" transport errors for an offline model if an ensemble is run for the parent model with greenhouse gases (e.g., GEOS5 for GEOS-Chem).

If the authors would like to revise their manuscript and make it scientifically significant enough for this journal, I can offer two different suggestions. Either they need to extend their GOSAT analysis to 5+ years and address questions such as long term trends and interannual variability of CO_2 fluxes. Or they need to more or less excise the GOSAT inversions and focus on the performance of GEM-MACH-GHG in simulating atmospheric CO_2 and its meteorological errors. For the first choice, I would suggest questions such as:

1. Do GOSAT retrievals estimate a stronger European sink consistently over time, as first suggested by Reuter et al (2014) with SCIAMACHY and a single year of GOSAT data?
2. Do GOSAT retrievals require a stronger northern hemisphere uptake consistently, as noted by Houweling et al (2015) for one year?
3. According to GOSAT, which region contributes most to the interannual variability of atmospheric CO_2, the Tropics or semi-arid ecosystems? This has been an ongoing debate in the atmospheric carbon community, see e.g., Baker et al (2006), Poulter et al (2014) and Ahlström et al (2015).
4. Are there persistent differences between GOSAT and surface data inversions across multiple years?

These are just some suggestions, and I'm sure the authors can think of many such questions to address with a multi-year GOSAT inversion. On the other hand, if the authors choose to focus on GEM-MACH-GHG, then that would make for a very interesting paper as well. The authors have already addressed some of the interesting questions that arise from using a high resolution online model for CO_2 transport. Some additional questions could be:

1. Are high frequency variations of CO_2 near the surface better represented by the higher resolution model? If yes, we could potentially move to assimilating more data from surface measurement sites in the future with online models such as GEM-MACH-GHG.
2. Can one construct a "look up table" for the baseline transport-driven errors using GEM-MACH-GHG, varying (say) by region and season? How do those errors differ between surface and total column measurements? I'm looking for something like Figure 17, but much finer grained than three zonal bands. At the very least, ocean sites, coastal sites and continental sites should be separated. Similarly, for total column measurements, ocean and land soundings should be separated.
3. If inversions were performed using errors from step 2, versus more traditional prescription of errors, how do the fluxes change?
4. Is it true that transport errors matter less in assimilating a total column than assimilating surface sites or a vertical profile? This was first suggested by Rayner & O'Brien (2001), but to my knowledge never explicitly demonstrated. The crucial thing to compare here would be the size of the transport error and the size of the flux signal, since that is small as well in the total column.
5. Is there any covariance between transport error and CO_2 variation, especially along weather fronts? This has also been a topic of much debate, especially whether assimilating high frequency CO_2 measurements can improve weather forecasts (Engelen et al, 2001), and whether CO_2 inversions need to assimilate met observations. Again, these are just some suggestions, and I'm sure the authors could come up with an interesting set of questions relevant to the atmospheric CO_2 community that they could answer with GEM-MACH-GHG.

Response: We are grateful to the Reviewer for the comments and suggestions. It is clear from the comments that the organization of our original manuscript led to some confusion about the focus of the manuscript. Specially, the main focus of the manuscript is on the new diagnostic associated with the posterior atmospheric CO_2 adjustment. We felt that it was necessary to provide a thorough evaluation of the posterior fluxes so that the reader would be able to interpret the main results of the work. As we noted in our manuscript, our fluxes are for the most part documented in the literature. Nevertheless, it would be impossible for us to proceed without describing them (at least briefly) here for two reasons. (1) Modeling and data assimilation systems are constantly changing and improving. Because of the passage of time, the inversions done here are close to but not identical to those shown in Deng et al. (2014, 2016). It is therefore important to assure the reader that our inversion results are understandable and reasonable. (2) The flux inversion estimates under study here were described in two separate papers (Deng et al. 2014, 2016) and the two inversions results were never presented together. Because the main part of the paper compares the impact of these two posterior fluxes on atmospheric distributions, it is useful to see them in a side-by-side comparison. Furthermore, we felt that it would be unreasonable to expect the reader to be familiar with both Deng et al. papers to be able to interpret the results presented in the manuscript. However, we acknowledge the Reviewer's concern and have shortened the discussion of the flux inversion results in section 3.1 to only those remarks necessary for understanding the later sections. Specifically, we stick to only a discussion of zonally averaged fluxes. Figure S6 replaces Figures 5 which was moved to the supplemental material. Figure 6 was deleted. We also now explicitly state that the reasons for very briefly describing the posterior fluxes.

Another reason we felt that it was necessary to go into detail about the evaluation of the flux inversions is because our diagnostic is based on atmospheric adjustments from a prior distribution, therefore, when we compare adjustments from multiple posterior fluxes, we cannot determine which is more "correct". However, we can infer which is "better" by comparing posterior CO_2 fields to measurements. Thus, the comparisons to observations is not done to validate the fluxes, but rather to inform the discussion of the posterior atmospheric adjustments resulting from the fluxes. The importance of these comparisons is recognized by Reviewer 1 since his/her comments primarily focus on improving the discussion related to validation of the posterior CO_2 distributions. In retrospect, the narrative in the original manuscript may have been deficient in this regard. However, in the revised manuscript, the focus of our work is squarely on the new diagnostic and its potential value for learning about flux inversion results. This involved rewriting the abstract and revising portions of the introduction and discussion sections as well as adding explanatory sentences throughout the results section. Finally, we appreciate the enthusiastic comments from the Reviewer regarding our new approach of comparing posterior atmospheric adjustments due to fluxes with those due to meteorological uncertainty.

In summary, as a result of the Reviewer's comments, we have rewritten portions of the manuscript to improve clarity and to focus on our main points: the introduction of a new diagnostic which is useful for studying flux inversion model results.

Other comments

1. The prior fluxes in Figure 5 look strange. It is rare for me to see a terrestrial flux prior that is positive in the annual aggregate over North America, and Boreal and Temperate Eurasia. Where do those priors come from?

Response: As mentioned in Deng et al. (2014), the priors come from the Boreal Ecosystem Productivity Simulator (BEPS) model (Chen et al. 1999) driven by NCEP reanalysis data and remotely sensed leaf area index. Deng and Chen (2012) scaled the hourly GPP and Respiration (RSP) to generate a set of GPP and RSP that are annually neutral for each grid box as priors for atmospheric inversion modeling. The positive priors mentioned here is/are caused by adding the biomass burning emissions. The addition of biofuel and biomass burning sources to the natural fluxes was noted in the caption for Figure 5. However, this figure was moved to the supplementary section (Figure S6) in the revised manuscript.

Chen, J. M., Liu, J., Cihlar, J., and Goulden, M. L.: Daily canopy photosynthesis model through temporal and spatial scaling for remote sensing applications, Ecol. Model., 124, 99–119, 1999.

2. In Figure 7, I would prefer to see time averages, say over a week or month, instead of snapshots. Snapshots often display misleading variations that do not matter for what the authors are considering. This comment only holds, of course, if an equivalent of Figure 7 still exists in the revised manuscript.

Response: In general, time averages are typically preferred for the reasons the reviewer presents. However, in our manuscript, we need snapshots and not time averages. Figure 7 is an encapsulation of the full time animations provided in the supplemental material. The evolution of the flux signal reveals interesting differences and hints at transport pathways that are explored in the section on adjoint sensitivity (and Figure 12). The time evolution of the animations (which the snapshots summarize) also corresponds to the time evolution of flux signals seen in later figures (Figures 13-18). Furthermore, the qualitative consistency of differences between the two types of flux signals across the two years, given that these are snapshots, is additional useful information.

3. I was surprised to see no data providers as co-authors in an inverse modeling paper. It is usual in this field to offer co-authorship to data providers, which they may or may not accept. In fact the ObsPack fair use policy explicitly states:

> *"Your use of this data product implies an agreement to contact each contributing laboratory to discuss the nature of the work and the appropriate level of acknowledgment. If this product is essential to the work, or if an important result or conclusion depends on this product, co-authorship may be appropriate. This should be discussed with each data provider at an early stage in the work. Contacting the data providers is not optional; if you use this data product, you must contact the data providers."*

Were the data providers contacted, at the very least to let them know that an inversion study using their data was about to be submitted? If not, that is a significant oversight that needs to be corrected.

Response: We are well aware of protocols for data usage and we fully appreciate the dedication and effort (by our close colleagues and by all measurement scientists) required to make high quality measurements. For that reason, we always try to acknowledge the expertise and effort required to make measurements and to provide them to researchers. Here are some specific details, regarding this manuscript.

a) TCCON. Some of our authors are co-located with TCCON PI Kim Strong at the University of Toronto. As with previous work, we contacted all TCCON PIs whose data appears in the tables and Figures. We also had discussions with Kim Strong about Eureka data, but we had no requests from any TCCON PIs for co-authorship. This is the same procedure and same result we got in our previous article (Polavarapu et al. 2016, ACP). The references for all 14 sites were cited in the text and all PIs were thanked in the acknowledgements.

b) HIPPO. We contacted Steve Wofsy by email (21 March 2017) and received no reply. This was also the case with our previous publication. (Also, in the case of the Deng et al. (2016) manuscript, Steve Wofsy declined co-authorship.) In the absence of a reply for this manuscript, we referenced his papers and the dataset DOI and added an acknowledgement. Note that the data usage protocol found at https://www.eol.ucar.edu/system/files/HIPPO_Full_Data_Policy_lah_20170915_1.pdf requests only the following: (1) Acknowledge with references and use the DOI number, (2) Acknowledge NSF and NOAA in the acknowledgements, (3) add "HIPPO, HIAPER Pole-to-Pole Observations, National Science Foundation, NSF, NSF/NCAR Gulfstream-V (GV)" to keywords. Note that we had done all of these in the original manuscript.

c) NOAA aircraft profiles. We contacted Colm Sweeney by email (8 Nov 2017) and provided the manuscript, figures and supplemental material and received no response. In the absence of a response, we cited his publications, added an acknowledgement to him, and submitted the manuscript on 29 Dec 2017. NOAA aircraft profiles were obtained from ObsPack2013 which was acknowledged as noted in (d).

d) NOAA surface measurements. For ObsPack, the contact in the datafiles mentioned is Ken Masarie. But we heard from NOAA colleagues that Ken had retired. Therefore, we contacted Arlyn Andrews (8 Nov 2017). Again, we provided the manuscript, figures and supplemental information. We did not get a reply. In the absence of a response, we cited Conway and Tans (2012), Conway et al. (2011), Masarie et al. (2014) and the DOI (http://dx.doi.org/10.3334/OBSPACK/1001).

4. I have a problem with the terminology "flux signal", even though the authors made the explicit caveat that this "signal" by definition depends on the inverse model and the prior. The term "flux signal" makes it sound like it's an inherent property of the observations, which it is not. I would recommend using a different term, such as "CO_2 adjustment" or "mole fraction update".

Response: Reviewer 1 had exactly the same concern and suggested an alternative expression which we like: "Posterior Atmospheric Adjustment". We adopted this new terminology and its acronym (PAA) in the revised manuscript.

References

A. Ahlström, M. R. Raupach, G. Schurgers, B. Smith, A. Arneth, M. Jung, M. Reichstein, J. G. Canadell, P. Friedlingstein, A. K. Jain, E. Kato, B. Poulter, S. Sitch, B. D. Stocker, N. Viovy, Y. P. Wang, A. Wiltshire, S. Zaehle, and N. Zeng, "The dominant role of semi-arid ecosystems in the trend and variability of the land CO2 sink," Science (80-.)., vol. 348, no. 6237, 2015.

D. F. Baker, R. M. Law, K. R. Gurney, P. Rayner, P. Peylin, A. S. Denning, P. Bousquet, L. Bruhwiler, Y.-H. Chen, P. Ciais, I. Y. Fung, M. Heimann, J. John, T. Maki, S. Maksyutov, K. Masarie, M. Prather, B. Pak, S. Taguchi, and Z. Zhu, "TransCom 3 inversion intercomparison: Impact of transport model errors on the interannual variability of regional CO2 fluxes, 1988-2003," Glob. Biogeochem. Cycles, vol. 20, no. 1, p. GB1002, Jan. 2006.

S. Basu, S. Guerlet, A. Butz, S. Houweling, O. Hasekamp, I. Aben, P. Krummel, P. Steele, R. Langenfelds, M. Torn, S. Biraud, B. Stephens, A. Andrews, and D. Worthy, "Global CO2 fluxes estimated from GOSAT retrievals of total column CO2," Atmos. Chem. Phys., vol. 13, pp. 8695–8717, 2013.

F. Chevallier, P. I. Palmer, L. Feng, H. Boesch, C. W. O'Dell, and P. Bousquet, "Toward robust and consistent regional CO2 flux estimates from in situ and spaceborne measurements of atmospheric CO2," Geophys. Res. Lett., vol. 41, no. 3, pp. 1065–1070, 2014.

R. J. Engelen, G. L. Stephens, and A. S. Denning, "The effect of CO2 variability on the retrieval of atmospheric temperatures," Geophys. Res. Lett., vol. 28, no. 17, pp. 3259–3262, 2001.

S. Houweling, D. Baker, S. Basu, H. Boesch, A. Butz, F. Chevallier, F. Deng, E. J. Dlugokencky, L. Feng, A. Ganshin, O. Hasekamp, D. Jones, S. Maksyutov, J. Marshall, T. Oda, C. W. O'Dell, S. Oshchepkov, P. I. Palmer, P. Peylin, Z. Poussi, F. Reum, H. Takagi, Y. Yoshida, and R. Zhuravlev, "An intercomparison of inverse models for estimating sources and sinks of CO2 using GOSAT measurements," J. Geophys. Res. Atmos., vol. 120, no. 10, pp. 5253–5266, 2015.

S. M. Polavarapu, M. Neish, M. Tanguay, C. Girard, J. de Grandpré, K. Semeniuk, S. Gravel, S. Ren, S. Roche, D. Chan, and K. Strong, “Greenhouse gas simulations with a coupled meteorological and transport model: the predictability of CO2,” Atmos. Chem. Phys., vol. 16, no. 18, pp. 12005–12038, 2016.

B. Poulter, D. Frank, P. Ciais, R. B. Myneni, N. Andela, J. Bi, G. Broquet, J. G. Canadell, F. Chevallier, Y. Y. Liu, S. W. Running, S. Sitch, and G. R. van der Werf, “Contribution of semi-arid ecosystems to interannual variability of the global carbon cycle.,” Nature, vol. 509, no. 7502, pp. 600–3, May 2014.

P. J. Rayner and D. M. O’Brien, “The utility of remotely sensed CO2 concentration data in surface source inversions,” Geophys. Res. Lett., vol. 28, no. 1, pp. 175–178, 2001.

M. Reuter, M. Buchwitz, M. Hilker, J. Heymann, O. Schneising, D. Pillai, H. Bovensmann, J. P. Burrows, H. Bösch, R. Parker, A. Butz, O. Hasekamp, C. W. O’Dell, Y. Yoshida, C. Gerbig, T. Nehrkorn, N. M. Deutscher, T. Warneke, J. Notholt, F. Hase, R. Kivi, R. Sussmann, T. Machida, H. Matsueda, and Y. Sawa, “Satellite-inferred European carbon sink larger than expected,” Atmos. Chem. Phys., vol. 14, no. 24, pp. 13739–13753, 2014.

A comparison of posterior atmospheric CO_2 ~~flux signal~~adjustments obtained from ~~GEOS-Chem~~ in situ and GOSAT constrained flux inversions ~~constrained by in situ or GOSAT observations~~

Saroja M. Polavarapu[1], Feng Deng[2], Brendan Byrne[2], Dylan B. A. Jones[2], Michael Neish[1]

[1]Climate Research Division, Environment and Climate Change Canada, Toronto, Ontario, M3H 5T4, Canada
[2]Dept. of Physics, University of Toronto, Toronto, Ontario, M5S 1A7, Canada

Correspondence to: Saroja Polavarapu (saroja.polavarapu@canada.ca)

Key points:

1. ~~The potential for GOSAT data to better resolve zonally asymmetric structures in the tropics year round and in the northern extratropics except during boreal winter is demonstrated.~~ Inversions constrained with GOSAT data introduce zonally asymmetric structures in posterior atmospheric adjustments that exceed those due to uncertain meteorology in the lower troposphere year round in the tropics and outside the boreal winter in the northern extratropics.
2. ~~In the lower troposphere, zonal asymmetries in the flux signal exceed that arising from meteorological uncertainties only in boreal summer, when in situ data constrain posterior fluxes.~~Inversions constrained with in situ data produce zonal asymmetries in posterior atmospheric adjustments in the lower troposphere that exceed those arising from meteorological uncertainties only in boreal summer.
3. The ~~GEOS-Chem~~ flux inversion constrained by in situ data better agrees (by 0.5 ppm) with independent observations on the global annual scale compared to the inversion constrained with GOSAT observations but the inversion with GOSAT data better captures the seasonal cycle of CO_2 at northern extratropical TCCON sites.

Keywords: data assimilation, carbon dioxide, GOSAT, CO_2 flux estimation, greenhouse gas sources and sinks, HIPPO, HIAPER Pole-to-Pole Observations, National ScienceFoundation, NSF, NSF/NCAR Gulfstream-V (GV).

Abstract. The CO_2 flux signal is defined as the difference of the four-dimensional CO_2 field obtained by integrating an atmospheric transport model with posterior fluxes and that obtained with prior fluxes. It is a function of both the model and the prior fluxes and it can provide insight into how posterior fluxes inform CO_2 distributions. Here, we use the GEOS-Chem transport model constrained by either GOSAT or in situ observations to obtain two sets of posterior flux estimates in order to compare the flux signals obtained from the two different observing systems. Flux signals are also computed using two different models. The global flux signal in the troposphere primarily reflects the northern extratropics whereas the global flux signal in the stratosphere mainly reflects tropical contributions. While both observing systems constrain the global budget for 2010 equally well, stronger seasonal variations of the flux signal are obtained with GOSAT. Posterior CO_2 distributions obtained with in situ observations better agree with TCCON measurements over an 18-month time period, but GOSAT-informed posterior fluxes better constrain the seasonal cycle at northern extratropical sites. Zonal standard deviations of the flux signal exceed the minimal value (defined by uncertainty in meteorological analyses) through most of the year when GOSAT observations are used, but when in situ observations are used, the minimum value is exceeded only in boreal summer. This indicates a potential for flux estimates constrained by GOSAT data to retrieve spatial structures within a zonal band throughout the year in the tropics and through most of the year in the northern extratropics. Verification of such spatial structures will require a dense network of independent observations.

Posterior fluxes obtained from inverse modeling are difficult to verify because there is no dense network of flux measurements available to evaluate estimates against. Here we present a new diagnostic to evaluate structures in posterior fluxes. First, we simulate the change in atmospheric CO_2 fields between posterior and prior fluxes, referred to as the posterior atmospheric adjustments due to updated fluxes (PAAF). Second, we calculate the uncertainty in atmospheric CO_2 fields due solely to uncertainty in the meteorological fields, referred to as the posterior atmospheric adjustments due to imperfect meteorology (PAAM). We argue that PAAF can only be considered robust if it exceeds PAAM, that is, the changes in atmospheric CO_2 between the posterior and prior fluxes should at least exceed atmospheric CO_2 changes arising from imperfect meteorology. This diagnostic is applied to two CO_2 flux inversions: one which assimilates observations from the in situ CO_2 network and the other which assimilates observations from the Greenhouse Gas Observing SATellite (GOSAT). On the global scale, PAAF in the troposphere reflects northern extratropical fluxes whereas stratospheric adjustments primarily reflect tropical fluxes. In general, larger spatiotemporal variations in PAAF are obtained for the GOSAT inversion than the in situ inversion. Zonal standard deviations of the PAAF exceed the PAAM through most of the year when GOSAT observations are used, but the minimum value is exceeded only in boreal summer when in situ observations are used. Zonal spatial structures in GOSAT-based PAAF exceed PAAM throughout the year in the tropics and through most of the year in the northern extratropics, suggesting GOSAT flux inversions can constrain zonal asymmetries in

fluxes. However, we cannot discount the possibility that these structures are influenced by biases in GOSAT retrievals. Verification of such spatial structures will require a dense network of independent observations.

1 Introduction

Flux inversion systems have become useful tools for understanding the global carbon budget as evidenced by their presence in Intergovernmental Panel on Climate Change (IPCC) reports (Ciais et al., 2013). However, even with the expansion of the near surface in situ network, limitations remain in the ability to retrieve regional-scale fluxes (Bruhwiler et al., 2011). Thus, with the promise of retrieving fluxes with higher spatial resolution, the first satellite missions dedicated to greenhouse gas measurements from space were launched: the Greenhouse gas Observing SATellite (GOSAT) in 2009 (Kuze et al., 2009) and the Orbiting Carbon Observatory (OCO-2) (Crisp et al., 2015; 2017) in 2014. The expectation was that not only should space-based measurements of column integrated CO_2 offer better spatial coverage, but the column amount should be less sensitive to modelling errors associated with the Planetary Boundary layer (PBL) and its representativeness should better correspond to that of coarse model grids (Keppel-Aleks, 2011). This occurs because mainly long range fluxes are seen in column data whereas both local and long-range flux signals are seen by surface in situ observations (Keppel-Aleks et al., 2011). Thus, space-based measurements of column integrated CO_2 offered the promise of alleviating some of the challenges associated with the assimilation of near surface in situ measurements in flux inversion systems. However, that promise has yet to be realized. Regional flux estimates have not been robust (e.g. Maksyutov et al., 2013; Basu et al., 2013; Chevallier et al., 2014; Deng et al., 2014, Houweling et al., 2015) and they are sensitive to biases in satellite retrievals (Basu et al., 2013, Deng et al., 2014, Takagi et al., 2014). Retrieved ~~fluxes from Europe~~ uptake by the European biosphere is ~~are~~ twice as large in GOSAT inversions compared to in situ inversions (Reuter et al., 2014; 2017), with many studies finding such increased sinks (Houweling et al., 2015; Feng et al., 2016). It has been suggested that the GOSAT-based inversions shift some uptake from North Africa to Europe which reduces the north-south gradient in CO_2 and reduces agreement with observations (Houweling et al., 2015). The issue may also be due to the impact of nonlocal observations in flux inversion systems since biases in upstream CO_2 contribute 60-90% of the European sink (Feng et al., 2016). On the other hand, the uneven spatial coverage of the in situ network may also be playing a role in the discrepancy. Bruhwiler et al. (2011) found that the inclusion of newer European sites results in a large rebalancing of uptake from Europe to boreal Eurasia in comparison to an inversion with existing older sites. Kim et al. (2016) found that after adding Siberian in situ measurements to their inversion system, the carbon uptake in Europe was enhanced while it decreased in the Eurasian boreal TransCom region. The point is that within the context of flux inversion systems, this new type of measurement poses new challenges. These challenges are related to aspects of the data specific to satellite column measurements. For example, biases arise from sampling only clear skies (Corbin et al., 2009; Parazoo et al., 2012) and from the seasonal variation of observational coverage (Liu et al., 2014; Byrne et al., 2017). At the same time, model transport errors remain an issue for inversions using column measurements. Model errors in simulating boundary layer mixing are still important for assimilating column measurements (Lavaux and Davis, 2014), isentropic transport needs to be correctly modelled (Parazoo et al., 2012; Barnes et al. 2016) and model biases in the high latitude upper troposphere can impact the north-south distribution of fluxes (Deng et al., 2015). Thus, it is important to get not only the low level vertical gradients correct in the transport model, but also the upper tropospheric and lower stratospheric distributions that the satellites are sensitive to. Ultimately, the best network will combine surface and satellite measurements (Baker et al., 2006, Basu et al., 2013, Lavaux and Davis, 2014). The question is how to use the different types of observations to their strengths within a given data assimilation system.

The goal of this work is to improve our understanding of how the different types of CO_2 observing systems can inform model simulations of CO_2 by (1) examining the imprint of inversion flux corrections in atmospheric CO_2 and (2) determining if this imprint is larger than CO_2 changes that arise solely from meteorological uncertainties. The imprint of flux corrections in atmospheric CO_2 can be found by simulating the change in atmospheric CO_2 fields between posterior and prior fluxes, which we refer to as the posterior atmospheric adjustments due to updated fluxes (PAAF).

The PAAF assumes that the meteorological fields are known exactly. However, there are known to be significant uncertainties in meteorological fields. For instance, Liu et al., (2011) estimate the uncertainty due to meteorology as 1.2–3.5 ppm at the surface and 0.8–1.8 ppm in a column mean CO_2 fields. This level of uncertainty can be calculated using an online weather and greenhouse gases transport model. Meteorological observations can be assimilated into the analysis to produce an error estimate in atmospheric transport (using an ensemble Kalman filter in our set-up). From this error estimate one can quantify a minimum level of uncertainty in CO_2 distributions arising from imperfect knowledge of wind fields, referred to as posterior atmospheric adjustments due to imperfect meteorology (PAAM). If PAAF is larger than PAAM it implies that the change in atmospheric CO_2 is robust against uncertainties in meteorological fields. Thus, we argue that atmospheric CO_2 adjustments due to retrieved fluxes should at least exceed the minimum level of uncertainty in CO_2 distributions arising from imperfect knowledge of wind fields for subsequent model intercomparisons to be meaningful.

~~The goal of this work is to improve understanding of how the different types of observations (near surface in situ observations versus space-based column measurements) inform model simulations of CO_2. To do this, we examine the flux signal which is defined as the difference between the CO_2 distribution obtained with retrieved fluxes and that obtained with prior fluxes. The flux signal reflects the impact of the observing system as manifested in the posterior fluxes convolved with a time history of atmospheric transport for a given inversion system and is a function of both the model and prior fluxes. In particular~~To illustrate the utility of this new diagnostic, we compare the 3-D structure of the ~~flux signal~~(PAAFs) estimated from the in situ observing network and from GOSAT. Because satellite data are sensitive to the full column of CO_2 concentrations, accurate forward model simulations throughout the troposphere and lower stratosphere are needed in order to be able to correctly attribute model-data mismatch to upstream surface fluxes. Thus we focus on assessing posterior CO_2 distributions at various heights by comparing to observations. In addition, the spatio-temporal evolution of the ~~flux signal~~PAAFs is examined through its global mean evolution, zonal mean structures, and zonal asymmetries. Two different tracer transport models, GEOS-Chem (http://geos-chem.org) and GEM-MACH-GHG (Polavarapu et al., 2016), are used to simulate the propagation of the ~~flux signal~~PAAF. This allows an investigation of the sensitivity of our results to transport errors between the models. ~~An additional benefit of using GEM-MACH-GHG is that we can obtain baseline estimates of uncertainty in the results by determining a "minimal" level of uncertainty in CO_2 distributions arising from imperfect knowledge of wind fields. The idea is that model-simulated CO_2 distributions have uncertainties due to a variety of sources (flux estimation errors, initial concentration field errors, model formulation errors, and wind field errors) but, at the very minimum, they will be impacted by wind field errors which can be substantial. For instance, Liu et al., (2011) estimate the uncertainty due to meteorology as 1.2–3.5 ppm at the surface and 0.8–1.8 ppm in a column mean CO_2 fields.~~ Furthermore, s~~S~~ince GEM-MACH-GHG is a coupled weather and greenhouse gases (GHG) transport model, we are able to determine uncertainties in our diagnostics that arise due to imperfections in meteorological analyses (PAAM). Only when ~~flux signal~~PAAF diagnostics exceed such minimum uncertainty levels do we find potential benefits of a given observing system.

The article is organized as follows. The experimental design is presented in section 2. Here the observations used for assimilation and verification, the transport models and the flux inversion system, are all described. Section 3 presents the results. First the posterior fluxes are briefly compared (section 3.1) before the impact of posterior fluxes on CO_2 distributions is examined (section 3.2). Diagnostics focus on ~~comparison to independent observations of CO_2 and~~ variations of the ~~flux signal~~PAAF on global scales and in three zonal bands. Because PAAF cannot be directly verified, comparisons to independent observations of CO_2 are also made, to inform the discussions of PAAF differences due to the different observing systems. Section 4 summarizes the results and considers their implications and generality.

2 The experimental design

In order to understand how the PAAF~~flux signal~~ retrieved from assimilating atmospheric observations propagates into the vertical, we must first perform some flux inversions. There are two sets of flux inversions performed with the GEOS-Chem model and these are based on either the in situ observation network or on GOSAT column measurements. In order to assess the quality of the CO_2 distributions from the two observing systems, we compare posterior CO_2 distributions to independent measurements that contain some information about the vertical distribution of CO_2, namely, aircraft profiles from measurement campaigns, routine NOAA aircraft profiles and the ground-based column measurement network. These comparisons will inform subsequent discussions of PAAF. Section 2.1 describes the observation systems used in the flux inversions as well as those used for validation of modelled CO_2 distributions. The models used are presented in section 2.2. The posterior atmospheric adjustment and its components (PAAF, PAAM) are defined mathematically ~~while the flux signal and uncertainty estimate calculations are described~~ in section 2.3 while section 2.4 explains how they are computed.

2.1 The observations

The in situ observation network primarily consists of CO_2 mixing ratios measured by a nondispersive infrared absorption technique applied to air samples collected in glass flasks at the NOAA ESRL Carbon Cycle Cooperative Global Air Sampling Network sites (Conway et al., 2011) and at the Environment and Climate Change Canada (ECCC) sampling sites. We use the same 72 NOAA sites and 6 ECCC sites that were used by Deng et al. (2014). **Figure 1** shows the approximate distribution of the insitu observations, as well as the validating observations (described below). Since observing stations may have missing data or may start or stop during the period of interest, the figure is only meant to provide a general idea of the spatial distribution of the in situ observation network. While the coverage is global, the density of the stations is sparse, particularly in the tropics and southern hemisphere. On the other hand, the measurements are accurate, to better than 0.2 ppm (Tans and Thoning, 2016). The CO_2 measurements reflect the influence of local as well as remote sources (Keppel-Aleks et al., 2012; Byrne et al., 2017).

The satellite data used this paper are version b3.4 of the NASA Atmospheric CO_2 Observations from Space (ACOS) GOSAT XCO_2 product, spanning July 2009 to December 2011, and have been bias corrected (Osterman et al., 2013). The ACOS retrievals employ an optimal estimation approach to infer atmospheric profile abundances of CO_2, from which XCO_2 is calculated. The details of the retrieval are described in O'Dell et al. (2012). Takagi et al. (2014) and Deng et al. (2014) showed that the biases of different versions of GOSAT products impact regional flux estimates but Deng et al. (2016) found that version b3.4 inferred fluxes result in CO_2 distributions that compare well to independent measurements. Hence, the XCO_2 data used here are exactly those used in Deng et al. (2016). In addition, Deng et al. (2016) found that assimilating ocean glint measurements in addition to land nadir measurements results in generally improved agreement with independent observations and so both types of GOSAT data are used here also. **Figure 2** shows that, in contrast to the fixed locations of the ground-based in situ observations, satellite observations have a seasonal variation. In particular, in boreal summer when CO_2 uptake by the terrestrial biosphere in the Northern Hemisphere dominates the global CO_2 evolution, observations are dense. In austral summer, the satellite's observational coverage shifts southward and the southern midlatitudes is observed well. Throughout the year, ocean glint measurements observe the tropical oceans and improve the estimation of tropical fluxes (Deng et al., 2016).

Since posterior atmospheric adjustments are not directly verifiable, tThe impact of the inversion results on CO_2 distributions are evaluated by comparing posterior CO_2 fields with atmospheric CO_2 observations from the Total Carbon Column Observing Network (TCCON) (http://tccon.ornl.gov/) (Wunch et al., 2011). At the TCCON sites, solar-viewing ground-based Fourier transform spectrometers are used to measure high-resolution spectra (0.02 cm^{-1}) in the near infrared (3800–15,500 cm^{-1}), from which XCO_2 is retrieved. For the comparisons, we use observations from the current TCCON GGG2014 data set from 14 different sites (Blumenstock et al., 2014; Deutscher et al., 2014; Griffith et al., 2014a,b; Hase et al., 2014;

Kivi et al., 2014; Notholt et al., 2014; Sherlock et al., 2014; Strong et al., 2014; Sussmann and Rettinger 2014; Warneke et al., 2014; Wennberg et al., 2014a,b). While total column measurements can indicate the quality of modelled CO_2 simulations throughout the troposphere, they do not provide information on vertical distributions. For a more direct indication of model performance in the middle and upper troposphere, we also evaluate the inversions using aircraft data from the HIAPER Pole-to-Pole Observations (HIPPO) aircraft campaign (http://hippo.ornl.gov/) as well as NOAA aircraft profiles (Sweeney et al., 2015). Specifically, the 10 s averaged data from the HIPPO-3 campaign (Wofsy et al., 2012, 2011) are used for 24 March to 16 April 2010. The NOAA aircraft profiles were limited to flights over Canada and the continental U.S. during 2010. The model comparisons to TCCON, HIPPO and NOAA aircraft profiles will be used to inform the discussions of posterior atmospheric adjustments in section 3.

2.2 The models

2.2.1 The GEOS-Chem inversion system

The GEOS-Chem 4-dimensional variational (4D-Var) data assimilation system was used to estimate global regional CO_2 fluxes. The GEOS-Chem global 3-dimensional chemical transport model is driven by assimilated meteorological observations from the Goddard Earth Observing System (GEOS-5) of the NASA Global Modeling Assimilation Office (GMAO). The model configuration is the same as that used in Deng et al. (2014). The horizontal resolution of the model is 4° x 5°, with 47 vertical levels extending from the surface to 0.01 hPa. The prior CO_2 fluxes, as described in Deng et al. (2014), include CO_2 fluxes from fossil fuel combustion and cement production from the Carbon Dioxide Information Analysis Center (CDIAC) (Andres et al., 2011), monthly mean shipping emissions of CO_2 from the International Comprehensive Ocean-Atmosphere Data Set (ICOADS) (Corbett, 2004; Corbett and Koehler, 2003; Endresen et al., 2004; Endresen et al., 2007) , 3-D aviation CO_2 emissions (Friedl, 1997; Kim et al., 2007; Wilkerson et al., 2010), a climatology of monthly mean ocean-atmosphere CO_2 flux by Takahashi et al. (2009), biofuel CO_2 emission based on Yevich and Logan (2003), and monthly mean biomass burning CO_2 emissions from the Global Fire Emissions Database version 3 (GFEDv3) from van der Werf et al. (2010). The model includes 3-hourly Terrestrial ecosystem exchange from the Boreal Ecosystem Productivity Simulator (BEPS) (Chen et al., 2012), which was driven by NCEP reanalysis data (Kalnay et al., 1996) and remotely sensed leaf area index (LAI) (Deng et al., 2006). The annual terrestrial ecosystem exchange imposed in each grid box is neutral (Deng and Chen, 2011).

Two sets of inversions were performed using the two different observing networks for the 1 July 2009 to 30 June 2011 period (**Figure 3**). The first six months are treated as a spin up period and we mainly consider the estimated fluxes for January 2010 – July 2011. The initial 3-D CO_2 mixing ratio fields were generated by running the model from January 1996 to December 2007 without assimilating any data, and then by assimilating surface CO_2 flask data from January 2008 to July 2010, following Deng et al. (2014). The optimized CO_2 mixing ratio field at 00:00 UTC on 1 July 2009, was used as the initial CO_2 field for the inversion analysis. As described in Deng et al. (2014), in assimilating the GOSAT data the model is transformed using the averaging kernels and prior CO_2 profiles from the XCO_2 retrievals. The assimilation did not account for horizontal correlations in the observation and prior error covariance matrices. The uncertainties applied to the GOSAT and in situ data are the same as in Deng et al. (2016) and Deng et al. (2014), respectively. Specifically, the reported XCO_2 retrieval uncertainties were inflated by 1.90 over land and 1.02 over ocean. Uncertainties applied to in situ data were determined from model-observation statistics for each site. Prior flux uncertainties are 16%, of fossil fuel emissions and 38% of biomass burning per gridbox per month. An uncertainty of 44% is assumed for the ocean flux and a 22% uncertainty is assigned to both the gross primary production and total ecosystem respiration per 3h per gridbox. Detailed explanations for these choices are found in Deng et al. (2014; 2016). Each set of inversions used a different assimilation window: 18 months for the insitu network but 12 months for the GOSAT network. This difference is necessitated by the different data densities. With the sparse insitu network, sufficient~~more~~ time is needed to collect enough observations to determine upstream fluxes, therefore, we use, an 18-month window as in Deng et al. (2014). However, with the more dense GOSAT observations (**Figure 2**), flux perturbations~~signal~~s have a greater chance of being observed quickly after injection into the atmosphere so a shorter window will suffice. Thus we used a 12-month assimilation window for the GOSAT inversion, as in Deng et al. (2016). Differences in the two inversion setups are inevitable because some parameters must necessarily differ (such as observation and representativeness error variances for the two measurement types). So, choosing exactly the same setup for both would force one system (and observation network) to be unfairly disadvantaged. Moreover, our intention is to examine the fluxes retrieved from what we believe to be the "best" configuration for each.

2.2.2 The GEM-MACH-GHG model

GEM-MACH-GHG is a global, coupled weather and greenhouse gas prediction model with approximately 0.9° horizontal grid spacing and 80 vertical levels spanning the ground to the mesosphere (0.01 hPa). It is derived from the operational weather forecast model used for global and regional predictions by the Canadian Meteorological Centre and is described in detail in Polavarapu et al. (2016). A semi-Lagrangian advection scheme is used for meteorology and constituent transport. For the latter, a global mass fixer was implemented. Convective transport of tracers through the deep convection scheme of Kain and Fritsch (Kain and Fritsch, 1990; Kain, 2004) was also implemented. The same initial condition used by GEOS-Chem was regridded to GEM-MACH-GHG's grid. Because of the large differences in model resolution and topography, the global air masses in the two models differ so forcing mass conservation during the regridding process introduced local differences. In particular, the GEM-MACH-GHG initial condition has a bias of about 0.5 ppm in the southern hemisphere. Since all model integrations use the same initial conditions, diagnostics involving a difference in model integrations (section 2.3) are not affected by the initial state differences between the two models. The posterior fluxes from the GEOS-Chem assimilation are inserted every model time step with 3 h updates. Note that posterior fluxes contain ~~total fluxes from unoptimized as well as optimized fluxes.~~ the total of all optimized (GPP, Respiration, ocean, biomass burning and anthropogenic) fluxes and the small amount of un-optimized fossil fuel emissions from shipping (~0.19 PgC/yr) and aviation (~0.16 PgC/yr). Since GEM-MACH-GHG does not yet have the ability to insert 3-dimensional emissions as GEOS-Chem does, the aircraft emissions were not inserted. This will lead to an underestimate in global CO_2 of less than 0.1 ppm per year.

2.3 The posterior atmospheric adjustment

In this section, we introduce a new diagnostic for flux inversion results. To do this, we first mathematically define the posterior atmospheric adjustment and show that, in general, it is comprised of a number of components. In our work, we will compute two of these components: the component due to flux adjustments and that due to meteorological uncertainty. By comparing these two components we can determine which is the dominant one. In particular, we are interested in identifying when changes in CO_2 fields introduced by flux analysis increments exceed CO_2 changes obtained from random perturbations on the size and shape of meteorological analysis errors. When this does not occur, CO_2 adjustments due to fluxes are smaller than those due to transport error and are therefore not robust against transport error.

Consider a transport model:

$$c_n = T\left(x_{0,n-1}, c_0, s_{0,n-1}\right) \qquad (1)$$

where T is the transport model which evolves the constituent (c) from time step 0 to time step n and which depends on the meteorological states, $x_{0,n-1}$, the constituent initial condition, c_0, and the fluxes, $s_{0,n-1}$. This same transport model is integrated twice: once with a set of prior fluxes, $s^b_{0,n-1}$, and a second time with the posterior fluxes, $s^a_{0,n-1}$. The posterior fluxes are related to the prior fluxes as follows.

$$s^a_{0,n-1} = s^b_{0,n-1} + \Delta s_{0,n-1} \qquad (2)$$

The second term on the right side is the flux increment obtained from inverse modelling and its spatial structure strongly depends on the observations used within the inversion model. The Posterior Atmospheric Adjustment (Δc_n) can be defined as:

$$\Delta c_n = T\left(x^a_{0,n-1}, c^a_0, s^a_{0,n-1}\right) - T\left(x^b_{0,n-1}, c^b_0, s^b_{0,n-1}\right). \qquad (3)$$

The superscript *a* in (3) denotes the "after adjustment" value and the superscript *b* refers to the "before adjustment" value. This is a general form which allows for the initial state of the constituent and the meteorological states to change when the posterior flux changes (i.e. uncertainty in initial conditions and meteorology is permitted). If the initial state of the constituent is not adjusted in the flux inversion (as in our case), we can drop the superscripts on c_0. However, let us retain the possibility of meteorological analysis uncertainty where

$$x^a_{0,n-1} = x^b_{0,n-1} + \varepsilon_{0,n-1}. \qquad (4)$$

The second term on the right side in (4) is a realization of meteorological analysis errors. If a meteorological data assimilation system computes analysis error covariances, such an estimate of uncertainty can be obtained. Then, as in Polavarapu et al. (2016), we expand the transport terms in Taylor series about the posterior state as follows:

$$\Delta c_n = \frac{\partial T}{\partial s}\left(x^a_{0,n-1}, c_0, s^a_{0,n-1}\right)\Delta s_{0,n-1} + \frac{\partial T}{\partial x}\left(x^a_{0,n-1}, c_0, s^a_{0,n-1}\right)\varepsilon_{0,n-1} + \mathrm{O}\left(\Delta s_{0,n-1}\varepsilon_{0,n-1}\right) \qquad (5)$$

To first order, the Posterior Atmospheric Adjustment (PAA) is comprised of two components (because in this work we do not consider the components of PAA related to imperfect initial concentrations).

$$\Delta c_n \cong \Delta c_n^s + \Delta c_n^x \qquad (6)$$

Note that for a given set of meteorological analyses, the transport model is a linear function of the flux and the linearized model is then the same as the original transport model in (5). We can approximate the components of the PAA using finite differences:

$$\Delta c_n^s = T\left(x_{0,n-1}^a, c_0, s_{0,n-1}^a\right) - T\left(x_{0,n-1}^a, c_0, s_{0,n-1}^b\right) = PAAF \qquad (7)$$

$$\Delta c_n^x = T\left(x_{0,n-1}^a, c_0, s_{0,n-1}^a\right) - T\left(x_{0,n-1}^b, c_0, s_{0,n-1}^a\right) = PAAM \qquad (8)$$

PAAF is the component of PAA due to flux adjustments while PAAM is the component of PAA due to uncertain meteorology. PAAF is computed by integrating the transport model with a set of posterior fluxes and again with the prior fluxes but both integrations use the same set of meteorological analyses ($x_{0,n-1}^a$) and initial concentrations. However, this is only one component of the posterior flux adjustment because the meteorological analyses are not perfectly known, and we can simulate that uncertainty by perturbing the meteorological analyses with realizations of meteorological analysis error (see supplemental material for a detailed description of how this was done). In other words, for a given set of fluxes, the meteorological fields could have been slightly different but equally valid in the context of the meteorological analysis errors. This is what PAAM defines and it is computed by integrating the model twice (with perturbed and unperturbed meteorology) for a given set of posterior fluxes and where we again use the same initial concentrations in both integrations. **Figure 4** illustrates these concepts schematically. Note that the impact of the meteorological uncertainty on posterior distributions is a different matter from transport biases that result from biased meteorology. The latter will be present in PAAF when it is computed with a single set of analyses but the former requires PAAM to be computed with two or more sets of analyses. A novel aspect of our work is the ability to compare the component of posterior atmospheric adjustment due to flux increments (PAAF) with that due to meteorological uncertainty (PAAM). If the PAA component due to flux increments alone (PAAF) does not exceed the component due to meteorological errors (PAAM), then it may not be the dominant contribution in (5) and therefore it should not be accorded much significance. In reality, the story will be complex because the PAA is a 4-dimensional field and the dominant component will likely be a function temporal and spatial scale. Therefore, in what follows, we consider some broad statistics of the PAA and its subcomponents such as global means and zonal means and zonal standard deviations.

2.43 Estimating the flux signal and meteorological analysis errorsComputing contributions to posterior atmospheric adjustments

Once the flux estimates have been obtained, they are inserted into a forecast model to obtain posterior CO_2 distributions. Prior CO_2 distributions are also obtained by inserting prior fluxes into the same model and then the flux signal PAAF is determined by subtracting the prior CO_2 distribution from the posterior CO_2 distribution. Both model integrations use the same CO_2 initial states and meteorological fields. Here we use GEOS-Chem as well as GEM-MACH-GHG (Polavarapu et al., 2016) for this purpose. The advantage of using two models is that we can get a sense of the robustness of the results since the models will have different model errors. The disadvantage of using a different model (from that used for the flux inversions) to obtain the flux signal PAAF is that posterior fluxes contain an imprint of transport model errors from the model used for the flux inversion, so integrating these into another model will convolve the two transport models' errors (as seen in Polavarapu et al., 2016). If the two models' transport errors are fortuitously similar, then this problem is avoided. However, this is unlikely to be the case for any two models on all time and spatial scales. Thus, we assess the ability of GEM-MACH-GHG to simulate CO_2 with fluxes derived from inversions performed with GEOS-Chem in order to identify where convolution of the two transport models' errors is evident.

By comparing CO_2 distributions from GEM-MACH-GHG obtained with posterior fluxes from GEOS-Chem with observations, we can assess the ability of this model to simulate CO_2 and search for instances of convolution of transport model errors. **Figure 45** shows two-year time series of modelled and measured CO_2 at the NOAA or ECCC stations of Alert, Mauna Loa, Sable Island and South Pole. Both The two model simulations correspond to use the two different flux estimates obtained with either in situ (red curves) or GOSAT (blue curves) observations. At Alert, which is far from CO_2 sources and sinks, a good comparison between the model simulation and measurements indicates a good ability of the model to transport the flux signalPAAF from the midlatitudes to the high latitudes on seasonal timescales. Indeed, **Figure 45** shows that the GEM-MACH-GHG both model simulations agree rather well with observations at Alert with in situ posterior fluxes. using either set of fluxes although iIn boreal summer GOSAT-retrieved fluxes produce a better match than insitu-based fluxes for both models (Table 2). The better match with observations in boreal summer is consistent with the increased density of GOSAT observations in the northern hemisphere at that time (Byrne et al., 2017). The overestimation in boreal spring of both years with GOSAT-based fluxes (Table 2) was also seen in Deng et al. (2016) and suggests fortuitously similar transport by the two models to this location. The overall agreement of both GEM-MACH-GHG simulations with Alert measurements is rather good especially considering the poorer agreement obtained with

CarbonTracker 2013B (Peters et al., 2007, http://carbontracker.noaa.gov) fluxes in Polavarapu et al. (2016). This does not mean that GEOS-Chem posterior fluxes are superior in any way to those of CT2013B, but rather that the transport errors of GEOS-Chem and GEM-MACH-GHG are fortuitously commensurate, at this location and time period. At Mauna Loa and Sable Island, which are far from sources but are also affected by synoptic scale variability, both model simulations compare well to measurements. At the South Pole, any differences in transport errors between the two models that accumulate over long timescales are visible. Here a bias appears but it is mostly (~0.5 ppm) is due to the regridded initial conditions with another 0.1 ppm arising after 2 years of simulation. The bias with GEM-MACH-GHG occurs with both sets of fluxes but the bias is smaller with in situ-based posterior fluxes (see also Table 2). From the bias in the simulation with in situ fluxes we infer a mismatch of transport times to the southern hemisphere between the two models since GEOS-Chem simulations with the in situ-based fluxes match this station's time series well (~~not shown~~Table 2) and since a similar bias is also present between the two model simulations at other southern hemisphere stations (not shown). ~~However~~In addition, a positive bias of 0.5 ppm ~~does~~ appears when GOSAT-based posteriors are used with GEOS-Chem (~~not shown~~Table 2). Thus the increased bias with GOSAT-data is seen by both models (Table 2) and is a separate issue from the convolution of transport errors.

The GEOS-Chem inversion was performed with a coarse 4°×5° resolution grid whereas GEM-MACH-GHG uses a much higher 0.9° resolution. So, the fact that the forward model simulations agree well with observations on synoptic time scales supports the contention of Agusti-Panareda et al. (2014) that the large scale gradients of CO_2 are captured in the retrieved fluxes due to an adequate density of observations whereas the high resolution model captures and adds the correct synoptic scale variability. Overall, we conclude that GEM-MACH-GHG simulates CO_2 reasonably well with GEOS-Chem fluxes on a variety of timescales in the northern hemisphere, but there is mismatch of transport times to the southern hemisphere. The fact that there are differences in the posterior CO_2 distributions with the two models (and evidence of convolution of transport errors) will inform discussions of atmospheric adjustments (PAAF and PAAM) in section 3.

Polavarapu et al. (2016) showed that the existence of uncertainty in meteorological fields limits the spatial scales that can be depicted in CO_2 fields. Although it is only one of the many sources of error impacting CO_2 model distributions, it will always be present and may be considered a minimum error level. To estimate this error (PAAM), the forward simulations of GEM-MACH-GHG were repeated with perturbed meteorological fields and the difference in CO_2 defines this inescapable error. To perturb the meteorological fields, Polavarapu et al. (2016) simply computed the difference between the meteorological analyses valid at the required time and those valid 6h prior to the required time, and then removed the diurnal signal from this perturbation. Here we improve on the methodology by using actual realizations of analysis error from our operational ensemble Kalman Filter (EnKF) system (Houtekamer et al., 2014), which is used to determine meteorological forecast uncertainty on the medium range. Because the ensemble members were not available in the archives of the Canadian Meteorological Centre for the period of study here, we use analysis error estimates from a different year. The supplemental material describes how the perturbations were computed and demonstrates that the method used to estimate analysis errors is considerably better that used in Polavarapu et al. (2016) despite some unavoidable approximations. In this work, meteorological fields perturbed by EnKF-derived meteorological analysis errors will be used to define minimum error levels in the diagnostics of sections 3.2.4 and 3.2.5.

3 Results

The two sets of posterior fluxes that will be used to study the atmospheric CO_2 flux signalsadjustments are described in section 3.1 before considering the vertical propagation structure of the flux signal PAAF in section 3.2. While some of the figures below include results from both models, others show those from a single model. In such cases, results from the GEOS-Chem model are shown, while corresponding figures obtained with GEM-MACH-GHG are relegated to the supplemental information. This choice was made because GEOS-Chem was used in the flux inversions, so posterior CO_2 distributions with GEOS-Chem are obtained with consistent model errors while posterior distributions obtained with GEM-MACH-GHG will convolve the transport errors from the two models. However, despite this convolution of errors, consistent patterns emerge with both models, lending greater confidence in the robustness of results in the face of transport error.

3.1 Posterior flux estimates

The inversion results used here are similar to those presented in Deng et al. (2014, 2016). However, we briefly present those results again here because (1) the runs used here are not identical (e.g. observation sets) to those published, and (2) we will be comparing the CO_2 adjustments arising from these two sets of fluxes so it is worth directly comparing them here.

The global total flux estimates for 2010 obtained from the two observation networks studied here are 5.01 Pg C (in situ) and 4.95 Pg C (GOSAT). Here positive values indicate fluxes from the Earth's surface into the atmosphere. The actual annual growth rate for 2010 from Conway and Tans (2012) is 2.41±0.06 ppm or 5.12±0.13 Pg C (using a conversion factor of 2.124 Pg C ppm^{-1}). The general agreement of both sets of posterior fluxes with the 2010 annual total flux suggests that both inversions are sufficiently well configured.

While the global annual totals for 2010 are similar with the two different observation networks, the spatial distributions of the fluxes for the 11 TransCom (Gurney et al., 2003) land regions differ (**Figure S6**). **Figure 5** shows the spatial distributions of the annual flux for 2010 for the 11 TransCom (Gurney et al., 2003) land regions. The prior and the in situ-based posterior fluxes are similar to those shown in Figure 4 of Deng et al. (2014) while the GOSAT-based posterior fluxes are similar to those presented in Figure 8 of Deng et al. (2016). As in Deng et al. (2014), **Figure S65** reveals that in situ data result in more uptake in the Americas whereas fluxes retrieved from GOSAT data put more uptake in Eurasia. As noted in this Introduction, this increase in European uptake with GOSAT data was also seen by Reuter et al. (2014) and Houweling et al. (2015).

~~Both sets of posterior fluxes have the same sign for most regions except North and South Africa and Australia.~~ In the north-south direction, in situ fluxes produce more uptake in the three tropical regions compared to GOSAT-derived fluxes, while the latter have relatively more uptake in temperate and boreal Eurasia. This was also seen in Houweling et al. (2015). This difference in north-south distributions of fluxes is more readily evident in **Figure 6~~S6~~** which shows the temporal variation of the fluxes accumulated over three large latitudinal bands: the northern extratropics, the tropics and the southern extratropics. (Here the dividing latitude between the tropics and extratropics is taken as 19.47° or $\sin^{-1}$ (1/3) because it results in exactly equal areas for all three regions. This advantage is exploited later to interpret the diagnostics of section 3.2.) **Figure 6~~S6~~a** reveals that both sets of fluxes are generally similar on the global scale with two exceptions: (1) the peak boreal summer uptake occurs in June with GOSAT data, but in July with in situ data, and (2) GOSAT data produces larger outgassing of CO_2 in October and November. The larger outgassing with GOSAT data in boreal autumn is due to larger contributions from both the northern extratopics (**Figure 6~~S6~~b**) and the tropics (**Figure 6~~S6~~c**). The larger global uptake in June with GOSAT data is due to the northern extratropics (**Figure 6~~S6~~b**). In the southern extratropics, GOSAT generally results in more uptake than in situ data but the magnitude of the uptake and the difference between the two posterior fluxes is small (**Figure 6~~S6~~d**). ~~The temporal variation of the flux is further broken down into the 11 TransCom land regions in **Figure 6**. The greater outgassing in boreal autumn with GOSAT data is seen in the Boreal and Temperate North American regions, as it was in Deng et al. (2014, their Figure 5). In temperate North America, the CO_2 source is greater throughout the boreal winter months but in boreal North America, the GOSAT fluxes are larger only in October and November, as seen in **Figure S6a-b**. Also, as noted by Deng et al. (2014), the boreal Eurasian sources in boreal winter are close to their prior values due to the dearth of observations there combined with low prior flux values (implying low prior flux uncertainty). In the tropics, there is little agreement between the two sets of fluxes. In Australia, the in situ flux stays close to the prior value but GOSAT-derived fluxes tend to decrease the prior through most of the year. This adjustment with GOSAT data occurs because the measurements observe the southern hemisphere well through ocean glint measurements (Byrne et al., 2017) whereas in situ observations are sparse in that region.~~

In summary, the posterior fluxes produced here bear similarities to those produced by other inversion systems constrained by similar observation sets, and are consistent with the range of results of the multi-inversion intercomparison of Houweling et al. (2015). Thus the two sets of posterior fluxes may be considered as reasonable examples representative of the two observing systems. Furthermore, the results obtained here should be relevant to other flux inversion systems.

3.2 Vertical propagation of the PAAF~~flux signal~~

Given the two sets of posterior fluxes, we now consider how they inform atmospheric CO_2 distributions. Although column measurements contain information about CO_2 concentrations throughout the depth of the troposphere, ultimately, in a flux inversion, this information is used to update a surface flux. It is unclear how this updated surface flux ~~signal~~perturbation is then ~~propagates~~ vertically transported to inform the middle and upper troposphere. Intuitively, one might expect the assimilation of column measurements to result in better CO_2 depictions in the middle and upper troposphere. However, as will be shown, this is not necessarily the case.

3.2.1 Zonal mean patterns

The PAAF~~flux signal~~ was computed for both sets of posterior fluxes resulting in four sets of 4-dimensional CO_2 fields—two sets for each model. To encapsulate the vertical motion, zonal mean fields were computed. The GEOS-Chem fields are animated in **Figure S7** and snapshots from the animation, taken every 3 months from 1 October 2009 to 1 July 2011 are shown in **Figure 7**. Qualitatively similar results are obtained with GEM-MACH-GHG (~~see supplementary material~~ **Fig. S9**). Immediately obvious from **Figure 7** is that the PAAF~~flux signal~~ is largely negative for both experiments at all times. This occurs because the prior flux has a terrestrial component that produces an annually balanced biospheric flux. Thus, the fact that the terrestrial biosphere annually takes up approximately 30% of the anthropogenic emissions entering the atmosphere (Le Quéré et al., 2015) is not assumed by the prior fluxes. This is done intentionally because of the desire that observations determine the existence and amount of uptake by the terrestrial biosphere. Here, the impact of using annually balanced biospheric fluxes and ocean prior fluxes from Takahashi (2009) that only account for 1.4 of the expected 2.5 Pg C per year is that the prior CO_2 distribution has a continually increasing global total relative to the actual increase. Then, once the flux inversion is performed and the fluxes are pulled toward realistic values, the posterior distributions reduce the overestimated CO_2. Thus the difference between the posterior and the prior CO_2 distributions is always negative, in a global sense—hence the overwhelming negative values seen in **Figure 7**.

Comparing the distributions obtained with the two observing systems reveals some clear patterns. In October 2009 (which is still in the spin up period), the patterns are similar except that the GOSAT data produce a smaller PAAF~~flux signal~~ in the tropics. This is even more evident by January 2010, where the GOSAT-derived ~~flux signal~~PAAF has ~~high~~smaller CO_2 adjustments in the northern hemisphere as well. At this time, there is a clear difference in the vertical gradient of the ~~flux signal~~PAAF between the tropics and northern extratropics, ~~with~~and GOSAT data produc~~ing~~es reduced meridional gradients. This was also seen by the inversion systems in Houweling et al. (2015, their Fig. 8), but the reduced gradient was not supported by independent measurements. By April 2010, the in situ data are continuing to reduce CO_2 in the northern hemisphere and tropics, while the GOSAT data seem to not have much impact. On the other hand, in July 2010, GOSAT data produce a large negative ~~flux signal~~ PAAF in the northern hemisphere when the satellite observes this region well

(**Figure 2**). However, the tropical upper troposphere retains a stronger ~~flux signal~~PAAF with the in situ data. In the second year of simulation, these patterns are repeated as the troposphere slowly adjusts to more realistic global mean values resulting from the observationally constrained terrestrial biospheric uptake. Specifically, October 2010 sees similar patterns for the two simulations in the northern hemisphere and tropics while January 2011 reveals larger CO_2 (smaller adjustments) throughout the troposphere in GOSAT-based simulations. April 2011 again sees a greater reduction in CO_2 throughout the tropics with in situ data so that the GOSAT-based ~~flux signal~~PAAF is relatively lower throughout the troposphere. Finally, by the end of June 2011, the large ~~flux signal~~PAAF obtained with GOSAT data is seen once again in the northern hemisphere while in situ data retain~~s~~ a large ~~flux signal~~PAAF in the tropical troposphere. When these patterns are animated (**Figure S7**), it appears that the in situ data provide a constant injection of information from northern hemispheric fluxes which is transported upward and equatorward to inform the tropical middle and upper troposphere. GOSAT data provide large updates to fluxes in boreal summer in the northern hemisphere, but when boreal autumn comes and the satellite tracks shift southward, the ~~flux signal~~PAAF diminishes. In boreal winter, GOSAT observes the southern hemisphere well, but the northern hemisphere dominates the global CO_2 seasonal variation (Keeling, 1960) and so GOSAT misses the northern hemisphere emissions and the ~~flux signal~~PAAF diminishes in this hemisphere with subsequent missing transport of the ~~flux signal~~PAAF to the tropics. In fact, Houweling et al. (2015) argue that this seasonal variation of GOSAT data coverage plays a role in amplifying the European sink. This difference in the seasonality between inversions with in situ and GOSAT data is also consistent with the results of Byrne et al. (2017). Although both simulations only adjust surface fluxes, the in situ-based posterior fluxes constantly inform the northern hemisphere and the adjusted CO_2 patterns are transported upward to the tropics. This transport of information relies on the accuracy of the model's transport and hence may not be correct. Transport error has long been known to be a major source of error in flux inversion systems (e.g., Chevallier et al., 2014; Chevallier et al., 2010; Houweling et al., 2010; Law et al., 1996). Thus, to see which of the two posterior fluxes better depicts the middle and upper troposphere, we compare to independent measurements in the next subsection.

3.2.2 Comparison to observations

Since the PAAF is defined as the CO_2 change relative to a given prior, it is not clear which pattern is more correct when the PAAFs are compared. Thus in order to inform subsequent discussions about PAAF diagnostics, we compare CO_2 posteriors directly to independent measurements. Total column measurements from the TCCON provide indirect information about CO_2 concentrations throughout the troposphere. The dominant feature seen in seasonally-aggregated comparisons of modelled CO_2 to TCCON is the larger bias resulting from GOSAT-based fluxes (**Figures 8, 9).** At all stations, except Eureka, a difference of about 0.5 ppm between the biases of the two simulations is present, with in situ data providing a closer fit to the measurements (**Figure 8**). However, if we look beyond this time-mean bias (by subtracting it out), GOSAT-based fluxes are seen to better define the seasonal cycle (**Table S1**) at most northern extratropical sites. Visually, this means the black curves are generally flatter than the red curves in **Figure 9**. At most of the northern sites (Bialystok, Garmisch, Izana, Karslruhe, Lamont, Orleans, Park Falls, Sodankyla) the seasonal variation of the statistics obtained with GOSAT is better since the means of absolute anomalies are lower than those obtained with in situ data (compare columns 6 and 7 in **Table S1**). (The results from Eureka seem anomalous relative to other TCCON sites so this is a topic currently under investigation by Kimberly Strong. Explanations under consideration include sampling issues, site-to-site differences, model transport errors and unknown issues with the data.) The improved ability of inversions constrained by GOSAT data to capture the seasonal cycle was also found by previous analyses (e.g., Deng et al., 2014; Liu et al., 2014; and Reuter et al., 2014). Butz et al. (2011) and Lindqvist et al. (2015) showed that GOSAT/ACOS data alone can match the seasonal cycle at TCCON locations (typically within 1 ppm in the Lindqvist study). In addition to better capturing the seasonal cycle, the GOSAT-based simulations result in lower mean residuals at many of the northern hemisphere sites in June, July and August (**Figures 9**). Improved agreement with independent observations using posterior fluxes from the GOSAT inversion relative to the in-situ inversion during boreal summer was also found by Basu et al. (2013), Deng et al. (2014) , and Reuter et al. (2014) and suggests that the summer drawdown in the in-situ inversions is too weak over the northern extratropics. Overall, however, the posterior fluxes obtained with in situ observations provide better agreement with TCCON overall since 61 of the 76 (80%) comparisons favour the simulation based on in situ data (**Figure 9**). The standard deviations are rather similar for the two simulations and are frequently smaller than the means (**Figure 9**).

Comparisons to TCCON obtained with GEM-MACH-GHG posterior CO_2 distributions are found in **Figures S10 and S11**. The same conclusions hold: there is an overall larger mean mismatch with TCCON when GOSAT-based posteriors are used (**Figure S10**) but the seasonal cycle is better captured at most northern extratropical sites (**Table S1**) and the agreement in boreal summer is better at many northern extratropical sites (**Figure S11**). Additionally, a ~~convolution of the two models' transport errors is evident in **Figure S10** in that a~~ larger bias with TCCON at southern hemisphere sites is seen with GEM-MACH-GHG compared to that obtained with GEOS-Chem (**Figure 8**). This bias was also seen in **Figure 5~~3~~** (South Pole station) and arises mainly from the initial condition but is affected by the ~~due to~~ differing transport times from the tropics to the southern hemisphere in the two models. GEOS-Chem transports CO_2 more rapidly to the southern hemisphere and its posterior fluxes reflect this rapid transport (see animation in **Figure S8,** especially July-August 2010). When inserted into GEM-MACH-GHG, the fluxes obtained assuming a fast transport to the southern hemisphere result in a too-slow departure from the prior CO_2 distribution and a larger bias with respect to observations. However, because GEM-MACH-GHG is disadvantaged by the convolution of transport errors, these results do not identify which model's interhemispheric transport to the south is more realistic. As a weather and environmental forecast model, knowledge of the age-of-air for GEM-MACH is not essential for its time scales of interest so this work identifies a need to better characterize interhemispheric transport with the GHG version of this model. At the same time, this work shows little evidence for the convolution of transport errors on shorter time scales or in the northern hemisphere (as was seen when GEM-MACH-GHG used CT2013b fluxes in Polavarapu et al., 2016). Moreover, despite the existence of some convolution of transport errors, conclusions regarding the agreement with independent measurements hold for both models, increasing confidence in the robustness of results in the face of model errors.

A more direct assessment of middle and upper tropospheric CO_2 distributions is obtained by comparing to aircraft profiles. Comparisons of both GEOS-Chem simulations to measurements from the HIPPO-3 campaign in 24 March to 16 April 2010 are shown in **Figure 10**. The results are aggregated by latitude and vertical bands. The in situ-based posterior fluxes result in lower mean differences from measurements in the middle to upper troposphere (panel c) and the lower stratosphere (panel d) in the northern extratropics. However, the GOSAT-based posterior fluxes generally agree better with measurements in the southern extratropics at all heights. Similar results are also obtained with GEM-MACH-GHG (**Figure S12**) in the northern extratropics but in the southern extratropics, in situ fluxes better match observations because of initial condition differences and the convolution of transport errors which leads to increased CO_2 in the southern hemisphere for all fluxes. Note that in the stratosphere for both comparisons with HIPPO-3 (**Figures 10d** and **S12d**), the mean mismatch exceeds the standard deviation. This means that both model simulations are biased in the stratosphere as was seen in Deng et al. (2015). Such a bias can adversely affect flux estimates in the northern hemisphere (Deng et al. 2015). Comparing **Figures 10** and **S12** (panels c and d) reveals that GEM-MACH-GHG has better agreement with HIPPO-3 than does GEOS-Chem in the middle to upper troposphere and in the stratosphere. This makes sense given the finer vertical and horizontal resolution of GEM-MACH-GHG and is expected from the results of Deng et al. (2015, their Figures 11-12). The number of realizations used in each comparison in **Figures 10** and **S12** ranges from 94 to 2570 and the differences in the mean values of the two experiments are significant at the 90% level. Thus, overall, we conclude that the middle and upper tropospheric distributions of CO_2 are better in the northern hemisphere in boreal spring 2010 when posterior fluxes use in situ data rather than GOSAT column measurements.

Since measurement campaigns occur only in select time windows (HIPPO-3 was in March-April 2010), we also consider the more routine NOAA aircraft profile measurements from continental U.S. and Canadian sites in **Figure 11**. The observations are from ObsPack2013 (Masarie et al., 2014). As in Agusti-Panareda et al. (2014), mean model profiles at the nearest grid point and time step to the observation locations and times are averaged over a season. Observed values are binned into 1 km layers and compared to model values at mid-layer. Hourly GEOS-Chem fields are used. When the entire 2010 year is considered, the bias throughout the troposphere with respect to the aircraft profiles is much smaller with in situ-based posterior fluxes (**Figure S13**) for both models. However, the results are more variable if broken down by season. In boreal winter, in situ data produce better agreement with NOAA aircraft near the surface but from 2-6 km GOSAT data give a better result (**Figure 11**). This variation in fit is related to the fact that vertical profiles from GEOS-Chem have stronger than observed gradients in the lowest 1-2 km. GEM-MACH-GHG profiles better match observed gradients (**Figure S14**) and GEM-MACH-GHG profiles consistently favour the same simulation in both height ranges. In Dec.-Feb. 2010, the in situ-based simulation better matches observations although it is partly in the spin up period, whereas in Dec.-Feb. 2011, the GOSAT-based simulation better matches mean NOAA aircraft profiles at all heights (**Figure S14**). In boreal spring (**Figures 11 and S14**) in situ data produce better agreement not just near the surface, but at all heights. In boreal summer, GOSAT data result in much better agreement from 1-3 km but from 3-6 km there is little difference between the two simulations. However, in boreal autumn, GOSAT data achieves a better match from 2-6 km, whereas in situ data has a better match near the surface (**Figures 11**). As in boreal spring, incorrect vertical gradients obtained with GEOS-Chem are likely playing a role in the inconsistent results since GEM-MACH-GHG's vertical gradient is closer to that observed and it favors the GOSAT-based simulations at all heights (**Figure S14**). Overall, from 3-6 km, simulations with both posteriors produce similar model profiles in boreal summer and fall, but in boreal winter and spring there is a difference between the two, with in situ data producing lower CO_2. The lower CO_2 values obtained with in situ data agree better with aircraft data in boreal spring, but not in boreal winter. From 1-2 km, in situ data better match aircraft data in boreal spring while GOSAT achieves the better match in boreal summer, for both models. These results once again confirm that in boreal summer when GOSAT views and samples the northern hemisphere well, the estimated fluxes are improved in the lower troposphere.

In summary, the results that are consistent are as follows. (1) Despite the reliance on faithful model transport, in situ-based posterior fluxes produce CO_2 distributions that better agree with independent observations of the middle troposphere in the northern hemisphere in boreal spring. This may partly be due to the propagation of the near surface improvements obtained in boreal winter. (2) GOSAT-based posterior fluxes consistently achieve better agreement with independent observations in the northern hemisphere in boreal summer and in the middle to upper troposphere in boreal winter.

3.2.3 Adjoint Sensitivity

Figures 7 and **S9** as well as animations **S7** and **S8** imply a propagation of ~~flux signal~~the PAAF from the northern midlatitude lower troposphere to the tropical middle and upper troposphere with in situ-based posterior fluxes. The question of whether this is realistic or not was the subject of the previous subsection where model simulations were compared to independent observations. Here we consider whether such transport (realistic or otherwise) has implications for flux inversions. In other words, can CO_2 from the northern extratropics influence the CO_2 in the tropical upper troposphere a few months later? To see whether this occurs in the flux inversion system, we compute the sensitivity of CO_2 at one point in time with respect to the CO_2 state at an earlier point in time using the adjoint of GEOS-Chem (Henze et al., 2007). While Byrne et al. (2017) utilize the adjoint sensitivity with respect to surface fluxes, here we need to consider the entire CO_2 state in order to see vertical transport of information. The extension of the adjoint calculation needed to produce sensitivity to the CO_2 state is described in Appendix A, and **Figure 12** shows the sensitivity of the CO_2 field on 1 February 2010 to earlier states, at one month intervals. Each panel shows a snapshot of the zonally averaged sensitivity field. In February 2010, the sensitivity is initialized to a uniform value within a mask from 20°S-20°N and 500-250 hPa. Proceeding backward in time, this field is sensitive to the CO_2 field throughout the depth of the tropics in January 2010 with a hint of sensitivity beyond the tropics in the stratosphere. By November 2009, this stratospheric influence is more evident and by October 2009, extratropical tropospheric influence is also evident. By September 2009, the sensitivity is largest in the northern and southern extratropics. Tracing the pattern in the northern hemisphere forward in time through the panels reveals upward and equatorward propagation of the signal. Thus the CO_2 field in the northern tropics in the upper troposphere in boreal spring is sensitive to CO_2 in the northern midlatitude lower troposphere on September 1. In other words, observations near the surface at northern midlatitudes on September 1 can potentially impact CO_2 fields in the tropical upper troposphere, 3 to 6 months later. Because the adjoint calculation only reveals patterns without a magnitude (since the actual influence of an observation on CO_2 estimates also involves error covariances of observations and propagated prior flux errors), only a potential influence can be revealed in **Figure 12**. However, this potential influence is sufficient to demonstrate the atmospheric transport from the northern midlatitude lower troposphere to the tropical upper troposphere on the timescale of several months. This figure then supports the notion that observations of the northern midlatitudes combined with model transport can influence (rightly or wrongly) CO_2 distributions downstream in the middle and upper tropical troposphere.

3.2.4 Global mean ~~flux signals~~posterior atmospheric adjustments

F~~The f~~lux ~~signal~~perturbations modify~~ies~~ CO_2 fields locally but, eventually, gradients get diffused by atmospheric turbulence and only the impact on the background CO_2 field is retained. Thus, looking at the zonal or global mean ~~flux signal~~PAAF reveals long time scale information retained from flux adjustments after redistribution and dispersion by model transport. How long does it take for a flux ~~signal~~perturbation to modify the background CO_2 state? Deng et al. (2014) show that transit times of regional fluxes to the middle troposphere further downstream are shorter than two months and flux ~~signals~~perturbations have dispersed to the background within 3 months (see their Figure 15). Similarly, Liu et al. (2015) found that column measurements are unable to distinguish the locality of fluxes older than three months. **Figure 13** shows the globally averaged zonal mean ~~flux signal~~ PAAF for both models and both observing systems at selected model levels in the lower troposphere (panel a), the middle troposphere (panel b), the upper troposphere (panel c), the lower stratosphere (panel d), middle stratosphere (panel e) and the upper stratosphere (panel f). (It was possible to find similar model levels in terms of approximate pressure for the six representative pressures for the two models by assuming a 1000 hPa reference for each vertical coordinate. These are listed in **Table 1**.) From Deng et al. (2014) and Liu et al. (2015) we conclude that the time scales reflected in **Figure 13** are seasonal and longer time scales. The evolution of global CO_2 when forced by the prior flux is missing a trend due to the assumption of a balanced biosphere so the prior CO_2 fields drift from a realistic global mean, increasingly overestimating it. Since the posterior CO_2 fields are constrained by observations to resemble the actual atmospheric budget evolution, our global ~~flux signal~~ PAAF increases with time as the trend error accumulates (**Figure 13** black curves). (Here the posterior fields are subtracted from the prior fields to give positive values, for convenience.) **Figure 13** shows that the global ~~flux signal~~ PAAF increases not only for the atmosphere as a whole but also at all heights (except the upper stratosphere). In addition, for the GOSAT-based ~~flux signal~~PAAF, there is a large seasonal variation on top of the linear trend which has largest amplitude near the surface.

Figure 13 also shows that despite the differing transport errors, the global ~~flux signal~~PAAFs are very similar for the two models. The largest differences occur in the upper troposphere and lower stratosphere (UTLS) regions (panels c and d). As noted by Deng et al. (2015), the GEOS-Chem CO_2 simulation at a resolution of 4° x 5° is biased in the UTLS. Stanevich et al. (manuscript in preparation) found a similar bias in the coarse resolution CH_4 simulation in GEOS-Chem, which they attributed to excessive mixing across the tropopause at the 4° x 5° resolution. Also, as noted earlier, GEM-MACH-GHG compares better to HIPPO3 in the upper troposphere and stratosphere of the northern extratropics with the same posterior fluxes as GEOS-Chem. Compared to the ~~flux signal~~PAAF obtained with in situ data, the ~~flux signal~~PAAF derived from GOSAT data diminishes in boreal winter and spring throughout the troposphere. Recall that in boreal spring, in situ data provided the better match of CO_2 distributions to NOAA aircraft in the lower troposphere (**Figures 11, S14**). In the stratosphere, the overall signal is smaller with GOSAT data, but there is little seasonality to the signal for either experiment (**Figure 13d-f**). Because the ~~flux signal~~PAAF reflects the departure of the posterior from the prior CO_2 field, it is not clear whether a large or small seasonal variation should be expected. However, comparisons of posterior fields to measurements in section 3.2.2 revealed that the posterior CO_2 fields derived from in situ data have an approximately 0.5 ppm lower bias relative to TCCON at all sites except Eureka. They also agree better with NOAA aircraft and HIPPO-3 in the middle and upper troposphere in boreal spring and with NOAA aircraft at all heights when annual mean profiles are considered. This suggests that the larger signal seen in boreal spring with in situ data may be realistic. In boreal winter, near the surface, the CO_2 fields obtained from in situ posteriors agree better with NOAA aircraft profiles, but those based on the GOSAT posteriors yield better matches from 2-6 km. However, the NOAA aircraft data used corresponds to North America, whereas **Figure 13** illustrates global diagnostics while the overall TCCON comparison (**Figure 8**) suggests in situ distributions are more realistic. Thus, it is not entirely clear whether the larger signal seen in boreal winter with in situ data is more realistic than the lower one obtained with GOSAT data. What is clear is that our flux inversions that assimilate GOSAT data produce posterior distributions that are less consistent with observations in global, annual statistics than flux inversions using in situ data. In addition, the GOSAT-informed ~~flux signal~~PAAF has much stronger seasonal variations than the in situ-based ~~flux signal~~PAAF. Thus, sub-annual variations in the global mean CO_2 adjustments are sensitive to the observing system used. However, this sensitivity also depends on the choice of prior fluxes since, for example, a prior flux with reduced bias in boreal summer would reduce this effect.

How much can we trust the global ~~flux signal~~PAAF? The model transport of flux adjustments is not perfect and a major component of the transport model uncertainty is due to wind field errors (Liu et al., 2011). We can use the coupled meteorology and greenhouse gas transport model to identify the error due to wind field uncertainty on ~~flux~~

signalsatmospheric adjustments by simply repeating each simulation with perturbed meteorological fields (as described in the Supplemental material) to compute PAAM. The difference in posterior CO_2 distributions obtained with the control and perturbed meteorology defines this uncertainty. When PAAF and PAAM are comparable, PAAF is not the dominant component and should not be accorded great significance. This uncertainty PAAM is plotted in **Figure 13** but is not evident because the curves are near zero. This is not surprising because the global mean atmospheric CO_2 is independent of transport. It is the spatial distribution of CO_2 that is affected by atmospheric transport (as will be demonstrated shortly). However, by considering the global mean at various heights, there was the possibility that an influence of errors in atmospheric transport might be seen at some vertical levels.

Figure 14 shows how the tropics and extratropics contribute to the global flux signalPAAF based on GOSAT data and computed with the GEOS-Chem model. As noted earlier, the dividing latitude between the tropics and extratropics was chosen so that the three zonal bands have equal areas. Because the zonal bands have equal areas, we multiply the zonal contributions depicted in **Figure 14** by a factor of three, which means that each regional total (red, blue or green curves) can be compared to the global total (black curves). For example, **Figure 14a** reveals that in the lower troposphere, the dominant contribution to the global flux signalPAAF comes from the northern extratropics where there is a large seasonal variation due to the seasonality of observational coverage (**Figure 2**) in addition to the seasonality in the fluxes. This is also true for the middle troposphere (**Figure 14b**). However, in the lower and middle stratosphere, the tropics dominate the global flux signalPAAF (**Figure 14d-e**). The upper stratosphere is not much influenced by flux adjustments (**Figure 14f**) on the two-year time frame. Since the northern extratropics dominates the global flux signalPAAF, the concern of Houweling et al. (2015) that the excellent observational coverage of this region by GOSAT in boreal summer combined with the poorer coverage in boreal winter has implications on flux inversions seems warranted. **Figure S15** shows that these patterns also occur for flux signalPAAFs derived from assimilating in situ observations but the seasonal variation of the flux signalPAAF is greatly reduced. The flux signalPAAF is largest in boreal summer due to adjustments in the northern extratropics for both posterior fluxes (**Figures 14** and **S15**). As seen in **Figure 7**, these adjustments in July are much greater when GOSAT data is assimilated. Indeed Byrne et al. (2017) found large sensitivity of boreal summer fluxes to GOSAT data. This is also consistent with the large summertime flux adjustments of Liu et al. (2014) and the increased European fluxes seen from May-August in Houweling et al. (2015).

Figure 15 compares the regional contributions to the global flux signalsPAAF for the two models. The differences seen in the UTLS in **Figure 13c** are evidently due to differences seen in the northern extratropics (**Figure 15c**) in boreal summer and autumn. Since GEM-MACH-GHG agrees better with HIPPO-3 in the middle and upper troposphere and in the lower stratosphere, it is possible that its signal is more accurate in this region. However, given the limited temporal and spatial domain of the measurements, such a conclusion would be tentative at best. The overall agreement between the two very different models suggests that the diagnostic is primarily seeing the impact of the posterior fluxes (which were the same for both models) for the large zonal bands considered. In addition, because the diagnostic involves a difference between model integrations, the southern hemisphere bias in CO_2 seen in GEM-MACH-GHG initial conditions is common to all simulations with this model and thus is subtracted out in the PAAF and PAAM diagnostics. **Figure 15** also shows that when the global mean is subdivided into three zonal bands, a tiny (negligible) influence of atmospheric transport errors associated with imperfect meteorology becomes apparent near the surface (**Figure 15a-b**) in the northern extratropics during boreal spring and summer. In addition, the CO_2 ~~uncertainty~~ adjustment due to wind field uncertainty (PAAM) exceeds the ~~flux signal~~atmospheric adjustment obtained from assimilating either set of observations (PAAF) in the tropical upper stratosphere (not shown). Overall, however, the global ~~flux signals~~PAAFs are very similar between the two models, even after dividing them into regional contributions.

3.2.5 Zonal asymmetry in the posterior atmospheric adjustments~~flux signals~~

Departures from zonal mean ~~flux signal~~PAAFs can be used to examine shorter temporal and spatial scales in the ~~flux signal~~PAAF. The zonal mean flow has no zonal standard deviation (by definition) so large zonal standard deviations indicate greater zonal structure (or asymmetry within a zonal band). Moreover, once the flux ~~signal~~perturbation has diffused to the background (or zonal mean) state, it will not contribute to the zonal standard deviation. As noted earlier, in the troposphere, the flux perturbation~~signal~~ diffuses to the background state in about 3 months. Thus the zonal standard deviation field shown in **Figure 16** reflects shorter time scales than does the zonal mean of the ~~flux signal~~PAAF. That explains why curves in **Figure 16** do not have a trend in the troposphere as was seen in **Figures 13-15**. The zonal structure is largest in boreal summer in the lower troposphere (black curves in panels a-b) mainly due to the ~~flux signal~~PAAF in the northern extratropics (red curves). ~~This suggests GOSAT is capable of picking up finer spatial scales due to the high density of observations in this region when the satellite shifts its view to the northern hemisphere (**Figure 2**).~~ The impact of large flux increments in boreal summer was also seen in zonal mean fields in **Figures 7** and ~~**12**~~**S9**. In addition, a rather constant and large zonal standard deviation is seen in the tropics (blue curve in **Figure 16a**). This is consistent with the findings of Deng et al. (2016) and Byrne et al. (2017) that finer scale flux estimates can be obtained in the tropics with GOSAT glint observations. However, in the middle troposphere and above, the seasonal variation in zonal standard deviation diminishes, as occurred with the zonal mean ~~flux signal~~PAAF (**Figures 13-15**). Also the magnitude of the zonal standard deviation diminishes with height. In the stratosphere, while the magnitudes are small, a small trend is seen in the second year in panels d and e. This suggests that after one year of simulation some zonal asymmetry is being seen in the ~~flux signal~~PAAF and that transit times of surface flux perturbations to the stratosphere are longer than the three months needed to reach the mid-troposphere. This delayed response makes sense given that the mean age of air is about one year in the tropical lower stratosphere and increases to more than four years in the extratropical lower stratosphere (Andrews et al., 2001; Waugh and

Hall, 2002). Thus perturbations of stratospheric flow can be expected to have a delayed response to perturbations in surface fluxes.

Figure S16 is comparable to **Figure 16** but for the in situ-based fluxes. As with GOSAT data, seasonal variation in ~~flux signal~~PAAF is also seen in the lower and middle troposphere in the northern extratropics. There is also a seasonal variation in the zonal standard deviations in the tropics (**Figure S16a-b**). Spatial variations in the tropics are larger in boreal summer as well as in March 2011. The March 2011 event was also seen with GOSAT data and with both models (Fig. 18f) and may be related to the fact that enhanced CO_2 in tropical Asia was seen in commercial aircraft based in situ data in March to May 2011 (Basu et al., 2014, their figure 3). As with the GOSAT-based ~~flux signal~~PAAF, the magnitude of zonal standard deviations diminishes with altitude, and in the stratosphere, a trend in values is seen (**Figure S16d-e**). The differences in zonal asymmetry of ~~flux signal~~PAAF seen with the two observing systems are directly compared in **Figure 17**. Now it is clear that more zonal structure is apparent with GOSAT data in the lower and middle troposphere (**Figure 17a-b**). Also, the slightly greater zonal structure in stratospheric increments obtained with in situ data in the first year is also evident (**Figure 17d**). However, the ~~flux signal~~ PAAF in the stratosphere due to the assimilation of observations does not exceed that due to wind field uncertainty in the middle and upper stratosphere (**Figure 17e-f**). In the lower stratosphere (**Figure 17d**), the zonal structure in the first year is also not to be trusted. In the lower troposphere, zonal asymmetry in GOSAT ~~flux signal~~PAAFs exceeds that arising from wind field uncertainty except in November, December and January (**Figure 17a**). However, for in situ data, the zonal structure can only be trusted in boreal summer (June, July and August). Thus the satellite data are potentially able to retrieve fluxes on finer spatial scales than are in situ data through most of the year but it~~.~~ is important to note that more spatial structure does not mean correct spatial structure. Validation of spatial structures in posterior distributions needs to be made against a dense network of independent observations in order to determine if the increased spatial variation is correct. Given the difference in observation densities (**Figures 1** and **2**), this result is not surprising. The lack of ability of in situ data to produce zonal asymmetry in ~~flux signal~~posterior atmospheric adjustments (PAAFs) that are larger than those arising from uncertainty in wind fields (PAAMs) outside of boreal summer may indicate why it has been difficult for flux inversions to regionally attribute sources with this observation network (e.g. Gurney et al., 2002, Peters et al., 2010, Bruhwiler et al., 2011, Peylin et al., 2013).

Contributions of the 3 zonal bands to the globally averaged zonal standard deviations are shown in **Figure 18**. In the northern extratropics, GOSAT data produce zonal structures that exceeds errors due to wind field uncertainty from May to October in the lower troposphere (**Figure 18a**), from June to September in the middle troposphere (**Figure 18b**) and in July and August in the upper troposphere (**Figure 18c**). However, the in situ data produce zonal structure that cannot be trusted except in July, August and September in the lower troposphere (**Figure 18a**). In the tropics, zonal structure is evident in CO_2 fields forced by GOSAT posterior fluxes in the lower troposphere at all times (**Figure 18d**). In the middle troposphere, the tropical zonal structure can be trusted in August, September, October (**Figure 18e**). For the CO_2 fields informed by in situ observations, the zonal structure in the tropics is trustable only in July, August and September in the lower and middle troposphere (**Figure 18d-e**). In August and September 2010, in the upper troposphere (**Figure 18f**), both GOSAT and in situ data produce zonal structure that exceeds that arising from uncertain wind fields. Both models also produce qualitatively similar results with the exception of the tropical lower troposphere (**Figure 18d**) and the UTLS region in the second year (**Figure 18c, i**) where GEM-MACH-GHG produces more zonal structure. Given the much higher resolution (horizontally and vertically) of this model, it can generate finer scale structures from the coarse resolution fluxes that eventually propagate to the stratosphere. The differences may also be due to the higher resolution of GEM-MACH-GHG directly producing spatial variations in UTLS flow and in the tropics.

In this subsection, the zonal standard deviations of the ~~flux signal~~PAAF were examined in a global sense and in terms of contributions to the global values. The potential benefit of the higher density GOSAT observations is clearly evident in enhanced zonal structures particularly in the northern extratropics in boreal summer and in the tropics, year round. These values exceed the uncertainty in CO_2 due to uncertain meteorology much of the time. However, these diagnostics can only indicate a potential benefit since the increased zonal variation was not validated against independent measurements. While this type of validation is not yet possible because it requires high resolution, globally distributed, independent measurement networks, Houweling et al. (2015) found that flux inversions with GOSAT data do not agree with each other on subcontinental scales. They conclude that flux inversions using GOSAT data do not sufficiently constrain regional scale fluxes.

4 Summary and Discussion

The results from flux inversion analyses are difficult to verify due to the lack of a dense, global network of flux measurements. In this work, we demonstrate that it is possible to glean useful information about flux inversion results by looking at the changes made to the tracer fields. The data assimilation process yields updates to prior fluxes, or "flux increments", but here we consider the tracer field increment. This increment is denoted the posterior atmospheric adjustment (PAA) and refers to the change in concentrations obtained from a model integration using posterior fluxes, initial states and wind fields relative to those from another integration using prior fluxes, initial states and wind fields. We show that there are many components to the PAA and consider two of these: posterior atmospheric adjustments due to fluxes (PAAF) and those due to meteorological uncertainty (PAAM). By comparing PAAF and PAAM, we obtain a new diagnostic for assessing retrieved fluxes. Specifically, when PAAF exceeds PAAM, atmospheric changes due to fluxes exceed those due to random perturbations in meteorological fields and should be more thoroughly verified against independent measurements. When this does not occur, PAAF is not robust against some types of transport error (namely, that due to imperfect meteorology).

27

This information will be useful for inverse model intercomparisons. The diagnostic could also be extended to check that PAAF also exceeds adjustments arising from initial condition updates.

Although our new diagnostic depends on the model and prior fluxes used, as is always the case with diagnostics based on analysis increments, we demonstrate its utility by comparing flux inversion results obtained with the GEOS-Chem 4D-Var system and two different observing systems: in situ (Deng et al. 2014) and GOSAT (Deng et al. 2016). ~~In this work, we have examined how fluxes retrieved with the GEOS-Chem flux inversion system and in situ and GOSAT observations inform CO_2 model simulations throughout the troposphere and lower stratosphere. We defined the flux signal as the CO_2 distribution obtained with posterior fluxes minus that obtained with prior fluxes. The flux signal therefore reflects the influence of observations in the recent past as well as the accumulated influence of observations in the distant past. By definition, the flux signal is a function of both the transport model and the prior fluxes used.~~ The largest contribution to the global ~~flux signal~~PAAF in the troposphere is from the northern extratropics but the stratospheric signal primarily reflects tropical influence (**Figure 14~~2~~**). The global ~~flux signal~~PAAF due to GOSAT observations has much stronger seasonal variations than that due to in situ observations (**Figure 13**). Furthermore, a difference of about 0.5 ppm is seen between the simulations obtained using GOSAT and in situ posterior fluxes with the latter agreeing better with observations (TCCON, HIPPO-3 in the northern extratropics above the middle troposphere, and NOAA aircraft on annual time scales) (**Figures 8, 10, S10, S12, S13~~4~~**). The inversion constrained by GOSAT data does not recover the global mean flux as well as the in situ inversion on these long time scales. However, GOSAT-informed CO_2 distributions can be revealed to better capture the seasonal cycle at most northern extratropical TCCON sites (**Figure 9, S11~~2~~**). Zonal standard deviations of the ~~flux signal~~PAAF (which reveal spatial structures in the zonal direction) are much larger when GOSAT-informed posteriors are used (in the northern extratropics outside of boreal winter and in the tropics throughout the year) (**Figure 16, 17**). ~~This indicates a potential for GOSAT data to retrieve finer scale fluxes since the accuracy of such finer scale features requires a dense network of independent measurements to validate.~~

Since the ~~flux signal~~PAAF depends on the transport model used, we used two different models (GEOS-Chem and GEM-MACH-GHG) to define the ~~flux signal~~PAAF. Since GEOS-Chem was used for the flux inversions, subsequent integrations of posterior fluxes are consistent with the transport assumed during the flux inversion. However, the posterior CO_2 distributions obtained with GEM-MACH-GHG convolve its transport model error with that of GEOS-Chem. Indeed, a difference in model transport times to the southern hemisphere was seen. Yet despite this caveat, all of the main conclusions held for both models. Moreover, the use of GEM-MACH-GHG, which is a coupled meteorology-tracer transport model, permitted the calculation of uncertainties in posterior CO_2 distributions due to uncertain wind fields (PAAM). Actual meteorological analysis errors were used to perturb wind fields and repeat all simulations (see supplemental material). The impact of perturbed wind fields on CO_2 distributions was used to define a minimum level of uncertainty (since in reality, model integrations of CO_2 will also include errors from fluxes, model formulation and representativeness as well as the inevitable imperfections from meteorological analyses). This error was useful for determining when spatial scales (departure from zonal symmetry) ~~could be trusted~~ are robust against transport error arising from meteorological uncertainty although, being a minimum error, it provides an optimistic assessment. In situ observations were found to generate zonal standard deviations larger than this minimum level only in boreal summer whereas GOSAT data exceeded this threshold through most of the year (**Figure 17~~6~~, 18~~7~~**). This potential for retrieving finer spatial scales with GOSAT sampling relative to the in situ network makes sense given the density of GOSAT observations (**Figure 2**) and is consistent with the prediction of Takagi et al. (2014) or Deng et al. (2016). Moreover, the ability to retrieve zonal structure is evident throughout the year in the tropics and in all seasons except boreal winter in the northern extratropics is rather encouraging. However, verifying such finer scales will be challenging given the limited spatial coverage of validating measurements from TCCON or aircraft platforms and temporal and spatial scales resolved may depend on the characteristics of the flux inversion system. Indeed, the current dispute over the enhanced European sinks obtained with GOSAT data (Feng et al., 2016; Reuter et al., 2014; Houweling et al., 2015) indicates that the finer spatial scales retrieved are not necessarily correct and are difficult to validate. It is plausible that spurious zonal structures in the PAAF could be introduced by spatially varying biases in the observations or uneven spatial coverage. However, there is also evidence supporting the ability of space-based observations to recover zonal asymmetries in the CO_2 fields. Liu et al. (2017) use observations from GOSAT and OCO-2 to isolate tropical flux anomalies between continents during the 2015-2016 El Niño event, while Chatterjee et al. (2017) found that zonal asymmetries in XCO2 anomalies could be isolated during the same El Niño event. Furthermore, the fact that the spatial structure seen in ~~flux signals~~PAAFs obtained with in situ data surpassed the minimum uncertainty level only in boreal summer implies that regional attribution of fluxes may be challenging with the in situ observation network alone when the inversion integrates signals over many seasons. Because our uncertainty arises from imperfect meteorological analyses, its impact cannot be seen in flux inversions obtained from a single model forced by a single set of driving meteorological fields. However, this error source should be evident in multi-system comparison studies when the systems use different sources of meteorological fields.

By examining the behaviour of each observing system separately, it was possible to isolate differences in their impact on posterior fluxes obtained with our flux inversion system. In particular, it is found that the in situ observing system results in posterior fluxes that well define the global mean CO_2 on annual time scales and that there is a dependence of seasonal variations of the global ~~flux signal~~ PAAF on observation system. However both systems defined the annual budget for 2010 equally well. ~~GOSAT was also shown to potentially better retrieve finer spatial scales within a zonal band.~~ The importance of these results is two-fold. First, the implications are that caution should be exercised when drawing conclusions based on sub-annual variations of the global mean CO_2 because they depend on the observation sets used. Since CO_2 has strong seasonal variations, the ~~flux signal~~ PAAF in the lower atmosphere should also have seasonal variations if the prior fluxes have errors on seasonal timescales (e.g. as in Liu et al., 2014, or Ott et al., 2015). The challenge is that the seasonal variation of GOSAT data coverage will be convolved with an actual seasonal variation of fluxes. Second, our results identify ~~spati~~temporal scales of atmospheric CO_2 that are best constrained by each observing network, in the context of our flux inversion system. Specifically, the in situ network captures global mean (and the 18-month mean at most TCCON stations) well, while GOSAT better captures ~~zonally asymmetric structures and~~ the seasonal cycle at northern extratropical TCCON sites. Understanding the time scales resolved by different observing systems will be critical for the CO_2 assimilation problem with coupled meteorological and GHG transport models at operational centers which are geared toward short assimilation windows (e.g. Polavarapu et al., 2016; Agusti-Panareda et al., 2014; Massart et al., 2016; Ott et al., 2015). For such systems, long time scale information will be challenging to extract from observations and may require novel multi-time scale analysis approaches.

While our results regarding the behaviour of each observing system has important implications for flux estimation, they must be seen in the context of the inversion system used, namely, GEOS-Chem and 4D-Var with long assimilation windows. Aspects of the inversion system may impact the results. For this reason, repetition of our experiments with other inversion systems is desirable to determine the generality of results across inversion systems. Furthermore, we suggest that comparing ~~flux signal~~PAAFs obtained by integrating a single model with known transport behaviour with posterior fluxes from various different inversion systems could be a useful diagnostic because it will identify relative mismatches of transport times between models. For example, CT2013B fluxes with our weather model (GEM-MACH-GHG) identified a mismatch in transport of midlatitude fluxes in boreal summer to the high Arctic in autumn with TM5 (Polavarapu et al., 2016) as well as a too fast transport of GEOS-Chem from the tropics to the southern hemisphere relative to GEM-MACH-GHG. While this diagnostic cannot determine which model's transport is correct, if the reference model's transport issues were known (from age-of-air diagnostics, for example), the ~~flux signal~~PAAF comparison offers a fast, simple way to infer transport issues of other models. However, only obvious transport mismatches would be identifiable. Regional, or shorter timescale transport mismatches would be hard to identify with a sparse verifying observation network. Indeed, as a result of this work, we plan to identify GEM-MACH-GHG's transport issues through age-of-air diagnostics in the future.

Although only GOSAT-based flux inversions were considered here, it is natural to wonder if the results would apply to OCO-2. Byrne et al. (2017) note that OCO-2 has higher spatial resolution and higher precision (due to aggregation of measurements in 2x2.5 grid) and that OCO-2 is better at picking up NH extratropical fluxes than GOSAT (their Fig. 10). OCO-2 also had the best constraints on regional fluxes in the tropics. It is easy to speculate that even finer spatial scales than seen here with GOSAT data could be expected to exceed meteorological uncertainties. However, OCO-2 also has a seasonal variation in coverage which has been shown to produce a bias in global annual flux (Liu et al., 2014). Although Liu et al., (2014), and Houweling et al., (2015) suggest that flux inversion systems are partly to blame by not permitting seasonal correlations of error covariances, it may be desirable to obtain additional measurements of the northern hemisphere during boreal winter. GOSAT, OCO-2 and TanSat measure in the shortwave infrared range so their latitudinal coverage does vary seasonally. The seasonal variation of coverage could be reduced if more nadir observations over snow covered regions were processed for the winter or more ocean glint observations were made in winter. (However, signal-to-noise ratio for the CO_2 bands is lower over snow, so retrieving over snow will typically result in poorer precision than over other surfaces.) Furthermore, active measurements such as Active Sensing of CO2 Emissions over Nights, Days and Seasons (ASCENDS) (https://decadal.gsfc.nasa.gov/ascends.html) that do not depend on sunlight would complement the current network of in situ and satellite measurements.

In this work, we have separately considered the impact of in situ and GOSAT data on posterior CO_2 distributions in order to better understand the behaviour of each type of observation in the context of a flux inversion and modelling system. Ultimately, the best network will be a combination of both types of observation (Baker et al., 2006). By revealing the complementary benefits of the two types of observations, our results indicate a need for further research to understand how best to adapt flux inversion systems to take advantage of each type of observation. For example, in situ data could constrain biases in satellite data as in Feng et al. (2016) but perhaps also the long time scale global mean, with satellite data being used to improve regional scale fluxes.

5 Appendix A

The GEOS-Chem adjoint model (Henze et al., 2007) calculates the derivative of the modeled CO_2 concentration with respect to a set of model parameters, f. We use the adjoint model to calculate the sensitivity of modelled CO_2 concentrations to an earlier atmospheric CO_2 state over a volume of atmosphere with units of parts per million by volume (ppm) and use the adjoint model to calculate the gradient $\nabla_f J$. For this study, J is defined as the mean CO_2 concentration over 20°S-20°N and 500-250 hPa at instantaneous time t_0:

$$J = \left[\sum_{k=500hPa}^{250hPa} \sum_{j=-20°}^{20°} \sum_{i=0°}^{360°} \frac{C_{i,j,k,t_0}}{M_{i,j,k,t_0}} \right] \cdot 10^6 \quad \text{(A1)}$$

where C_{i,j,k,t_0} and M_{i,j,k,t_0} are the molar abundances of CO_2 and air at longitude i, latitude j, level k, and time t_0. Gas abundances are obtained by sampling a forward model simulation at the time t_0. The sensitivity is obtained by calculating the gradient of J with respect to an earlier atmospheric CO_2 state, $f_{i,j,k,t}$:

$$\gamma_{i,j,k,t} = \frac{\partial J}{\partial f_{i,j,k,t}}. \quad \text{(A2)}$$

Acknowledgements

Work at the University of Toronto was supported by funding from the Canadian Space Agency, Environment and Climate Change Canada, and the Natural Science and Engineering Research Council of Canada. We are grateful to Ray Nassar and Douglas Chan for helpful comments on an earlier version of this manuscript. ACOS GOSAT data were produced by the ACOS/OCO-2 project at the Jet Propulsion Laboratory (JPL), California Institute of Technology, and obtained from the JPL website, co2.jpl.nasa.gov. We acknowledge the GOSAT Project for acquiring these spectra. TCCON data were obtained from the TCCON Data Archive, hosted by the Carbon Dioxide Information Analysis Center (CDIAC) at http://tccon.ornl.gov/. We thank TCCON PIs Paul Wennberg, Caltech (Lamont, Park Falls), David Griffith, University of Wollongong (Darwin and Wollongong), Justus Notholt, University of Bremen (Bremen), Nicholas Deutscher, University of Bremen (Bialystok), Thorsten Warneke, University of Bremen (Orleans), Dave Pollard, NIWA (Lauder), Ralf Sussmann, IMKIFU (Garmisch), Kimberly Strong, University of Toronto (Eureka), Rigel Kivi, FMI (Sodankylä), Frank Hase, KIT (Karlsruhe), and Matthias Schneider, KIT (Izaña). We are grateful to Colm Sweeney (NOAA ESRL) for providing the NOAA aircraft profiles and to Ken Masarie of the NOAA Global Monitoring Division in Boulder, Colorado for compiling ObsPack2013. The National Oceanic and Atmospheric Administration (NOAA) North American Carbon Program has funded NOAA/ESRL Global Greenhouse Gas Reference Network Aircraft program. The ObsPack data were obtained for the period 2000-2012 (obspack_co2_1_PROTOTYPE_v1.0.4_2013-11-25) from http://dx.doi.org/10.3334/OBSPACK/1001. We are grateful to NSF and NOAA for producing and providing HIPPO-2 (http://hippo.ucar.edu) aircraft measurements (HIPPO Merged 10-second Meteorology, Atmospheric Chemistry, Aerosol Data (R_20121129)). We would like to thank Doug Worthy of Atmospheric Science and Technology Directorate (ASTD), Environment and Climate Change Canada, for developing and maintaining ECCC's greenhouse gas measurement network and for providing the CO_2 concentration measurement data.

References

Andrews, A. E., et al. :, Mean ages of stratospheric air derived from in situ observations of CO2, CH4, and N2O, J. Geophys. Res., 106(D23), 32295–32314, doi:10.1029/2001JD000465, 2001.

Agustí-Panareda, A., Massart, S., Chevallier, F., Boussetta, S., Balsamo, G., Beljaars, A., Ciais, P., Deutscher, N. M., Engelen, R., Jones, L., Kivi, R., Paris, J.-D., Peuch, V.-H., Sherlock, V., Vermeulen, A. T., Wennberg, P. O., and Wunch, D.: Forecasting global atmospheric CO2, Atmos. Chem. Phys., 14, 11959-11983, doi:10.5194/acp-14-11959-2014, 2014.

Andres, R. J., Gregg, J. S., Losey, L., Marland, G., and Boden, T. A.: Monthly, global emissions of carbon dioxide from fossil fuel consumption, Tellus B, 63(3), 309-327, doi:10.1111/j.1600-0889.2011.00530.x,2011.

Baker, D. F., Doney, S. C. and Schimel, D. S.: Variational data assimilation for atmospheric CO2, Tellus, 58B, 359-365, 2006.

Barnes, E. A., Parazoo, N., Orbe, C., and Denning, A. S.: Isentropic transport and the seasonal cycle amplitude of CO2 , J. Geophys. Res.-Atmos., 121(13), 8106–8124.

Basu, S., Guerlet, S., Butz, A., Houweling, S., Hasekamp, O., Aben, I., Krummel, P., Steele, P., Langenfelds, R., Torn, M., Biraud, S., Stephens, B., Andrews, A., and Worthy, D.: Global CO2 fluxes estimated from GOSAT retrievals of total column CO2, Atmos. Chem. Phys., 13, 8695-8717, https://doi.org/10.5194/acp-13-8695-2013, 2013.

Basu, S., Krol, M., Butz, A., Clerbaux, C., Sawa, Y., Machida, T., Matsueda, H., Frankenberg, C. , Hasekamp, O. P., and Aben, I.: The seasonal variation of the CO2 flux over Tropical Asia estimated from GOSAT, CONTRAIL, and IASI, Geophys. Res. Lett., 41, 1809–1815, doi:10.1002/2013GL059105, 2014.

Butz, A., Guerlet, S., Hasekamp, O., Schepers, D., Galli, A., Aben, I., Frankenbert, C. F., Hartmann, J.-M., Tran, H., Kuze, A., Keppel-Aleks, G., Toon, G., Wunch, D., Wennberg, P., Deutscher, N., Griffith, D. G., Macatangay, R., Messerschmidt, J., Notholt, J., Warneke, T.: Toward accurate CO2 and CH4 observations from GOSAT, Geophys. Res. Lett., 38, L14812, doi:10.1029/2011GL047888, 2011.

Blumenstock, T., Hase, F., Schneider, M., García, O. E., and Sepúlveda, E.: TCCON data from Izana, Tenerife, Spain, Release GGG2014R0, TCCON data archive, hosted by the Carbon Dioxide Information Analysis Center, Oak Ridge National Laboratory, Oak Ridge, Tennessee, USA, doi:10.14291/tccon.ggg2014.izana01.R0/1149295, 2014.

Bruhwiler, L. M. P., Michalak, A. M., and Tans, P. P.: Spatial and temporal resolution of carbon flux estimates for 1983–2002, Biogeosciences, 8, 1309-1331, doi:10.5194/bg-8-1309-2011, 2011.

Byrne, B., D. Jones, B. A., Strong, K., Zeng, Z.-C., Deng, F., and Liu, J.: Sensitivity of CO_2 surface flux constraints to observational coverage, J. Geophys. Res. Atmos., 122, 6672–6694, doi:10.1002/2016JD026164, 2017

Chaterjee, A.Gierach, M. M., Sutton, A. J., Feely, R. A., Crisp, D., Eldering, A., Gunson, M. R., O'Dell, C. W., Stephens, B. B. and Schimel, D. S.: Influence of El Niño on atmospheric CO_2 over the tropical Pacific Ocean: Findings from NASA's OCO-2 mission, Science 358 (6360), eaam5776. DOI: 10.1126/science.aam5776

Chen, J. M., Mo, G., Pisek, J., Liu, J., Deng, F., Ishizawa, M. and Chan, D.: Effects of foliage clumping on the estimation of global terrestrial gross primary productivity, Global Biogeochemical Cycles, 26, doi:10.1029/2010gb003996, 2012.

Conway, T. J. and Tans, P. P.: Trends in atmospheric carbon dioxide: http://www.esrl.noaa.gov/gmd/ccgg/trends, last access: April 2012.

Corbett, J. J.: Considering alternative input parameters in an activity-based ship fuel consumption and emissions model: Reply to comment by Øyvind Endresen et al. on "Updated emissions from ocean shipping", Journal of Geophysical Research, 109(D23), doi:10.1029/2004jd005030, 2004.

Chevallier, F., Feng, L., Bösch, H., Palmer, P.I. and Rayner: On the impact of transport model errors for the estimation of CO2 surface fluxes from GOSAT observations, Geophys. Res. Lett., 37, L21803, doi:10.1029/2010GL044652, 2010.

Chevallier, F., Palmer, P.I., Feng, L., Boesch, H., O'Dell, C. W. and Bousquet, P.: Toward robust and consistent regional CO2 flux estimates from in situ and spaceborne measurements of atmospheric CO2, Geophys. Res. Lett., 41, 1065–1070, doi:10.1002/2013GL058772, 2014.

Ciais, P., Sabine, C., Bala, G., Bopp, L., Brovkin, V., Canadell, J., Chhabra, A., DeFries, R., Galloway, J., Heimann, M., Jones, C., Le Quéré, C., Myneni, R.B., Piao S., and Thornton, P.: Carbon and Other Biogeochemical Cycles. In: Climate Change 2013: The Physical Science Basis. Contribution of Working Group I to the Fifth Assessment Report of the Intergovernmental Panel on Climate Change [Stocker, T.F., D. Qin, G.-K. Plattner, M. Tignor, S.K. Allen, J. Boschung, A. Nauels, Y. Xia, V. Bex and P.M. Midgley (eds.)]. Cambridge University Press, Cambridge, United Kingdom and New York, NY, USA, 2013.

Conway, T. J., Lang, P. M., and Masarie, K. A.: Atmospheric Carbon Dioxide Dry Air Mole Fractions from the NOAA ESRL Carbon Cycle Cooperative Global Air Sampling Network, 1968-2010, Version: 2011-10-14, ftp://ftp.cmdl.noaa.gov/ccg/co2/flask/event/ 2011, 2011.

Corbett, J. J., and Koehler, H. W.: Updated emissions from ocean shipping, J. Geophys. Res., 108(D20), 4650-4666, doi:10.1029/2003jd003751, 2003.

Corbin, K. D., Denning, A. S., and Parazoo, N. C.: Assessing temporal clear-sky errors in assimilation of satellite CO2 retrievals using a global transport model, Atmos. Chem. Phys., 9, 3043-3048, doi:10.5194/acp-9-3043-2009, 2009.

Crisp, D. and OCO-2 Science Team, Measuring Atmospheric Carbon Dioxide from Space with the Orbiting Carbon Observatory-2 (OCO-2) Proc. SPIE 9607, Earth Observing Systems XX, 960702. doi:10.1117/12.2187291, 2015.

Crisp, D., Pollock, H. R., Rosenberg, R., Chapsky, L., Lee, R. A. M., Oyafuso, F. A., Frankenberg, C., O'Dell, C. W., Bruegge, C. J., Doran, G. B., Eldering, A., Fisher, B. M., Fu, D., Gunson, M. R., Mandrake, L., Osterman, G. B., Schwandner, F. M., Sun, K., Taylor, T. E., Wennberg, P. O., and Wunch, D.: The on-orbit performance of the Orbiting Carbon Observatory-2 (OCO-2) instrument and its radiometrically calibrated products, Atmos. Meas. Tech., 10, 59-81, https://doi.org/10.5194/amt-10-59-2017 , 2017.

Deng, F., and Chen, J. M.: Recent global CO2 flux inferred from atmospheric CO2 observations and its regional analyses, Biogeosciences, 8(11), 3263-3281, doi:10.5194/bg-8-3263-2011, 2011.

Deng, F., Chen, J. M., Plummer, S., Chen, M. Z. and Pisek, J.: Algorithm for global leaf area index retrieval using satellite imagery, IEEE Transactions on Geoscience and Remote Sensing, 44(8), 2219-2229, doi:10.1109/tgrs.2006.872100, 2006.

Deng, F., Jones, D. B. A., Henze, D. K., Bousserez, N., Bowman, K.W., Fisher, J. B., Nassar, R., O'Dell, C., Wunch, D., Wennberg, P. O., Kort, E. A., Wofsy, S. C., Blumenstock, T., Deutscher, N. M., Griffith, D. W. T., Hase, F., Heikkinen, P., Sherlock, V., Strong, K., Sussmann, R., and Warneke, T.: Inferring regional sources and sinks of atmospheric CO2 from GOSAT XCO2 data, Atmos. Chem. Phys., 14, 3703–3727, doi:10.5194/acp-14-3703-2014, 2014.

Deng, F., Jones, D. B. A., Walker, T. W., Keller, M., Bowman, K. W., Henze, D. K., Nassar, R., Kort, E. A., Wofsy, S. C., Walker, K. A., Bourassa, A. E., and Degenstein, D. A.: Sensitivity analysis of the potential impact of discrepancies in stratosphere–troposphere exchange on inferred sources and sinks of CO2, Atmos. Chem. Phys., 15, 11773-11788, doi:10.5194/acp-15-11773-2015, 2015.

Deng, F., Jones, D. B. A., O'Dell, C. W., Nassar, R. and Parazoo, N. C.: Combining GOSAT XCO2 observations over land and ocean to improve regional CO2 flux estimates, J. Geophys. Res. Atmos., 121, 1896–1913, doi:10.1002/2015JD024157, 2016.

Deutscher, N., Notholt, J., Messerschmidt, J., Weinzierl, C., Warneke, T., Petri, C., Grupe, P., and Katrynski, K.: TCCON data from Bialystok, Poland, Release GGG2014R0, TCCON data archive, hosted by the Carbon Dioxide Information

Analysis Center, Oak Ridge National Laboratory, Oak Ridge, Tennessee, USA, doi:10.14291/tccon.ggg2014.bialystok01.R0/1149277, 2014.

Endresen, Ø., Sørgård, E., Bakke, J. and Isaksen, I. S. A.: Substantiation of a lower estimate for the bunker inventory: Comment on "Updated emissions from ocean shipping" by James J. Corbett and Horst W. Koehler, J. Geophys. Res., 109(D23), D23302, doi:10.1029/2004jd004853, 2004.

Endresen, Ø., Sørgård, E., Behrens, H. L., Brett, P. O. and Isaksen, I. S. A., A historical reconstruction of ships' fuel consumption and emissions, J. Geophys. Res., 112(D12), D12301, doi:10.1029/2006jd007630, 2007.

Feng, L., Palmer, P. I., Parker, R. J., Deutscher, N. M., Feist, D. G., Kivi, R., Morino, I., and Sussmann, R.: Estimates of European uptake of CO2 inferred from GOSAT XCO2 retrievals: sensitivity to measurement bias inside and outside Europe, Atmos. Chem. Phys., 16, 1289-1302, doi:10.5194/acp-16-1289-2016, 2016.

Friedl , R. R.: Atmospheric effects of subsonic aircraft: interim assessment report of the Advanced Subsonic Technology Program, edited, p. 168, National Aeronautics and Space Administration, Goddard Space Flight Center, Greenbelt, MD United States, 1997.

Griffith, D. W. T., Deutscher, N., Velazco, V. A., Wennberg, P. O., Yavin, Y., Aleks, G. K., Washenfelder, R., Toon, G. C., Blavier, J.-F., Murphy, C., Jones, N., Kettlewell, G., Connor, B., Macatangay, R., Roehl, C., Ryczek, M., Glowacki, J., Culgan, T., and Bryant, G.: TCCON data from Darwin, Australia, Release GGG2014R0, TCCON data archive, hosted by the Carbon Dioxide Information Analysis Center, Oak Ridge National Laboratory, Oak Ridge, Tennessee, USA, doi:10.14291/tccon.ggg2014.darwin01.R0/1149290, 2014a.

Griffith, D. W. T., Velazco, V. A., Deutscher, N., Murphy, C., Jones, N., Wilson, S., Macatangay, R., Kettlewell, G., Buchholz, R. R., and Riggenbach, M.: TCCON data from Wollongong, Australia, Release GGG2014R0, TCCON data archive, hosted by the Carbon Dioxide Information Analysis Center, Oak Ridge National Laboratory, Oak Ridge, Tennessee, USA, doi:10.14291/tccon.ggg2014.wollongong01.R0/1149291, 2014b.

Gurney, K. R., et al.: Towards robust regional estimates of CO2 sources and sinks using atmospheric transport models, Nature, 415, 626– 630, 2002.

Gurney, K. R., Law, R. M. , Denning, A. S., Rayner, P. J., Baker, D., Bousquet, P., Bruhwiler, L., Chen, Y.-H., Ciais, P., Fan, S., Fung, I. Y. , Gloor, M., Heimann, M., Higuchi, K., John, J., Kowalczyk, E., Maki, T., Maksyutov, S., Peylin, P., Prather, M., Pak, B. C., Sarmiento, J., Taguchi, S., Takahashi, T. and Yuen C.-W., TransCom 3 CO2 inversion intercomparison: 1. Annual mean control results and sensitivity to transport and prior flux information, Tellus, 55B, 555-579, 2003.

Hase, F., Blumenstock, T., Dohe, S., Groß, J., and Kiel, M.: TCCON data from Karlsruhe, Germany, Release GGG2014R1, TCCON data archive, hosted by the Carbon Dioxide Information Analysis Center, Oak Ridge National Laboratory, Oak Ridge, Tennessee, USA, doi:10.14291/tccon.ggg2014.karlsruhe01.R1/1182416, 2014.

Henze, D. K., Hakami, A. and Seinfeld, J. H.: Development of the adjoint of GEOS-Chem, Atmos. Chem. Phys., 7(9), 2413–2433, 2007.

Houtekamer, P.L., Deng, X., Mitchell, H.L., Baek, S.-J. and Gagnon, N.: Higher Resolution in an Operational Ensemble Kalman Filter, Mon. Wea. Rev., 142, 1143-1162, 2014.

Houweling, S., Aben, I., Breon, F.-M., Chevallier, F., Deutscher, N., Engelen, R., Gerbig, C., Griffith, D., Hungershoefer, K., Macatangay, R., Marshall, J., Notholt, J., Peters, W., and Serrar, S.: The importance of transport model uncertainties for the estimation of CO2 sources and sinks using satellite measurements, Atmos. Chem. Phys., 10, 9981-9992, doi:10.5194/acp-10-9981-2010, 2010.

Houweling, S., Baker, D., Basu, S. Boesch, H., Butz, A., Chevallier, F., Deng, F., Dlugokencky, E. J., Feng, L., Ganshin, A., Hasekamp, O., Jones, D., Maksyutov, S., Marshall, J., Oda, T., O’Dell, C. W., Oshchepkov, S., Palmer, P. I., Peylin, P., Poussi, Z., Reum, F., Takagi, H., Yoshida, Y., and Zhuravlev, R.: An intercomparison of inverse models for estimating sources and sinks of CO2 using GOSAT measurements. J. Geophys. Res. Atmos., 120, 5253–5266. doi:10.1002/2014JD022962, 2015.

Kain, J.S., and Fritsch, J.M.: A one-dimensional entraining/detraining plume model and its application in convective parameterizations, J. Atmos. Sci. 47, 2784-2802, 1990.

Kain, J.S.: The Kain-Fritsch convective parameterization: an update, J. Appl. Meteorol. 43, 170-181, 2004.

Kalnay, E., et al.: The NCEP/NCAR 40-Year Reanalysis Project, Bulletin of the American Meteorological Society, 77(3), 437-471, doi:10.1175/1520-0477(1996)077<0437:TNYRP>2.0.CO;2, 1996.

Keeling, C. D.: The concentration and isotopic abundances of carbon dioxide in the atmosphere. Tellus B, 12, 200–203, 1960.

Keppel-Aleks, G., Wennberg, P. O., and Schneider, T.: Sources of variations in total column carbon dioxide, Atmos. Chem. Phys., 11, 3581-3593, https://doi.org/10.5194/acp-11-3581-2011, 2011.

Keppel-Aleks, G., Wennberg, P. O., Washenfelder, R. A., Wunch, D., Schneider, T. and co-authors: The imprint of surface fluxes and transport on variations in total column carbon dioxide. Biogeosciences. 9, 875 891. DOI: 10.5194/bg-9-875-2012, 2012.

Kim, B. Y., et al.: System for assessing Aviation's Global Emissions (SAGE), Part 1: Model description and inventory results, Transportation Research Part D: Transport and Environment, 12(5), 325-346, doi:10.1016/j.trd.2007.03.007, 2007.

Kim, J., Kim, H. M., Cho, C.-H., Boo, K.-O., Jacobson, A. R., Sasakawa, M., Machida, T., Arshinov, M., and Fedoseev, N.: Impact of Siberian observations on the optimization of surface CO2 flux, Atmos. Chem. Phys., 17, 2881-2899, https://doi.org/10.5194/acp-17-2881-2017, 2017.

Kivi, R., Heikkinen, P., and Kyro, E.: TCCON data from Sodankyla, Finland, Release GGG2014R0., TCCON data archive, hosted by the Carbon Dioxide Information Analysis Center, Oak Ridge National Laboratory, Oak Ridge, Tennessee, USA, doi:10.14291/tccon.ggg2014.sodankyla01.R0/1149280, 2014.

Kuze, A., Suto, H., Nakajima, M. and Hamazaki, T.: Thermal and near infrared sensor for carbon observation Fourier-transform spectrometer on the Greenhouse Gases Observing Satellite for greenhouse gases monitoring, Appl. Opt., 48(35), 6716-6733, 2009.

Lauvaux, T., and Davis, K. J.: Planetary boundary layer errors in mesoscale inversions of column-integrated CO2 measurements, J. Geophys. Res. Atmos., 119, 490–508, doi:10.1002/2013JD020175, 2014.

Law, R. M., Rayner, P. J., Denning, A. S., Erickson, D., Fung, I. Y., Heimann, M., Piper, S. C., Romonet, M., Taguchi, S., Taylor, J. A., Trudinger, C. M., and Watterson, I. G.: Variations in modeled atmospheric transport of carbon dioxide and the consequences for CO2 inversions, Global Biogeochem. Cy., 10(4), 783–796, 1996.

Le Quéré, C., Moriarty, R., Andrew, R. M., Canadell, J. G., Sitch, S., Korsbakken, J. I., Friedlingstein, P., Peters, G. P., Andres, R. J., Boden, T. A., Houghton, R. A., House, J. I., Keeling, R. F., Tans, P., Arneth, A., Bakker, D. C. E., Barbero, L., Bopp, L., Chang, J., Chevallier, F., Chini, L. P., Ciais, P., Fader, M., Feely, R. A., Gkritzalis, T., Harris, I., Hauck, J., Ilyina, T., Jain, A. K., Kato, E., Kitidis, V., Klein Goldewijk, K., Koven, C., Landschützer, P., Lauvset, S. K., Lefèvre, N., Lenton, A., Lima, I. D., Metzl, N., Millero, F., Munro, D. R., Murata, A., Nabel, J. E. M. S., Nakaoka, S., Nojiri, Y., O'Brien, K., Olsen, A., Ono, T., Pérez, F. F., Pfeil, B., Pierrot, D., Poulter, B., Rehder, G., Rödenbeck, C., Saito, S., Schuster, U., Schwinger, J., Séférian, R., Steinhoff, T., Stocker, B. D., Sutton, A. J., Takahashi, T., Tilbrook, B., van der Laan-Luijkx, I. T., van der Werf, G. R., van Heuven, S., Vandemark, D., Viovy, N., Wiltshire, A., Zaehle, S., and Zeng, N.: Global Carbon Budget 2015, Earth Syst. Sci. Data, 7, 349-396, doi:10.5194/essd-7-349-2015, 2015.

Lindqvist, H., O'Dell, C. W., Basu, S., Boesch, H., Chevallier, F., Deutscher, N., Feng, L., Fisher, B., Hase, F., Inoue, M., Kivi, R., Morino, I., Palmer, P. I., Parker, R., Schneider, M., Sussmann, R., and Yoshida, Y.: Does GOSAT capture the true seasonal cycle of carbon dioxide?, Atmos. Chem. Phys., 15, 13023-13040, doi:10.5194/acp-15-13023-2015, 2015.

Liu, J., Fung, I., Kalnay, E., and Kang, J.-S.: CO2 transport uncertainties from the uncertainties in meteorological fields, Geophys. Res. Lett., 38,L12808, doi:10.1029/2011GL047213, 2011.

Liu, J., Bowman, K. W., Lee, M., Henze, D. K., Bousserez, N., Brix, H., Collatz, G. J., Menemenlis, D., Ott, L., Pawson, S., Jones, D. and Nassar, R.: Carbon monitoring system flux estimation and attribution: impact of ACOS-GOSAT XCO2 sampling on the inference of terrestrial biospheric sources and sinks. Tellus B, 66, 1600-0889, http://dx.doi.org/10.3402/tellusb.v66.22486, 2014.

Liu, J., Bowman, K. W. and Henze, D. K.: Source-receptor relationships of column-average CO2 and implications for the impact of observations on flux inversions, J. Geophys. Res. Atmos., 120, 5214–5236, doi:10.1002/2014JD022914, 2015.

Liu, J., Bowman, K. W., Schimel, D. S., Parazoo, N. C., Jiang, Z., Lee, M., Bloom, A. A., Wunch, D., Frankenberg, C., Sun, Y., O'Dell, C. W., Gurney, I. R., Menemenlis, D., Gierach, M. Crisp, D., Eldering, A.: Contrasting carbon cycle responses of the tropical continents to the 2015-2016 El Niño, Science, 358 (6360), eaam5690. DOI:10.1126/science.aam5690

Maksyutov, S., Takagi, H., Valsala, V. K., Saito, M., Oda, T., Saeki, T., Belikov, D. A., Saito, R., Ito, A., Yoshida, Y., Morino, I., Uchino, O., Andres, R. J., and Yokota, T.: Regional CO2 flux estimates for 2009–2010 based on GOSAT and ground-based CO2 observations, Atmos. Chem. Phys., 13, 9351-9373, https://doi.org/10.5194/acp-13-9351-2013 , 2013.

Masarie, K. A., Peters, W., Jacobson, A. R., and Tans, P. P.: ObsPack: a framework for the preparation, delivery, and attribution of atmospheric greenhouse gas measurements, Earth Syst. Sci. Data, 6, 375-384, doi:10.5194/essd-6-375-2014, 2014.

Massart, S., Agustí-Panareda, A., Heymann, J., Buchwitz, M., Chevallier, F., Reuter, M., Hilker, M., Burrows, J. P., Hase, F., Desmet, F., Feist, D. G., and Kivi, R.: Ability of the 4-D-Var analysis of the GOSAT BESD XCO2 retrievals to characterize atmospheric CO2 at large and synoptic scales, Atmos. Chem. Phys. , 16, 1653-1671, doi:10.5194/acp-16-1653-2016, 2016.

Notholt, J., Petri, C., Warneke, T., Deutscher, N., Buschmann, M., Weinzierl, C., Macatangay, R., Grupe. P.: TCCON data from Bremen, Germany, Release GGG2014R0. TCCON data archive, hosted by the Carbon Dioxide Information Analysis Center, Oak Ridge National Laboratory, Oak Ridge, Tennessee, USA, doi:10.14291/tccon.ggg2014.bremen01.R0/1149275, 2014.

O'Dell, C. W., et al.: The ACOS CO2 retrieval algorithm – Part 1: Description and validation against synthetic observations, Atmospheric Measurement Techniques, 5(1), 99-121, doi:10.5194/amt-5-99-2012, 2012.

Osterman, G., Eldering, A., Avis, C., O'Dell, C., Martinez, E., Crisp, D., Frankenberg, C. and Frankenberg, B.: ACOS Level 2 Standard Product version B3.4, Data User's Guide (https://co2.jpl.nasa.gov/static/docs/v3.4_DataUsersGuide-RevB_131028.pdf), edited, p. 48, Jet Propulsion Laboratory, Pasadena, California, USA, 2013.

Ott, L. E., Pawson, S., Collatz, G. J., Gregg, W.W., Menemenlis, D., Brix, H., Rousseaux, C. S., Bowman, K. W., Liu, J., Eldering, A., Gunson, M. R., and Kawa, S.R.: Assessing the magnitude of CO2 flux uncertainty in atmospheric CO2 records using products from NASA's CarbonMonitoring Flux Pilot Project, J. Geophys. Res. Atmos., 120, doi:10.1002/2014JD022411, 2015.

Parazoo, N. C., Denning, A. S., Kawa, S. R., Pawson, S., and Lokupitiya, R.: CO2 flux estimation errors associated with moist atmospheric processes, Atmos. Chem. Phys., 12, 6405-6416, https://doi.org/10.5194/acp-12-6405-2012, 2012.

Peters, W., Jacobson, A. R., Sweeney, C., Andrews, A. E., Conway, T. J., Masarie, K., Miller, J. B., Bruhwiler, L. M. P., Pétron, G., Hirsch, A. I., Worthy, D. E. J., van der Werf, G. R., Randerson, J. T., Wennberg, P. O., Krol, M. C., and Tans, P. P.: An atmospheric perspective on North American carbon dioxide exchange: CarbonTracker, Proc. Nat. Acad. Sci., 104, 18925–18930, 2007.

Peters, W., Krol, M. C., Van Der Werf, G. R., Houweling, S., Jones, C. D., Hughes, J., Schaefer, K., Masarie, K. A., Jacobson, A. R., Miller, J. B., Cho, C. H., Ramonet, M., Schmidt, M., Ciattaglia, L., Apadula, F., Heltai, D., Meinhardt, F., DiSarra, A. G., Piacentino, S., Sferlazzo, D., Aalto, T., Hatakka, J., Ström, J., Haszpra, L., Meijer, H. A. J., Van der Laan, S., Neubert, R. E. M., Jordan, A., Rodó, X., Morguí, J.-A., Vermeulen, A. T., Popa, E., Rozanski, K., Zimnoch, M., Manning, A. C., Leuenberger, M., Uglietti, C., Dolman, A. J., Ciais, P., Heimann, M. and Tans, P. P.: Seven years of recent European net terrestrial carbon dioxide exchange constrained by atmospheric observations. Global Change Biology, 16: 1317–1337. doi:10.1111/j.1365-2486.2009.02078.x, 2010.

Peylin, P., Law, R. M., Gurney, K. R., Chevallier, F., Jacobson, A. R., Maki, T., Niwa, Y., Patra, P. K., Peters, W., Rayner, P. J., Rödenbeck, C., van der Laan-Luijkx, I. T., and Zhang, X.: Global atmospheric carbon budget: results from an ensemble of atmospheric CO2 inversions, Biogeosciences, 10, 6699-6720, doi:10.5194/bg-10-6699-2013, 2013.

Polavarapu, S. M., Neish, M., Tanguay, M., Girard, C., de Grandpré, J., Semeniuk, K., Gravel, S., Ren, S., Roche, S., Chan, D., and Strong, K.: Greenhouse gas simulations with a coupled meteorological and transport model: the predictability of CO2, Atmos. Chem. Phys., 16, 12005-12038, https://doi.org/10.5194/acp-16-12005-2016 , 2016.

Reuter, M., Buchwitz, M., Hilker, M., Heymann, J., Schneising, O., Pillai, D., Bovensmann, H., Burrows, J. P., Bösch, H., Parker, R., Butz, A., Hasekamp, O., O'Dell, C. W., Yoshida, Y., Gerbig, C., Nehrkorn, T., Deutscher, N. M., Warneke, T., Notholt, J., Hase, F., Kivi, R., Sussmann, R., Machida, T., Matsueda, H., and Sawa, Y.: Satellite-inferred European carbon sink larger than expected, Atmos. Chem. Phys., 14, 13739-13753, https://doi.org/10.5194/acp-14-13739-2014 , 2014.

Reuter, M., Buchwitz, M., Hilker, M. Heymann, J., Bovensmann, H., Burrows, J.P., Houweling, S., Liu, Y.Y., Nassar, R., Chevallier, F., Ciais, P., Marshall, J. and Reichstein, M.: How Much CO2 Is Taken Up by the European Terrestrial Biosphere?. Bull. Amer. Meteor. Soc., 98, 665–671, https://doi.org/10.1175/BAMS-D-15-00310.1 , 2017.

Sherlock, V. B., Connor, Robinson, J., Shiona, H., Smale, D., and Pollard, D.: TCCON data from Lauder, New Zealand, 125HR, Release GGG2014R0, TCCON data archive, hosted by the Carbon Dioxide Information Analysis Center, Oak Ridge National Laboratory, Oak Ridge, Tennessee, USA, doi:10.14291/tccon.ggg2014.lauder02.R0/1149298, 2014.

Strong, K., J. Mendonca, D. Weaver, P. Fogal, J.R. Drummond, R. Batchelor, R. Lindenmaier. 2014. TCCON data from Eureka, Canada, Release GGG2014R0. TCCON data archive, hosted by the Carbon Dioxide Information Analysis Center, Oak Ridge National Laboratory, Oak Ridge, Tennessee, U.S.A, doi:10.14291/tccon.ggg2014.eureka01.R0/1149271, 2014.

Sussmann, R. and Rettinger, M.: TCCON data from Garmisch, Germany, Release GGG2014R0, TCCON data archive, hosted by the Carbon Dioxide Information Analysis Center, Oak Ridge National Laboratory, Oak Ridge, Tennessee, USA, doi:10.14291/tccon.ggg2014.garmisch01.R0/1149299, 2014.

Sweeney, C., Karion, A., Wolter, S., Newberger, T., Guenther, D., Higgs, J. A., Andrews, A. E., Lang, P. M., Neff, D., Dlugokencky, E., Miller, J. B., Montzka, S. A., Miller, B. R., Masarie, K. A., Biraud, S. C., Novelli, P. C., Crotwell, M., Crotwell, A. M., Thoning, K. and Tans, P. P..: Seasonal climatology of CO_2 across North America from aircraft measurements in the NOAA/ESRL Global Greenhouse Gas Refernce Network, J. Geophys. Res. Atmos., 120, doi:10.1002/2014JD022591, 2015.

Takagi, H., Houweling, S., Andres, R. J., Belikov, D., Bril, A., Boesch, H., Butz, A., Guerlet, S., Hasekamp, O., Maksyutov, S., Morino, I., Oda, T., O'Dell, C. W., Oshchepkov, S., Parker, R., Saito, M., Uchino, O., Yokota, T., Yoshida, Y., Valsala, V., Influence of differences in current GOSAT XCO2 retrievals on surface flux estimation, Geophys. Res. Lett., 41, 2598–2605, doi:10.1002/2013GL059174, 2014.

Takahashi, T., et al.: Climatological mean and decadal change in surface ocean pCO2, and net sea-air CO2 flux over the global oceans, Deep Sea Research Part II: Topical Studies in Oceanography, 56(8-10), 554-577, 2009.

van der Werf, G. R., J. T. Randerson, L. Giglio, G. J. Collatz, M. Mu, P. S. Kasibhatla, D. C. Morton, R. S. DeFries, Y. Jin, and T. T. van Leeuwen: Global fire emissions and the contribution of deforestation, savanna, forest, agricultural, and peat fires (1997–2009), Atmos. Chem. Phys., 10(23), 11707-11735, doi:10.5194/acp-10-11707-2010, 2010.

Tans, P. and Thoning, K.: How we measure background levels of CO2 on Mauna Loa, 2016. Available from https://www.esrl.noaa.gov/gmd/ccgg/about/co2_measurements.pdf

Waugh, D.W., and Hall, T.M.: Age of stratospheric air: Theory, observations, and models. Rev. Geophys., 40, no. 4, 1010, doi:10.1029/2000RG000101, 2002.

Warneke, T., Messerschmidt, J., Notholt, J., Weinzierl, C., Deutscher, N., Petri, C., Grupe, P., Vuillemin, C., Truong, F., Schmidt, M., Ramonet, M., and Parmentier, E.: TCCON data from Orleans, France, Release GGG2014R0, TCCON data archive, hosted by the Carbon Dioxide Information Analysis Center, Oak Ridge National Laboratory, Oak Ridge, Tennessee, USA, doi:10.14291/tccon.ggg2014.orleans01.R0/1149276, 2014.

Wennberg, P. O., Roehl, C., Wunch, D., Toon, G. C., Blavier, J.-F., Washenfelder, R., Keppel-Aleks, G., Allen, N., and Ayers, J.: TCCON data from Park Falls, Wisconsin, USA, Release GGG2014R0, TCCON data archive, hosted by the Carbon Dioxide Information Analysis Center, Oak Ridge National Laboratory, Oak Ridge, Tennessee, USA, doi:10.14291/tccon.ggg2014.parkfalls01.R0/1149161, 2014a.

Wennberg, P. O., Wunch, D., Roehl, C., Blavier, J.-F., Toon, G. C., Allen, N., Dowell, P., Teske, K., Martin, C., and Martin, J.: TCCON data from Lamont, Oklahoma, USA, Release GGG2014R0, TCCON data archive, hosted by the Carbon Dioxide Information Analysis Center, Oak Ridge National Laboratory, Oak Ridge, Tennessee, USA, doi:10.14291/tccon.ggg2014.lamont01.R0/1149159, 2014b.

Wilkerson, J. T., M. Z. Jacobson, A. Malwitz, S. Balasubramanian, R. Wayson, G. Fleming, A. D. Naiman, and S. K. Lele (2010), Analysis of emission data from global commercial aviation: 2004 and 2006, Atmospheric Chemistry and Physics, 10(13), 6391-6408, doi:10.5194/acp-10-6391-2010.

Wofsy, S. C., Team, H. S., Cooperating, M., and Satellite, T.: HIAPER Pole-to-Pole Observations (HIPPO): fine-grained, global- scale measurements of climatically important atmospheric gases and aerosols, Phil. Trans. A Math. Phys. Eng. Sci., 369, 2073–2086, doi:10.1098/rsta.2010.0313, 2011.

Wofsy, S. C., B. C. Daube, R. Jimenez, E. Kort, J. V. Pittman, S. Park, R. Commane, B. Xiang, G. Santoni, D. Jacob, J. Fisher, C. Pickett-Heaps, H. Wang, K. Wecht, Q.-Q. Wang, B. B. Stephens, S. Shertz, A.S. Watt, P. Romashkin, T. Campos, J. Haggerty, W. A. Cooper, D. Rogers, S. Beaton, R. Hendershot, J. W. Elkins, D. W. Fahey, R. S. Gao, F. Moore, S. A. Montzka, J. P. Schwarz, A. E. Perring, D. Hurst, B. R. Miller, C. Sweeney, S. Oltmans, D. Nance, E. Hintsa, G. Dutton, L. A. Watts, J. R. Spackman, K. H. Rosenlof, E. A. Ray, B. Hall, M. A. Zondlo, M. Diao, R. Keeling, J. Bent, E. L. Atlas, R. Lueb, M. J. Mahoney. 2012. HIPPO Merged 10-second Meteorology, Atmospheric Chemistry, Aerosol Data (R_20121129). Carbon Dioxide Information Analysis Center, Oak Ridge National Laboratory, Oak Ridge, Tennessee, U.S.A. http://dx.doi.org/10.3334/CDIAC/hippo_010 (Release 20121129)

Wunch, D., Wennberg, P. O., Toon, G. C., Connor, B. J., Fisher, B., Osterman, G. B., Frankenberg, C., Mandrake, L., O'Dell, C., Ahonen, P., Biraud, S. C., Castano, R., Cressie, N., Crisp, D., Deutscher, N. M., Eldering, A., Fisher, M. L., Griffith, D. W. T., Gunson, M., Heikkinen, P., Keppel-Aleks, G., Kyrö, E., Lindenmaier, R., Macatangay, R., Mendonca, J., Messerschmidt, J., Miller, C. E., Morino, I., Notholt, J., Oyafuso, F. A., Rettinger, M., Robinson, J., Roehl, C. M., Salawitch, R. J., Sherlock, V., Strong, K., Sussmann, R., Tanaka, T., Thompson, D. R., Uchino, O., Warneke, T., and Wofsy, S. C.: A method for evaluating bias in global measurements of CO2 total columns from space, Atmos. Chem. Phys., 11, 12317–12337, doi:10.5194/acp-11-12317-2011, 2011.

Yevich, R., and J. A. Logan (2003), An assessment of biofuel use and burning of agricultural waste in the developing world, Global Biogeochem. Cycles, 17(4), 1095-1134, doi:10.1029/2002gb001952.

Reference pressure (hPa)	GEOS-Chem Model level ref		GEM Model level ref	
	index	hPa	index	hPa
850	9	856.781	69	854.893
500	22	503.795	57	501.327
250	28	263.587	47	258.932
100	34	99.191	34	99.1268
33	38	33.814	19	32.9691
7	41	6.588	10	6.86514

Table 1: Comparable model levels used in later figures. An approximate pressure level is computed for each model level assuming a reference surface pressure of 1000 hPa.

Alert						
	DJF 2010	MAM 2010	JJA 2010	SON 2010	DJF 2011	MAM 2011
GEOS-Chem GOSAT	0.59 1.46	0.84 0.83	-0.02 0.96	0.58 1.08	0.13 1.48	1.11 1.03
GEOS-Chem insitu	-0.56 1.45	-0.16 0.88	1.14 0.90	-0.03 1.08	-1.09 1.46	0.20 1.07
GEM GOSAT	0.01 0.97	1.11 0.81	0.89 1.26	-0.84 0.80	-0.57 1.09	0.78 1.04
GEM insitu	-0.96 0.95	0.12 0.88	2.33 1.27	-0.96 0.79	-1.70 1.08	-0.13 1.14
No. obs.	2157	2195	2104	2079	2084	2145
Mauna Loa						
	DJF 2010	MAM 2010	JJA 2010	SON 2010	DJF 2011	MAM 2011
GEOS-Chem GOSAT	0.80 0.95	1.57 0.80	-0.67 1.45	-0.09 1.07	0.72 0.72	1.61 1.10
GEOS-Chem insitu	-0.14 0.91	0.54 0.78	-0.48 1.03	0.05 0.72	0.19 0.65	0.82 1.05
GEM GOSAT	1.17 0.99	1.41 0.90	-0.84 1.67	0.08 1.31	0.94 0.77	1.64 1.10
GEM insitu	0.22 0.98	0.45 0.89	-0.57 1.28	0.15 0.94	0.32 0.68	1.00 1.08
No. obs.	743	759	870	1011	994	879
Sable Island						
	DJF 2010	MAM 2010	JJA 2010	SON 2010	DJF 2011	MAM 2011
GEOS-Chem GOSAT	-0.64 4.14	0.52 3.92	-0.15 5.20	1.78 3.06	0.78 2.33	0.51 2.15
GEOS-Chem insitu	-1.89 4.09	0.39 3.85	0.46 4.56	-0.26 2.69	-0.57 2.28	0.12 2.01
GEM GOSAT	-0.91 3.97	0.73 3.78	-2.64 5.16	0.40 2.77	0.27 1.24	1.03 1.44
GEM insitu	-2.01 3.96	0.26 3.76	-1.58 4.91	-1.25 2.77	-0.97 1.18	0.59 1.63
No. obs.	2137	1961	1388	2032	2125	2184
South Pole						
	DJF 2010	MAM 2010	JJA 2010	SON 2010	DJF 2011	MAM 2011
GEOS-Chem GOSAT	0.22 0.18	0.52 0.16	0.29 0.11	0.52 0.12	0.49 0.20	0.56 0.17
GEOS-Chem insitu	0.19 0.17	0.05 0.15	-0.22 0.10	0.15 0.18	0.21 0.24	0.03 0.15

GEM GOSAT	0.67 0.22	1.23 0.17	1.27 0.09	1.23 0.15	1.09 0.21	1.29 0.13
GEM insitu	0.68 0.18	0.69 0.13	0.66 0.10	0.76 0.10	0.76 0.20	0.66 0.13
No. obs.	2027	2111	2103	2055	2035	2120

Table 2: Comparison of GEOS-Chem and GEM-MACH-GHG CO_2 to NOAA or ECCC continuous in situ observations. The 6-season averaged seasonal means and standard deviations from Figure 4 are given. Each box with statistics contains two numbers: the seasonal mean (left) and the standard deviation (right). Results from four experiments are shown. Two models (GEOS-Chem and GEM-MACH-GHG) were used to integrate posterior fluxes from GEOS-Chem inversions using only in situ or GOSAT observations. Units are ppm. Note that all observations (including night time) were used.

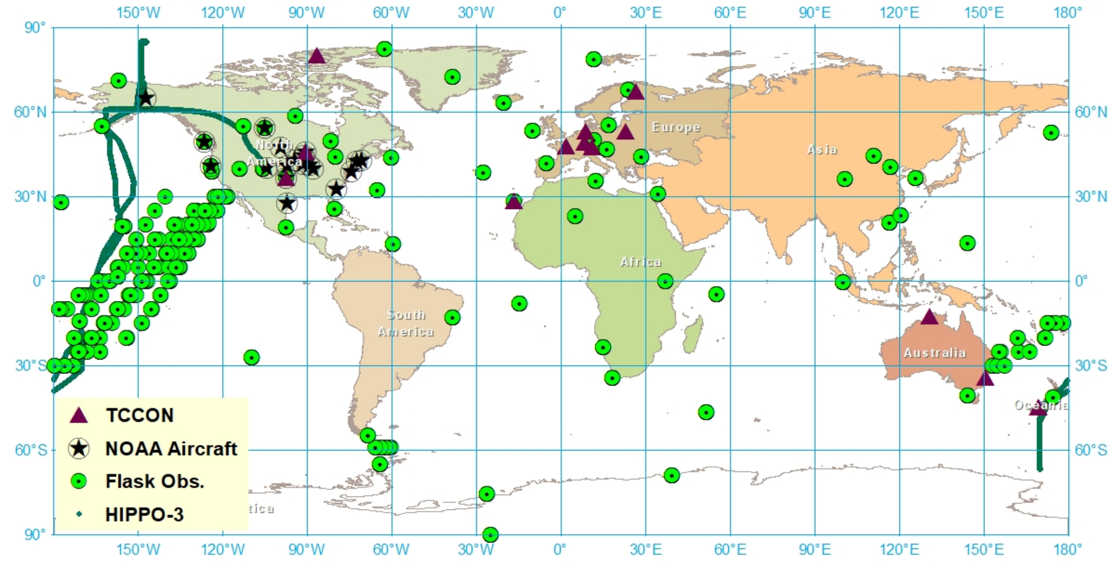

Figure 1. In situ observation network and observations used for verification. The in situ observations used in the GEOS-Chem flux inversion are indicated in green circles. Observations used for model assessment are also shown: TCCON (triangles), NOAA aircraft (stars) and HIPPO-3 aircraft (green line).

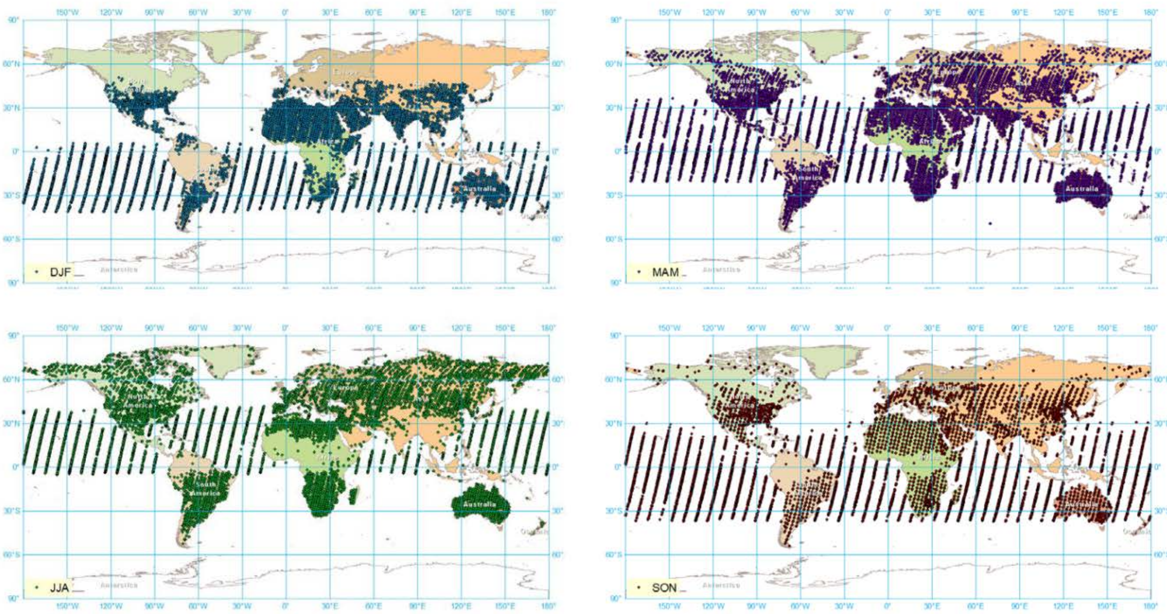

Figure 2. Seasonal variation of GOSAT observations. The observations used in the GOSAT-based flux inversions are shown for four seasons: boreal winter (December, January, February – top left), boreal spring (March, April, May – top right), boreal summer (June, July, August – bottom left) and boreal autumn (September, October, November – bottom right) for 2010.

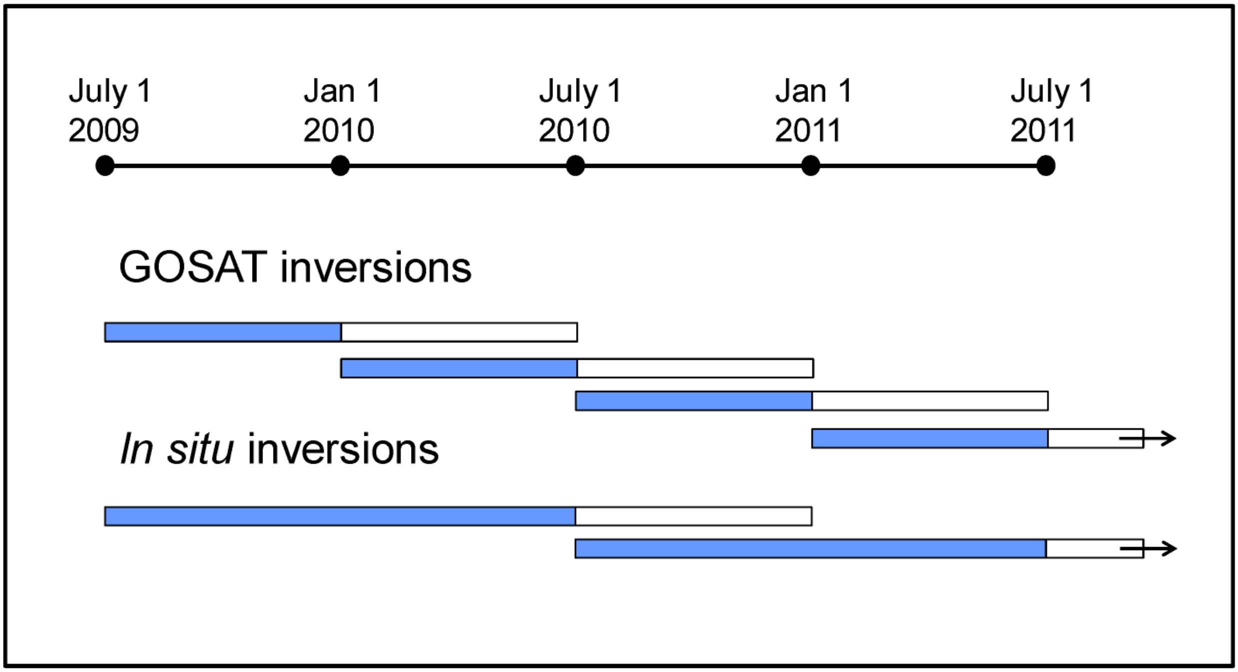

Figure 3. Schematic diagram of GEOS-Chem inversion experiments. The inversions involving the assimilation of GOSAT data were done in four 12-month segments. The fluxes obtained from the first 6 months of each segment were retained as the retrieved fluxes. The inversions involving in situ data were done in two 18-month segments with the fluxes retained from the first 12 months. Thus retrieved fluxes were available for the 24 months from 1 July 2009 to 30 June 2011 for both sets of flux inversions.

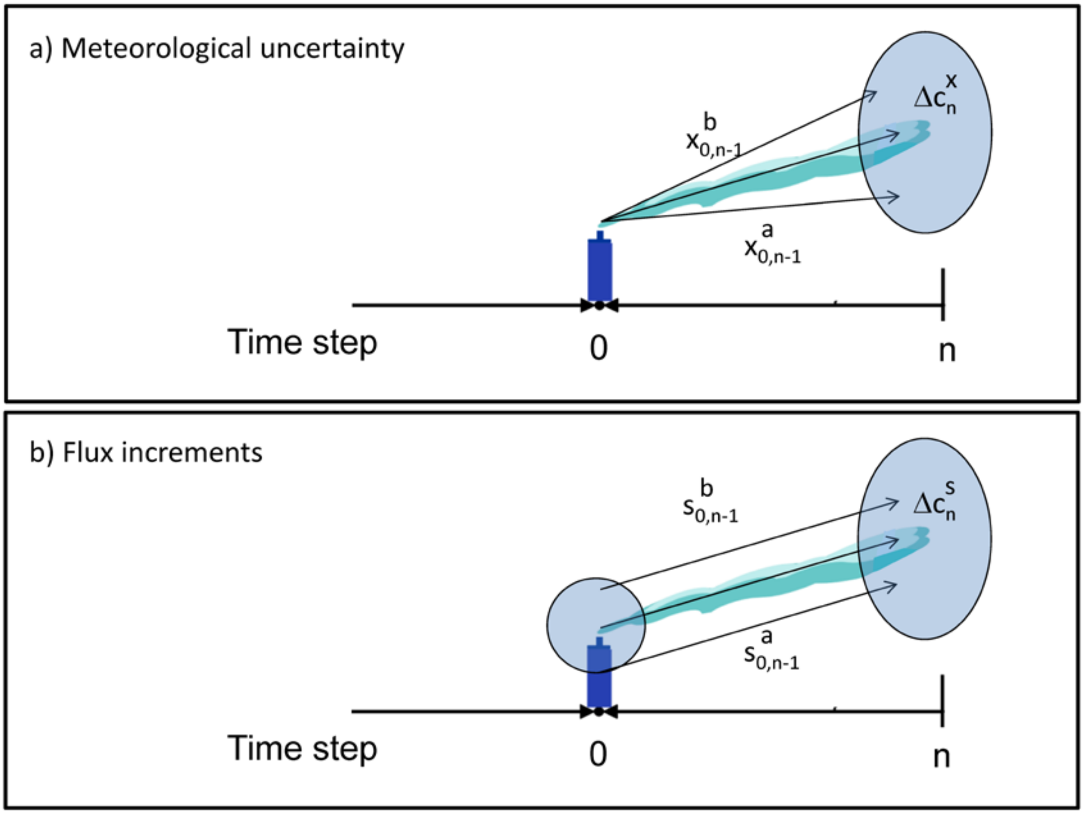

Figure 4. Components of the posterior atmospheric adjustment. a) The top panel is a schematic diagram illustrating the fact that uncertain wind fields (represented by the 3 arrows) would lead to a cloud of equally plausible downstream locations for a given sequence of fluxes. b) The lower panel is a schematic diagram illustrating the fact that flux increments (e.g. a prior versus a posterior flux) will lead to differences in concentrations downstream, for a given sequence of meteorological analyses. The parallel arrows are meant to indicate the use of the same meteorological fields for two flux estimates.

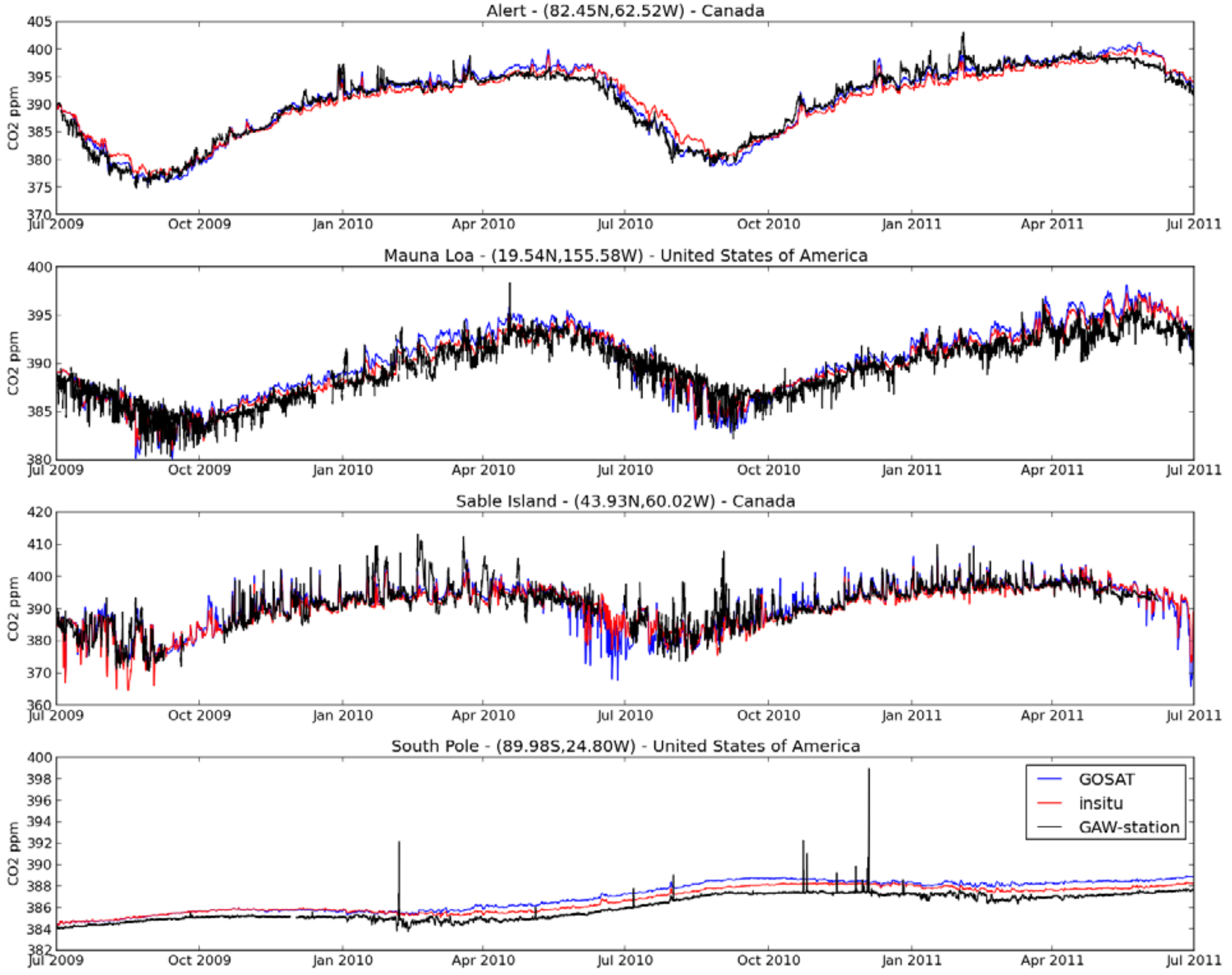
Alert - (82.45N,62.52W) - Canada
Mauna Loa - (19.54N,155.58W) - United States of America
Sable Island - (43.93N,60.02W) - Canada
South Pole - (89.98S,24.80W) - United States of America
CO2 ppm
Jul 2009
Oct 2009
Jan 2010
Apr 2010
Jul 2010
Oct 2010
Jan 2011
Apr 2011
Jul 2011
GOSAT
insitu
GAW-station

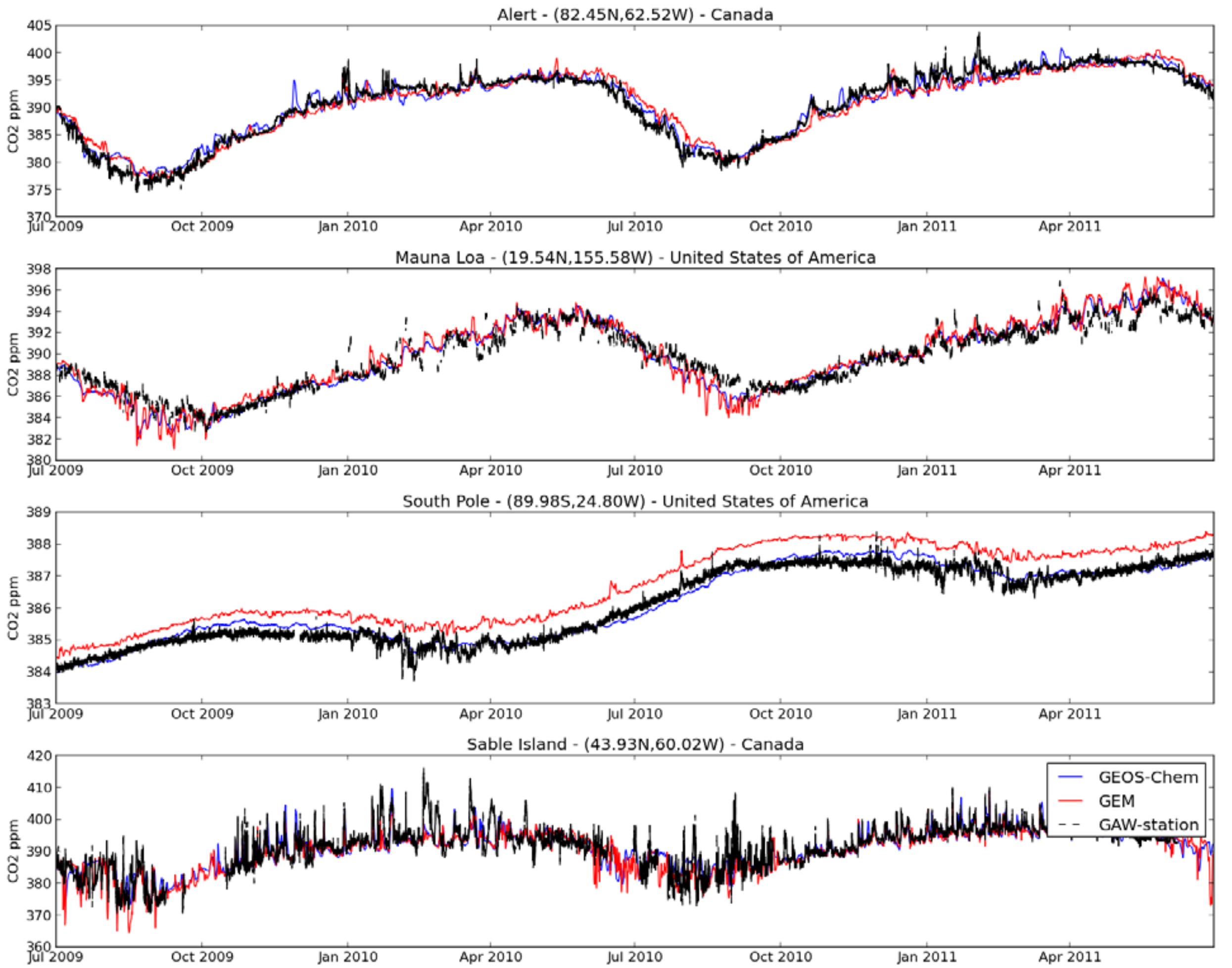

Figure 54. Time series of CO_2 observations and GEM-MACH-GHG model simulations for 1 July 2009 to 1 July 2011. The CO_2 observations are from ECCC or NOAA GHG in situ measurement networks for Alert (top), Mauna Loa (second), Sable Island South Pole (third) and South Pole Sable Island (bottom). The observations are indicated in black. The model simulations with GEM-MACH-GHG (red curves) and GEOS-Chem (blue curves) used posterior fluxes obtained from inversions with GEOS-Chem using in situ (red curves) or GOSAT (blue curves) observations.

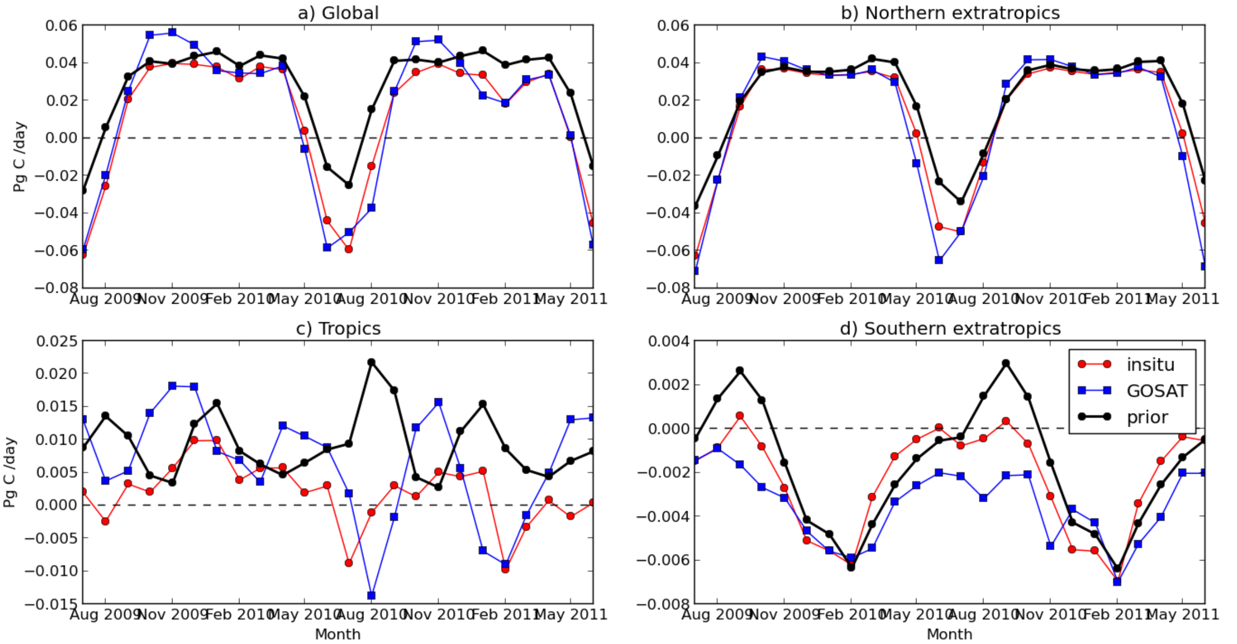

Figure 6. Prior and posterior fluxes area weighted and regionally averaged over (a) the whole globe, (b) the northern extratropics, (c) the tropics and (d) the southern extratropics. Fluxes are monthly averages from July 2009 to June 2011. Note the expanded vertical scales for panels c and d.

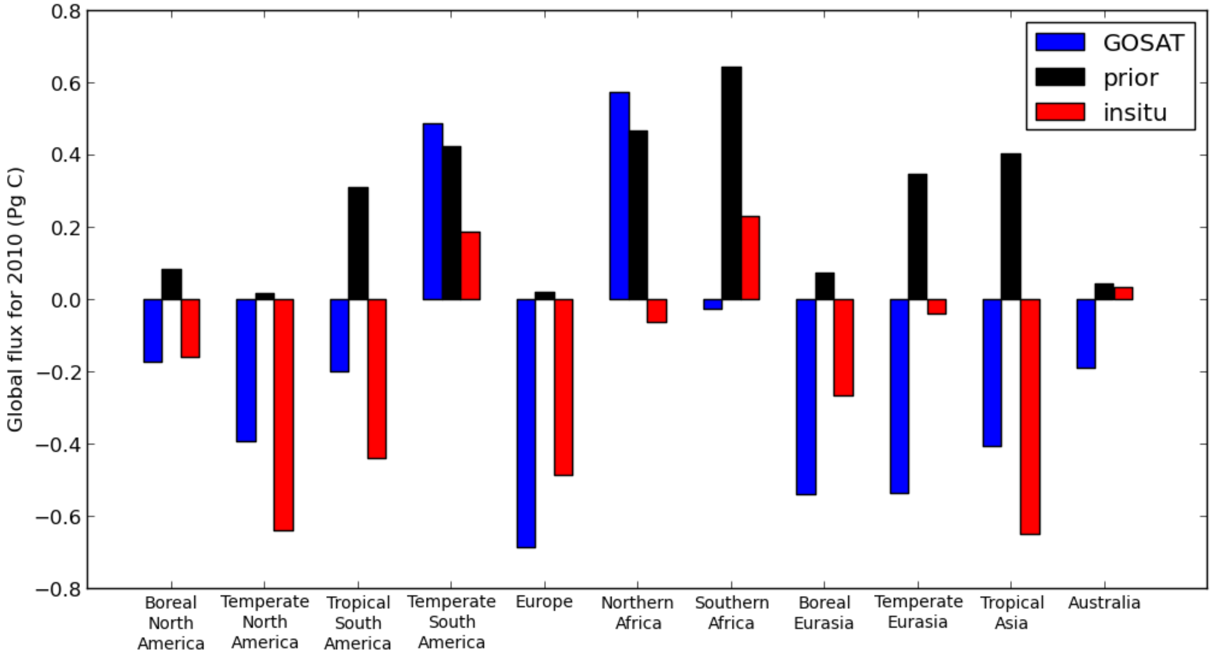

Figure 5. Annual fluxes for 2010 for the 11 TransCom regions inferred by GOSAT (blue) and in situ (red) data. Also shown is the prior flux (black). Values include natural fluxes as well as biofuel and biomass burning emissions.

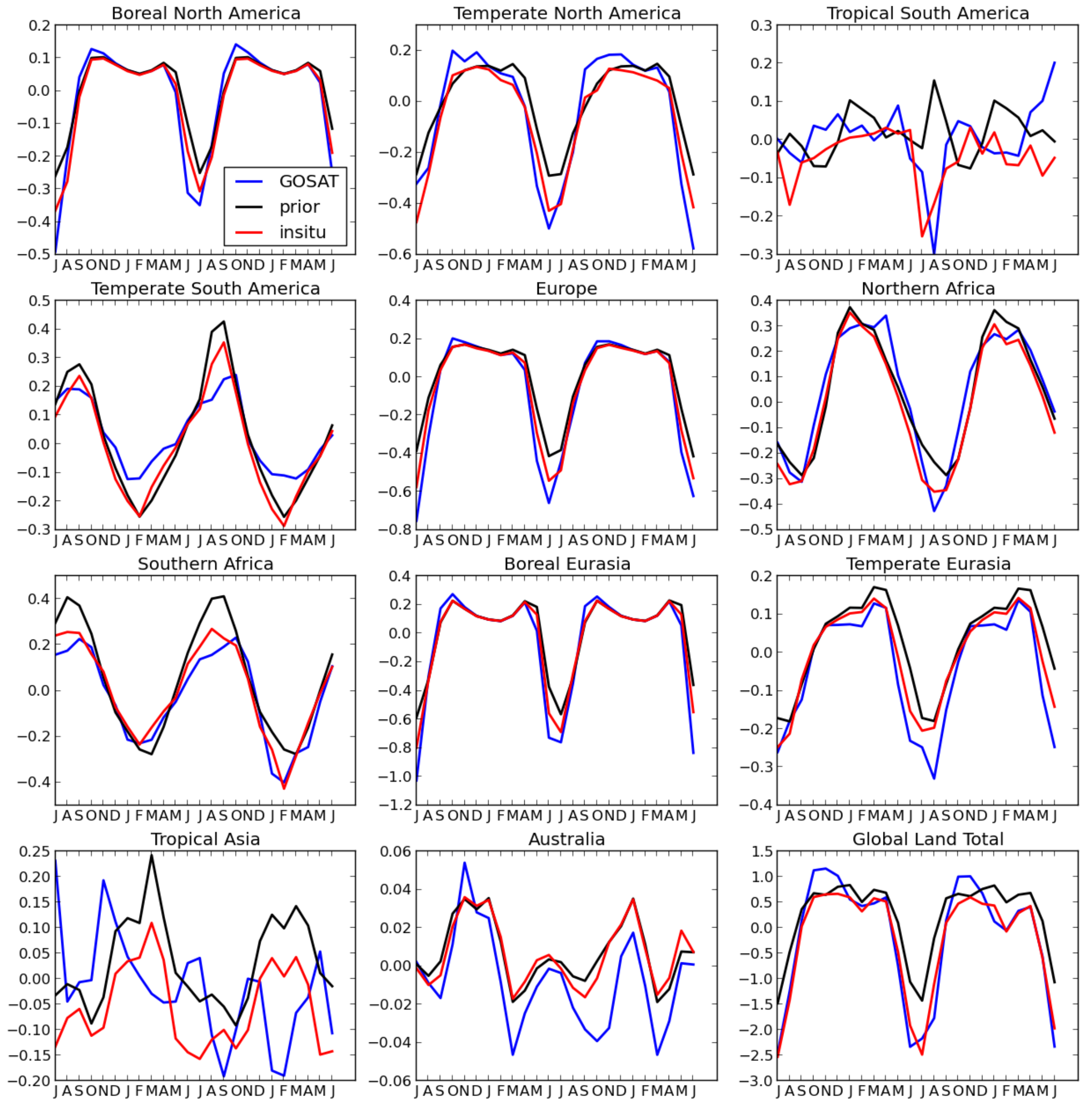

Figure 6: Monthly fluxes in PgC yr^{-1} for the 11 TransCom land regions and the global land total retrieved from GEOS-Chem 4D-Var inversions using GOSAT (Blue) or in situ (red) data. Also shown are prior fluxes (black). The full simulation period of July 2009 to June 2011 is shown, including the spin up period (July – Dec. 2009).

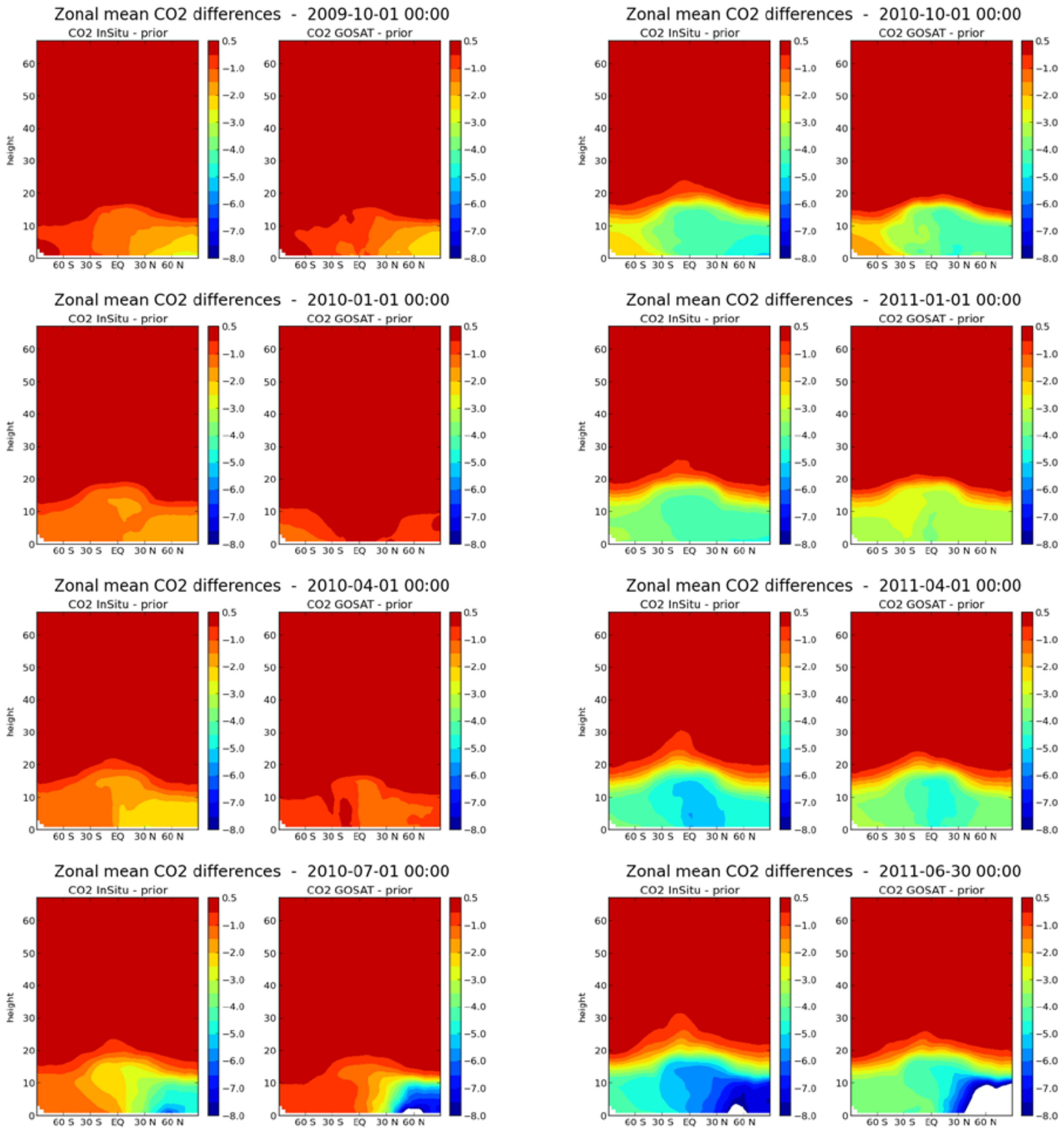

Figure 7. Time sequence of zonal mean ~~flux signals~~posterior atmospheric adjustment due to fluxes (PAAF) simulated with GEOS-Chem. Zonal mean fields are displayed as a function of height and latitude in units of ppm. Shown are the in situ (leftmost of each pair) and the GOSAT (rightmost of each pair) zonal mean ~~flux signal~~PAAFs. The earliest date is in the top left corner with subsequent dates following down the left side then continuing down the right side. Dates are indicated above each pair of panels starting on 1 October 2009 and continuing in three-month intervals to 30 June 2011.

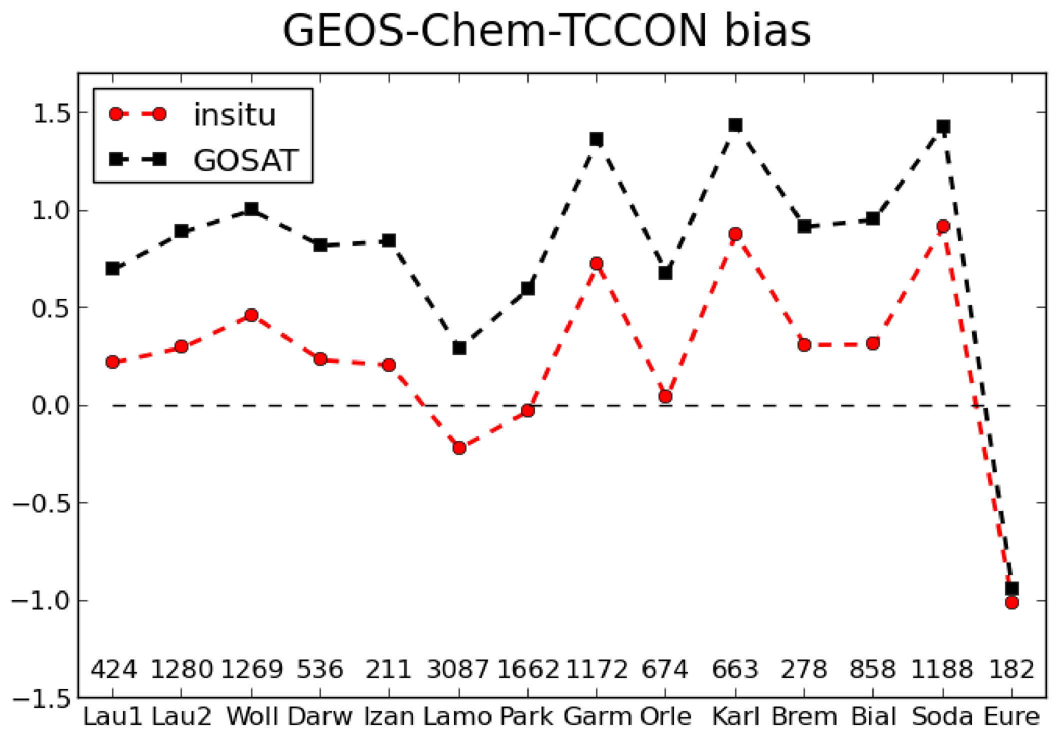

Figure 8. Comparison of GEOS-Chem CO_2 simulations with GOSAT-derived (black) and in situ (red) derived posterior fluxes to TCCON measurements at 14 sites (Darwin, Wollongong, 2 instruments at Lauder, Izaña, Lamont, Park Falls, Garmisch, Orléans, Karlsruhe, Bremen, Bialystock, Sodankylä, and Eureka). Stations are ordered by latitude from southernmost to northernmost. The mean residual in ppm was computed for each stations from December 2009 to May 2011, inclusive. Positive values mean the modelled CO_2 is generally higher than observed CO_2.

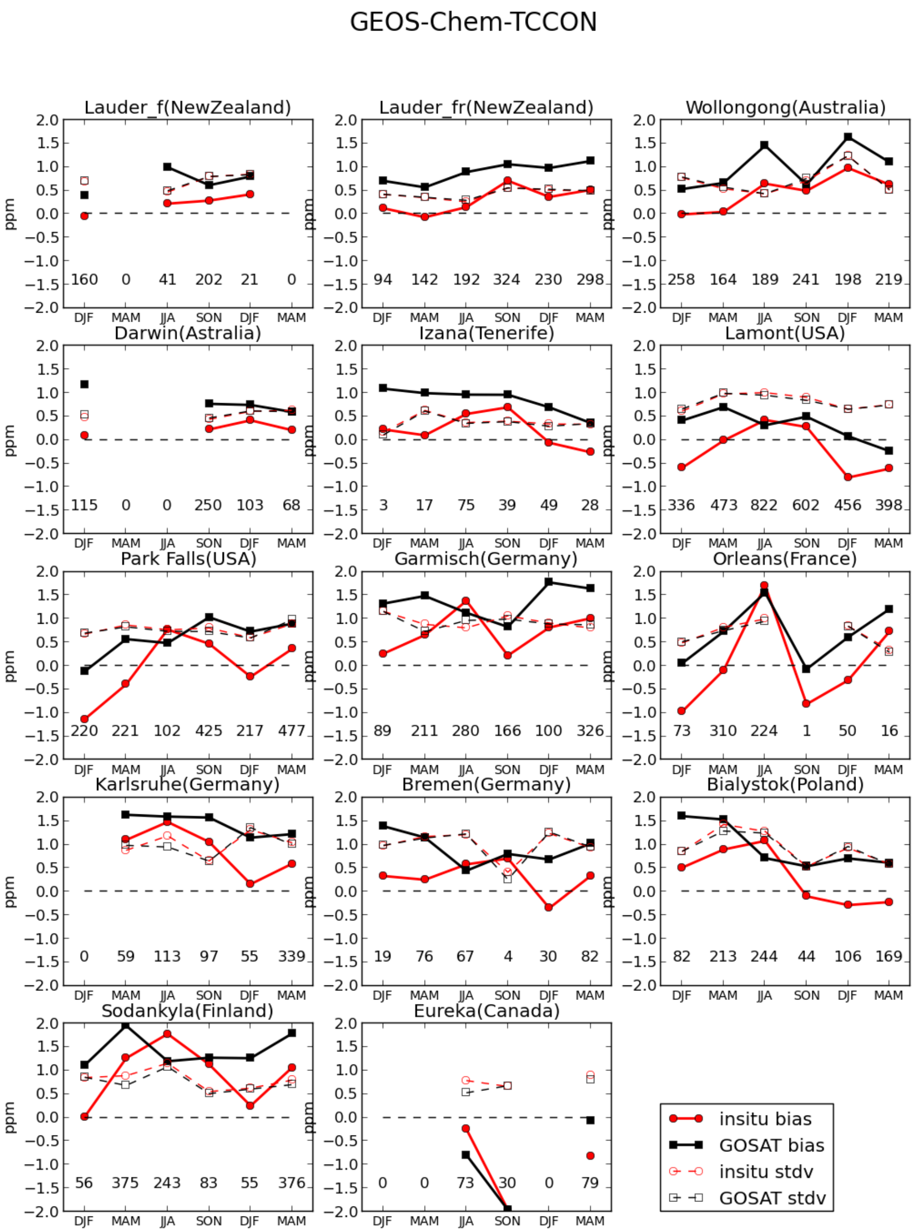

Figure 9. Comparison between TCCON measurements at 14 sites and the GEOS-Chem CO_2 simulations driven with posterior fluxes from the GOSAT (black) and in situ (red) inversions. Scores (bias and standard deviation) are aggregated by three-month seasons from December 2009 to May 2011. Lauder appears twice because there are two different instruments there.

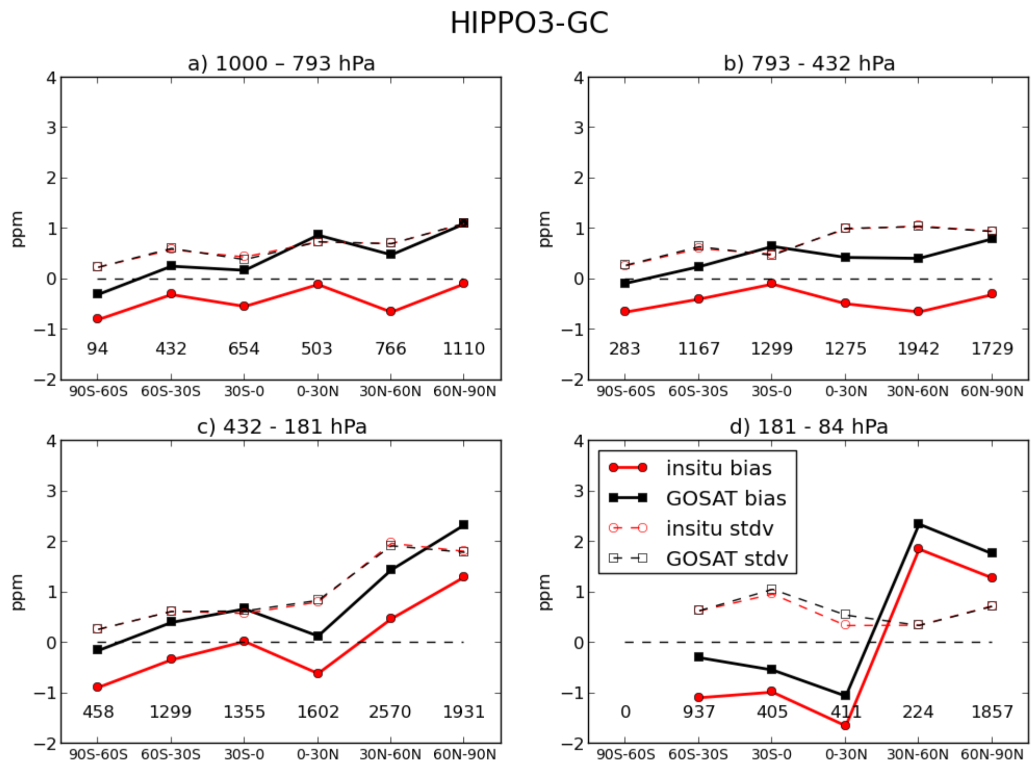

Figure 10. Comparison between the HIPPO-3 measurements and the GEOS-Chem CO_2 simulations driven with posterior fluxes from the GOSAT (black) and in situ (red) inversions. Scores (bias and standard deviation) of modelled minus observed values are aggregated by latitude band and over the pressure layers given above each panel. The numbers of observations used in each statistic are indicated within each panel. The flights occurred between 24 March to 16 April 2010.

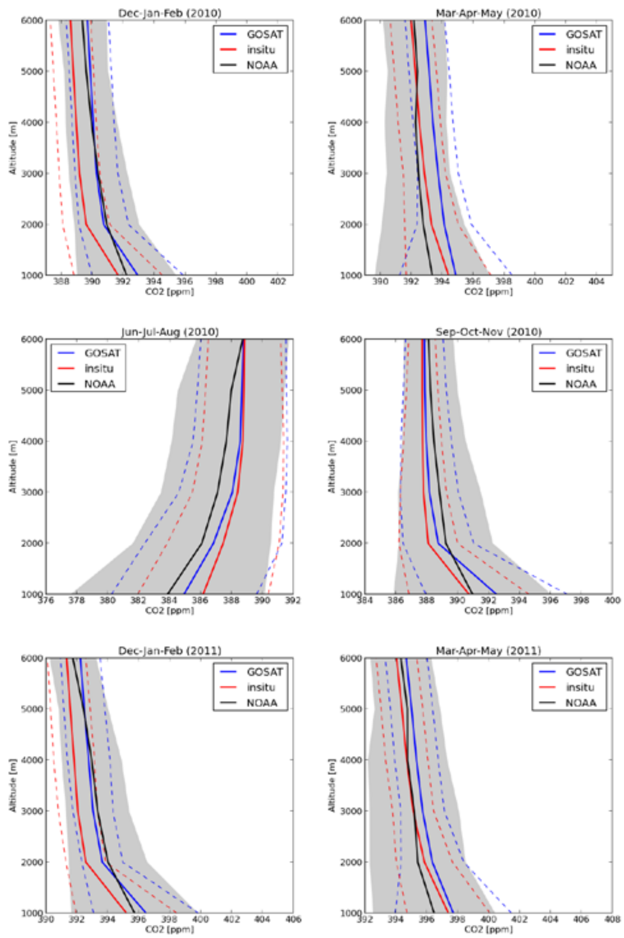

Figure 11. Comparison of mean GEOS-Chem model profiles of CO_2 to NOAA aircraft observations. Observations (black curves) are from obspack_co2_1_PROTOTYPE_v1.0.4_2013-11-25 for locations over continental U.S. and Canada, only. Observed and modelled profiles are binned over 3-month seasons as indicated above each panel. Model simulations used posterior fluxes from GEOS-Chem inversions with GOSAT (blue) or in situ (red) observations. The shaded grey regions indicate plus or minus one standard deviation for the observations while the dashed coloured lines indicate the same quantities but for the different model runs. Sites used are: Beaver Crossing, Nebraska; Bradgate, Iowa; Briggsdale, Colorado; Cape May, New Jersey; Charleston, South Carolina; Dahlen, North Dakota; East Trout Lake, Saskatchewan; Estevan Point, British Columbia; Fairchild, Wisconsin; Harvard Forest, Massachusetts; Homer, Illinois; Oglesby, Illinois; Park Falls, Wisconsin; Poker Flat, Alaska; Sinton, Texas; Southern Great Plains, Oklahoma; Trinidad Head, California; West Branch, Iowa; Worcester, Massachusetts.

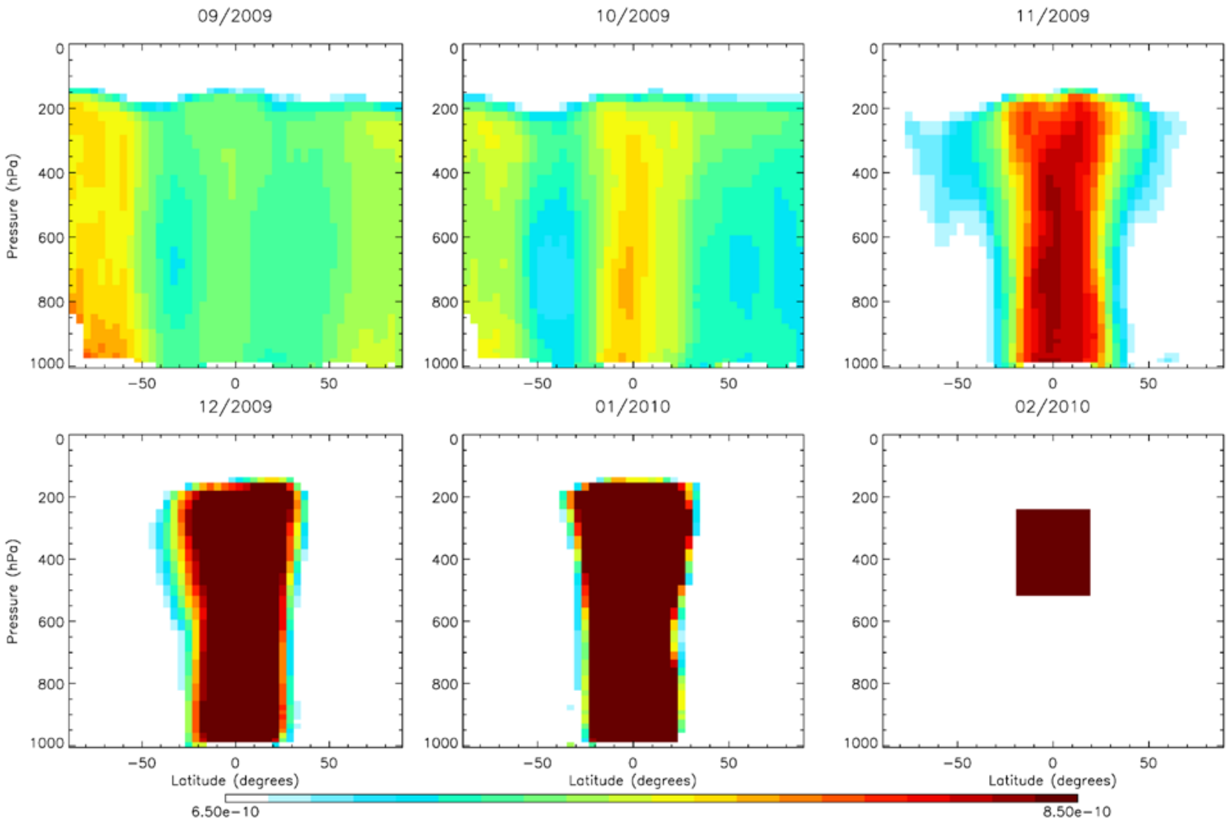

Figure 12: Sensitivity (in ppm/ppm) of the GEOS-Chem tropical tropospheric CO_2 on 1 February 2010 to the 3D modeled state on earlier dates. Sensitivity fields are zonally averaged instantaneous fields for the first day of each month from September 2009 to February 2010 in the various panels.

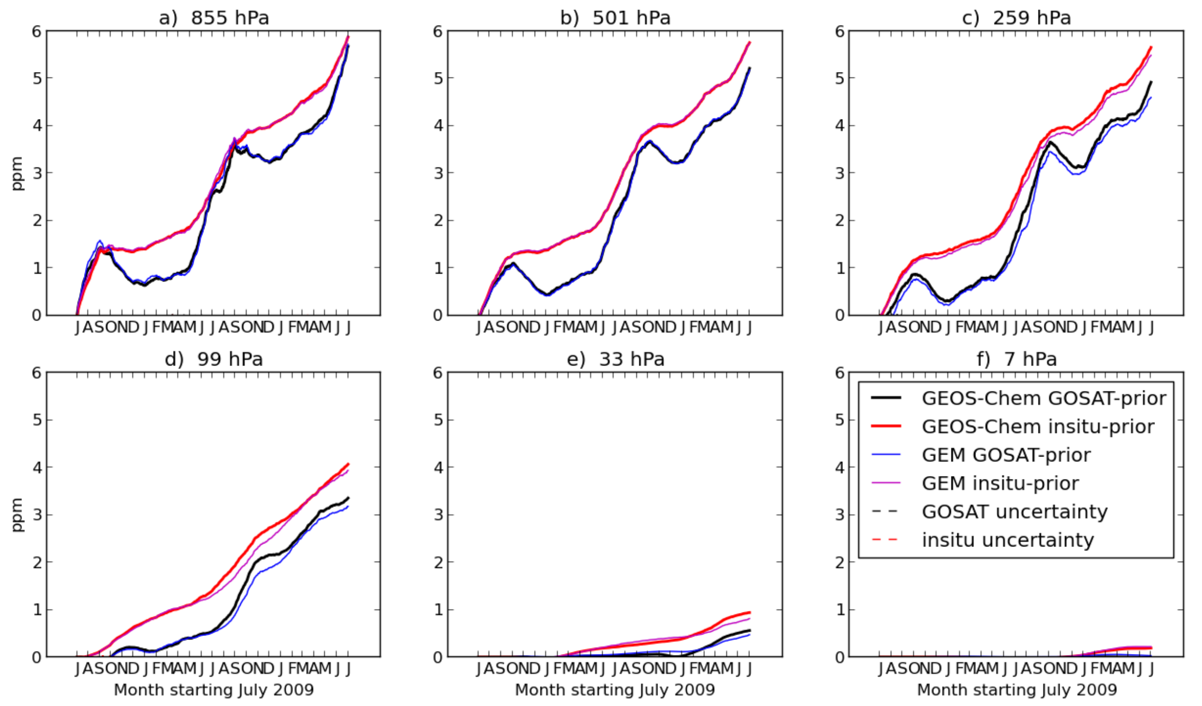

Figure 13. Global mean CO_2 ~~flux signal~~PAAF for 1 July 2009 to 30 June 2011 from the GOSAT-based posterior fluxes (solid black curves) and the in situ-based posterior fluxes (solid red curves). ~~Flux signal~~PAAFs (prior minus posterior CO_2 fields) are shown for the model level closest to the nominal pressure level indicated above each panel for both GEOS-Chem (thick lines) and GEM-MACH-GHG (thin lines). The global means of the CO_2 uncertainty are~~is~~ shown for the GOSAT posterior flux integration (black dashed curves) and the in situ posterior flux integration (red dashed curves) but are not visible because they are negligble. Uncertainty in CO_2 is estimated with GEM-MACH-GHG by perturbing the meteorological analyses and computing the difference from the unperturbed integration.

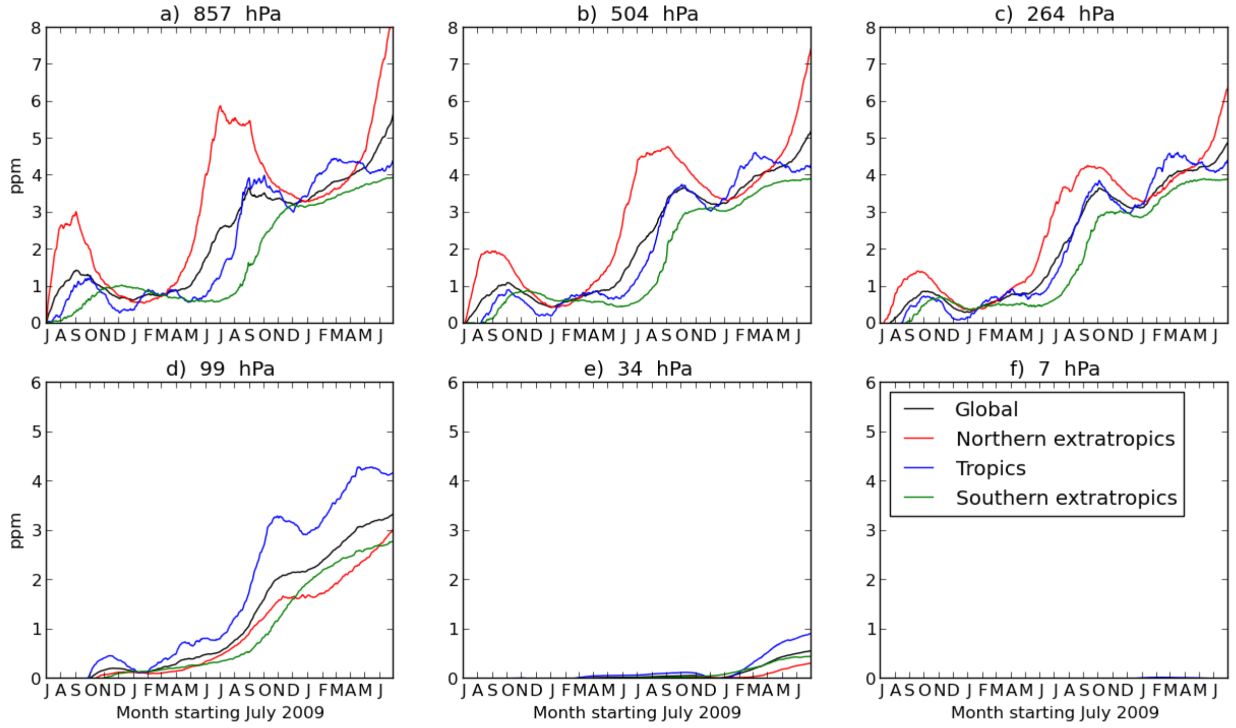

Figure 14. Global mean CO_2 ~~flux signal~~PAAF obtained with GEOS-Chem with GOSAT-based posterior fluxes. ~~Flux signal~~PAAFs (prior minus posterior CO_2 fields) are shown for the model level closest to the nominal pressure level indicated above each panel. The coloured curves represent the global total (black) and the contributions to this from the various subregions: northern extratropics (red), southern extratropics (green) and tropics (blue). Because the subregions were chosen to have equal areas, the contribution depicted for each subregion was scaled by a factor of three so that the mean of the contributions from the subregions gives the total contribution.

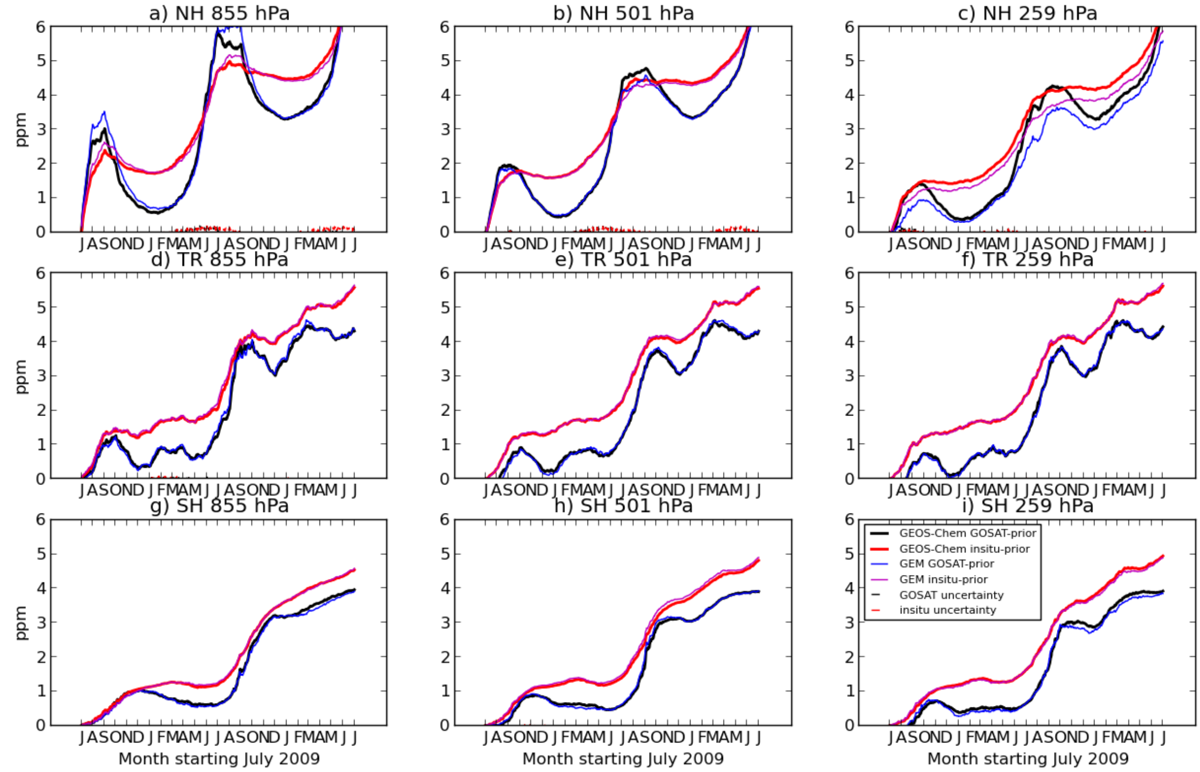

Figure 15. Regional contributions to the global mean CO_2 ~~flux signal~~PAAF for 1 July 2009 to 30 June 2011. The PAAF~~flux signal~~ is from the GOSAT-based posterior fluxes (solid black curves) and the insitu-based posterior fluxes (solid red curves). ~~Flux signal~~PAAFs (prior minus posterior CO_2 fields) are shown for the model level closest to the nominal pressure level indicated above each panel for both GEOS-Chem (thick lines) and GEM-MACH-GHG (thin lines). Regional contributions have been multiplied by a factor of three as in Figure 14. Uncertainty in global mean CO_2 is shown for the GOSAT posterior flux integration (black dashed curves) and the insitu posterior flux integration (red dashed curves). Uncertainty in CO_2 is estimated for each integration by perturbing the meteorological analyses and computing the difference from the unperturbed integration.

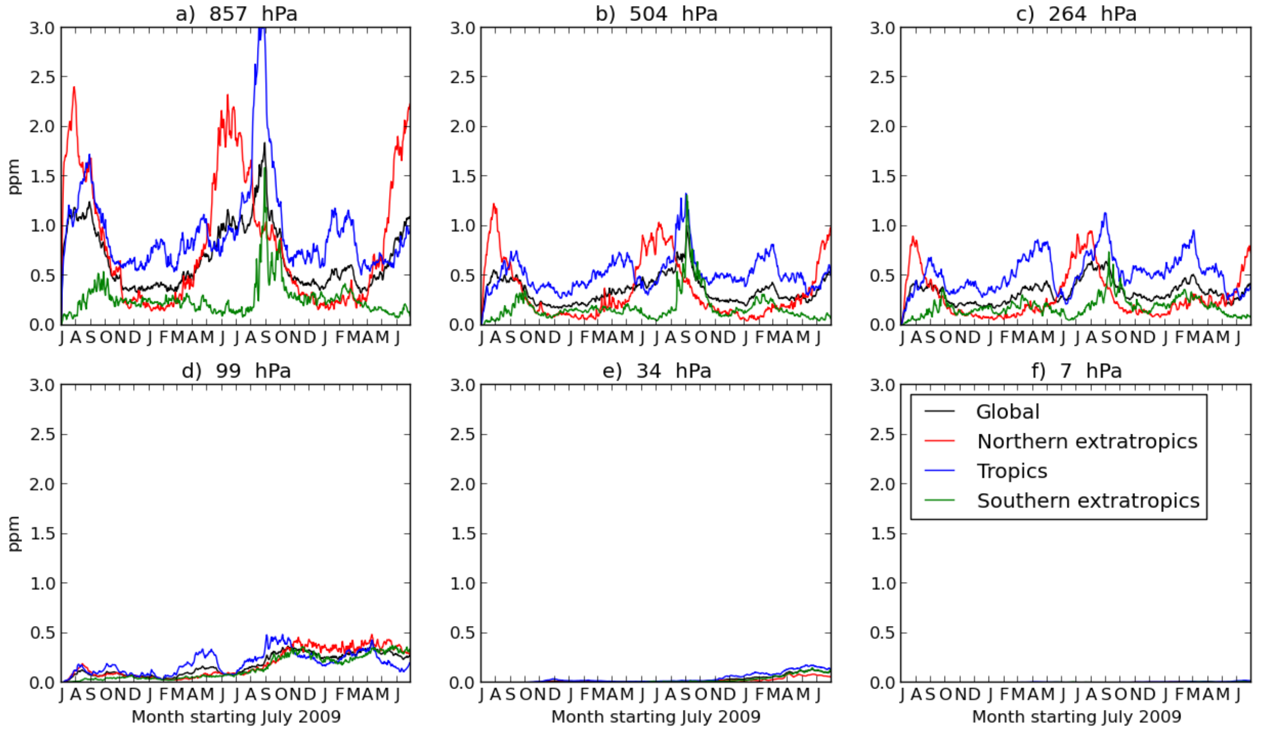

Figure 16. Global mean of zonal standard deviation of the CO_2 ~~flux signal~~PAAF obtained with GEOS-Chem using GOSAT-based posterior fluxes. Statistics are shown for the model level closest to the nominal pressure level indicated above each panel. The coloured curves represent the global total (black) and the contributions to this from the various subregions: northern extratropics (red), southern extratropics (green) and tropics (blue). Because the subregions were chosen to have equal areas, the contribution depicted for each subregion was scaled by a factor of three so that the mean of the contributions from the subregions gives the total contribution.

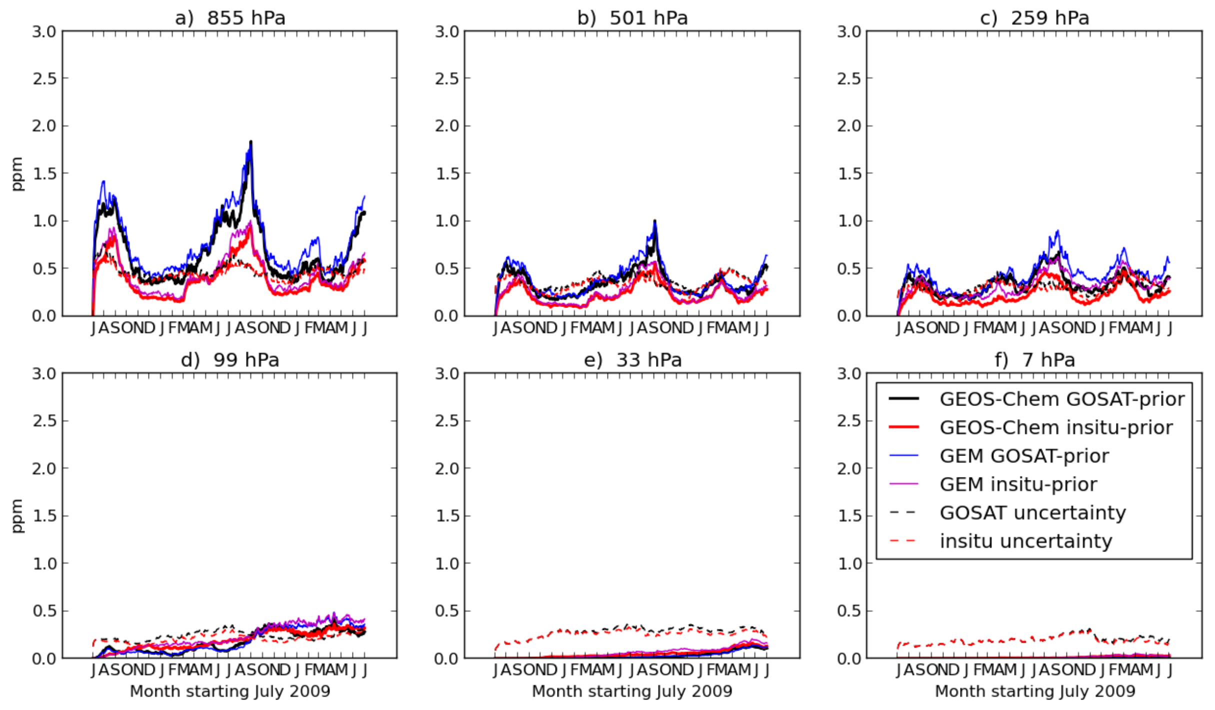

Figure 17. Global mean of the zonal standard deviation of the CO_2 ~~flux signal~~PAAF for 1 July 2009 to 30 June 2011 from the GOSAT-based posterior fluxes (solid black curves) and the insitu-based posterior fluxes (solid red curves). ~~Flux signal~~PAAFs are shown for the model level closest to the nominal pressure level indicated above each panel for both GEOS-Chem (thick lines) and GEM-MACH-GHG (thin lines). The zonal standard deviation of the CO_2 uncertainty is shown for the GOSAT posterior flux integration (black dashed curves) and the insitu posterior flux integration (red dashed curves). Uncertainty in CO_2 is estimated with GEM-MACH-GHG by perturbing the meteorological analyses and computing the difference in CO_2 from the unperturbed integration with a given set of posterior fluxes.

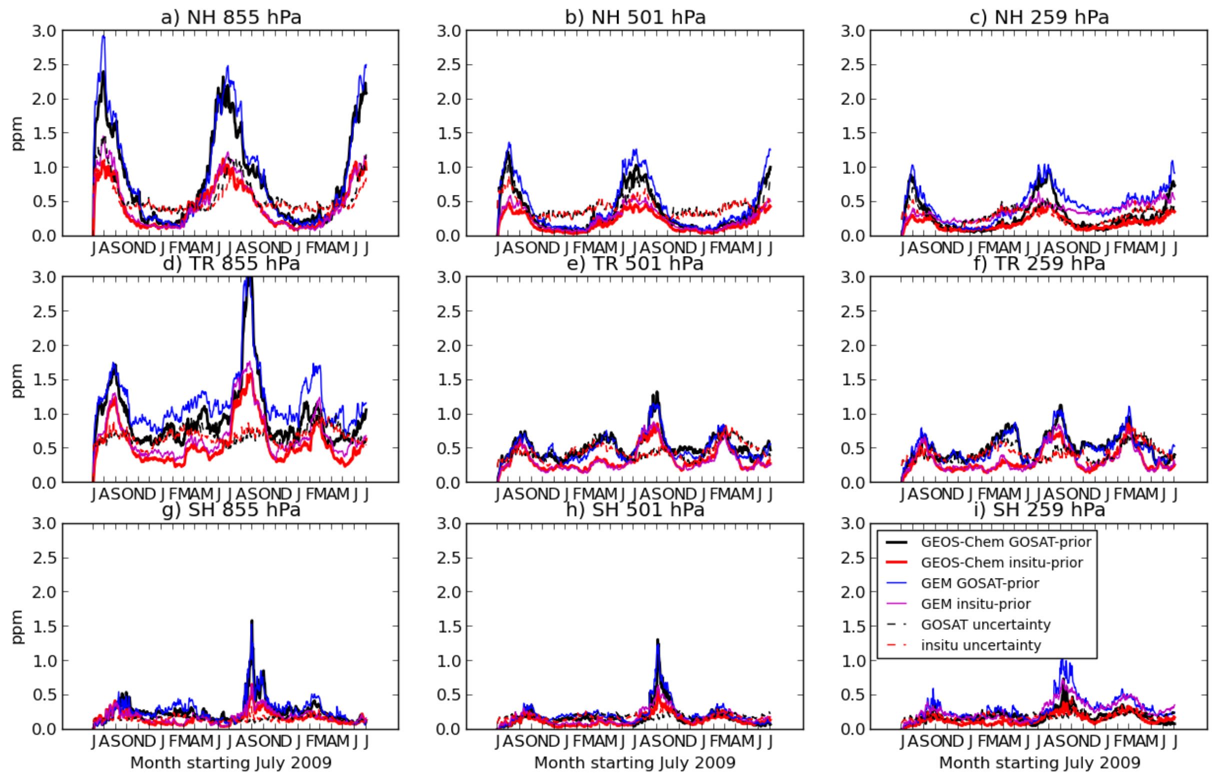

Figure 18. Regional contributions to the global mean of the zonal standard deviation of the CO_2 ~~flux signal~~PAAF for 1 July 2009 to 30 June 2011 from the GOSAT-based posterior fluxes (solid black curves) and the insitu-based posterior fluxes (solid red curves). ~~Flux signal~~PAAFs are shown for the model level closest to the nominal pressure level indicated above each panel for both GEOS-Chem (thick lines) and GEM-MACH-GHG (thin lines). Regional contributions have been multiplied by a factor of three as in Figure 14~~2~~. Uncertainty in zonal standard deviation of CO_2 is shown for the GOSAT posterior flux integration (dashed cyan curves) and the insitu posterior flux integration (dashed magenta curves). Uncertainty in CO_2 is estimated for each integration by perturbing the meteorological analyses and computing the difference from the unperturbed integration.